ADVANCEMENTS IN THE SIMULATION OF GROUND SOURCE HEAT PUMP SYSTEMS

By

JAMES R. CULLIN

Bachelor of Science in Mechanical Engineering
Oklahoma State University
Stillwater, Oklahoma
2006

Master of Science in Mechanical Engineering
Oklahoma State University
Stillwater, Oklahoma
2008

Submitted to the Faculty of the
Graduate College of the
Oklahoma State University
in partial fulfillment of
the requirements for
the Degree of
DOCTOR OF PHILOSOPHY
May 2014

ADVANCEMENTS IN THE SIMULATION OF

GROUND SOURCE HEAT PUMP SYSTEMS

Dissertation Approved:

Dr. Jeffrey D. Spitler

Dissertation Adviser

Dr. Daniel E. Fisher

Dr. Afshin J. Ghajar

Dr. Richard A. Beier

ACKNOWLEDGEMENTS

This work would not have been possible without the gracious support of my wonderful wife and best friend, Cassandra. I had a feeling once I met you that my life was about to change, but I could never have imagined the levels of joy and happiness you have brought me. Above all, going through life beside each other these past seven years has made me realize just how much the two of us can accomplish together. I could not ask for a better friend, companion, lover, and soulmate. Congratulations, my dear, on your own amazing accomplishment in earning your own doctorate. Cassandra, you are the love of my life, always and forever, with all my heart.

I also could not have done this without the encouragement of my parents, John and Celia, and sister, Nyssa. The same from my "second" family: Dan, Levata, Mellanie, and Nick. When I was struggling through, thinking I wouldn't make it, you were there for me.

My committee has been an invaluable resource of knowledge and mentorship during my time at OSU. Thanks go to Dr. Spitler, Dr. Fisher, Dr. Ghajar, Dr. Beier, and Dr. Bose (happy retirement!), for all of their contributions to my education.

All of my research group colleagues over the years have provided a great sounding board for ideas, as well as a fun bunch just to talk to. You all are too numerous to name here individually, but each of your influences on my time at OSU are greatly appreciated.

Special mention to the Oklahoma State University Quiz Bowl team, especially the early folks: Lenzy, Jacob, Colin, Jonathon, Carla, and Libbie. OSUQB gave me an outlet for my frustrations (and they were sometimes both numerous and profound), and I couldn't ask for a better group of lifelong friends. You are also responsible for introducing me to Cassandra; if only for that, I am forever in your debt.

Thank you all.

James R. Cullin
29 April 2014

Name: JAMES ROBERT CULLIN

Date of Degree: MAY 2014

Title of Study: ADVANCEMENTS IN THE SIMULATION OF GROUND SOURCE HEAT PUMP SYSTEMS

Major Field: MECHANICAL ENGINEERING

Abstract:

With ground source heat pump systems becoming an increasing focus in the building energy efficiency sector, fully understanding their behavior is key. For systems such as these, computer simulation is typically performed to design them, or to examine their potential energy performance. Therefore, having detailed simulations that take into account all relevant behaviors of these systems is of the utmost importance.

After discussing the current state of ground source heat pump system simulation, a first-order analysis shows that the horizontal piping in a vertical borehole system can play a very significant effect on the overall performance, and that the selection of the design temperatures can influence the long-term behavior of the system. To further delve into particular aspects of ground source heat pump behavior, a new, detailed model is developed that focuses much computational effort on the area surrounding the borehole, which possesses the highest temperature gradient and therefore the highest heat transfer rate.

The new model, as well as a widely-used existing model, are then validated against multiple experimental data sets. This validation shows that the new model performs well for smaller systems, but struggles when the number of boreholes increases due to computation time. Meanwhile, the existing model performs well for typical systems of all sizes; where it fails, though, is in failing to account for thermal short-circuiting inside the borehole, which becomes significant as the fluid residence time grows.

Finally, two notable design methodologies are also validated. One, a simulation-based standalone design tool, sizes systems very accurately, and the error falls within the range attributable to not using a more detailed hourly simulation. On the other hand, the current ASHRAE Handbook design equation fails to predict the lengths with any accuracy; this is predominantly due to the simplistic nature in which it represents the building loads.

TABLE OF CONTENTS

Chapter Page

Chapter Page

LIST OF TABLES

Table Page

LIST OF FIGURES

Figure Page

Figure Page

CHAPTER I

INTRODUCTION

As worldwide focus to conserve energy grows, the need for technologies to meet the demands of today's world becomes extremely important. In particular, energy-efficient buildings are one way in which total energy demands may be lessened, and one way to increase the efficiency of a building's heating and cooling systems is by utilizing a ground source heat pump (GSHP) system, sometimes also referred to as a geothermal heat pump system.

A ground source heat pump system consists of one or more heat pumps connected to a ground heat exchanger (GHX). In warmer months, the ground acts as a heat sink, allowing heat to be rejected to the ground; similarly, in cooler months, the ground can be a source of heat as heat is extracted from the ground. Thus, heat can be extracted from and rejected to the ground on a cyclic, annual basis. This cycle can last for many years, as equipment can be replaced as it ages; the limiting factor in the lifespan of a GSHP system is typically either the durability of the HDPE piping that comprises the GHX, or the functional life of the building itself. Any imbalance between the heat moving into or out of the ground, though, can lead to long-term drift in the ground temperature, which can reduce the system's efficiency. In the worst case, this thermal imbalance can lead to system failure, and/or an impractically expensive design. Additionally, the

efficiency of the GSHP system is also dictated by the thermal properties of the working fluid, soil, and any grouting used to fill a borehole.

Multiple methods exist for designing ground source heat pump systems. Implicit in nearly all of these methods is a core set of assumptions, some of which are often made automatically by design engineers without considering their ramifications, or even realizing that the assumptions are being made. While these effects are generally accepted by practicing designers to be secondary in nature (when they are acknowledged at all), their exact contributions to system performance have, to date, not been quantified in the published literature. Therefore, one goal of this work is to explore some of these assumptions, in order to gain a better understanding of how real ground source heat pump systems operate. This can be done through careful usage of existing models, but will also require development of a more detailed model to test particular aspects of GHSP behavior.

With any computer-based simulation, validation is an important step. A model that has been validated against experimental data has been shown to provide accurate results in the prediction of real system operation, and as such, can be trusted to provide accurate results in the future for systems that are still in the design phase. Consequently, another goal of this work is to provide a large-scale validation of both existing and new ground heat exchanger models, against multiple sets of experimental data. A validation on this scale provides great opportunity to demonstrate the limitations of individual models, as testing a single model against a single data set may not necessarily be indicative of the model's general performance across all ranges of feasible inputs.

In the same vein, several approaches exist that are used by design engineers to determine the required size (and, potentially, other features) of ground heat exchangers. These engineers place their faith in the accuracy of these methods, as sizing the GHX either too large or too small can result in severe consequences, either in terms of unnecessary added costs or equipment damage. Thus, the final goal of this work is to test these design methods in very much the same way that the system simulations were analyzed. By using experimental parameters from real, installed and monitored GSHP systems around the world, the design methods can be used to determine the GHX size required to meet the temperatures measured in these systems. The accuracy of these design methods when compared to the actual installed size will hopefully lead to some explanation of why real systems may be over- or undersized.

The overall aim of this work is to advance the current state of ground source heat pump system simulation, by analyzing new and existing models to explore in detail the behavior of these systems. Following, then, is a brief description of each of the chapters in this work.

Chapter 2 presents a thorough review of the state of the art of ground source heat pump simulation and design. It categorizes and emphasizes the assumptions made in practice, in order to provide recommendations of how to examine them in detail. Additionally, it explores past efforts in ground source heat pump model validation, with a focus on what constitutes the ideal validation.

Chapter 3 provides a first-order analysis of one assumption made in the design of ground source heat pump systems: that any horizontal connective piping between boreholes, or running from the borefield to the piping manifold, has no effect on the thermal performance of the system. In doing

this analysis, observations are made as to how this could be one potential explanation for GSHP users being unable to see a long-term change in ground temperature when using certain design methods.

Chapter 4 describes a new model that has been developed to analyze vertical ground heat exchangers. This model has been termed a "multi-coordinate model" due to its application of both Cartesian and (two separate) cylindrical coordinate systems, in an effort to focus the computational effort on areas around the borehole where temperature gradients, and as a result heat transfer rates, are highest. The initial development of this model is discussed, as well as revisions that make it more accurate. A basic validation is also presented, with further validation in the next chapter.

Chapter 5 presents a detailed validation of an existing ground heat exchanger model, as well as the new model developed in Chapter 4. Validation is done for four separate data sets from monitored ground source heat pump systems around the world. In addition to simply checking the accuracy of results, the issue of computation time is discussed, particularly in light of the more detailed multi-coordinate model. This chapter also delves into the issue of thermal short-circuiting in vertical ground heat exchangers, since the new model can directly account for this phenomenon while the existing model neglects it.

Chapter 6 explores the accuracy of two methods of designing vertical ground heat exchangers, namely a simulation-based design tool and the ASHRAE Handbook design equation. Multiple experimental data sets are used with the design methods to size VGHXs, utilizing experimental parameters and measured temperatures. The resulting sizes are compared to the actual installed

depths to gauge the accuracy of each method, and reasons for differences between the two methods are analyzed in depth.

Chapter 7 concludes by summarizing this work. General findings from each of the preceding chapters are discussed, and recommendations proffered for future work in simulating ground source heat pump systems.

CHAPTER II

CURRENT STATUS OF VERTICAL GROUND HEAT EXCHANGER SIMULATION

The idea of the ground source heat pump (GSHP), also known as a geothermal heat pump, can be traced back to a Swiss patent by Zoelly (1912). A typical ground source heat pump system will contain, at a bare minimum, a ground heat exchanger (GHX), one or more heat pumps, and a circulating pump. The ground loop heat exchanger can be oriented in either the horizontal or vertical direction, or coiled into a spiral shape. This review focuses on the vertical ground heat exchanger (VGHX). A VGHX consists of one or more boreholes; each borehole is drilled vertically to a depth of around 50-100m at a diameter around 4-6in, and filled with a standard-sized U-tube of nominal diameter from 3/4" to 1.5". While single U-tubes are the norm, double tubes and concentric tubes are also possible. The area between the tube and the borehole wall is typically filled with some form of bentonite grout, which can be thermally enhanced via the addition of silica. This practice, however, is less common in regions such as Sweden, which allow the boreholes to fill with ground water.

Because of the complex geometries involved, and due to the extreme range of relevant time constants (from a few minutes to multiple decades), VGHXs are designed by means of one of a number of methods; while these methods are frequently numerical in nature and require computer simulation, other, equation-based methods can also be utilized. In either case, these methods

require some sort of validation to prove that the can accurately predict system performance. This chapter details previous efforts in ground heat exchanger model validation, and outlines aspects of an "ideal" experimental validation.

No matter the method used in designing GHXs, simulation or not, all the physical phenomena in play cannot possibly be accounted for; assumptions must be made when dealing with systems of this complexity, and the simulations must focus on the most important elements. As the simulation of VGHXs has evolved, a set of assumptions has become prevalent. Witte (2012) explored the potential sources of error in performing thermal response tests to measure ground thermal conductivity and borehole resistance *in situ*; however, existing literature concerning the errors introduced in making these assumptions for simulations is scarce, at best. This chapter seeks to partially address this, by specifically identifying these assumptions, and the methods in which they are used.

2.1 History of Vertical Ground Heat Exchanger Simulation

2.1.1 Line Source and Cylinder Source Approximations

The simplest analytical model of a single borehole is the line source, first proposed by Kelvin (1884) and explicitly stated by Ingersoll et al. (1954). For an infinite line source in an infinite medium, Kelvin described the temperature in the surrounding medium as dependent on time, radial distance from the source, and the (constant) value of the heat flux from the source. In simplifying the problem to one dimension in the radial direction, Ingersoll et al. (1954) numerically computed integrals derived from Kelvin's work,

resulting in a table of values based on the Bessel function. For boreholes, assuming a constant flux and collapsing the entire borehole to a line approximates a system that can be modeled with the line source equation. However, this results in the individual effects of the pipe, grout, and fluid being lost, as the line is essentially a point in space extending down in the depth direction, with only single thermal resistance and capacitance terms. Additionally, since the line source is assumed to be of infinite length, any effects at the end of a finite source (such as the U-bend at the end of a typical borehole) cannot be assessed with this method. Finally, this approximation also assumes a uniform heat flux and non-interfering boreholes, so superposition both temporally and spatially is needed if multiple bores are being considered. The line source solution, then, takes the rate of heat input and ground thermal conductivity and, as a function of time and radial distance from the source, gives the change in temperature from an arbitrary reference state. In practice, this approach can be used in reverse for thermal response tests, as first described by Mogensen (1983). In a thermal response test, the rate of heat injection is known, while the temperature of the fluid circulating through the borehole is measured with time; by application of the line source solution, the thermal conductivity can be found indirectly via this temperature measurement.

Zeng et al. (2002) proposed an analytical solution to the line source of a finite length, *i.e.*, including end effects. This solution provides response factor terms akin to the "g-functions" put forth by Eskilson (1987) and discussed in the next section. The predominant difference between this expression and that based on Kelvin's work is that, since end effects are included, the finite line source tends to a steady-state temperature

solution at long time scales, while the infinite source goes to infinity. Lamarche and Beauchamp (2007) modified this technique and successfully compared it to numerical results for multiple boreholes from Eskilson and other authors.

Carslaw and Jaeger (1947) developed an analytical expression for the heat transfer in an infinite, homogeneous medium due to a constant heat flux from the surface of an infinite cylinder buried in the medium. Similar restrictions as with the line source apply when approximating a borehole as a cylinder source. Namely, the two halves of the U-tube, along with the working fluid and any grout or casing, fall inside the cylinder and are lumped together; thus, short-circuiting heat transfer between the upward and downward legs of the U-tube is by necessity neglected. Additionally, any thermal mass inside the borehole is neglected as well, meaning a steady-state thermal resistance term is needed to translate the wall temperature to a fluid temperature.

2.1.2 The "G-function" Approach

Simulation of vertical ground heat exchangers dates to the work of Eskilson (1987), who developed a set of computer programs for different aspects of the GHX design process, including dimensioning boreholes as well as determining heat rejection and extraction rates. For a borehole, the temperatures in the soil surrounding the borehole in response to a step change in heat input are computed as a function of time using a two-dimensional, transient finite difference scheme in a radial-axial coordinate system. Eskilson (1987) used the principles of superposition to determine the effects of multiple boreholes in combination over time. Superposition in space is possible since solutions to a linear partial differential equation—like the conduction equation—subject to varying boundary conditions may be added together to generate a solution for a linear

combination of those boundary conditions; while it is possible in time as a consequence of Duhamel's principle, which states that since the conduction equation is linear and inhomogeneous, it can be broken down into a set of homogeneous equations corresponding to discrete time intervals. These superposition computations lead to a set of discrete, non-dimensionalized time and temperature responses that depict the thermal behavior of a particular VGHX, as a function of the time and rate of heat input. Collectively, this set of response factors is termed the "g-function". Currently, there are a multitude of borefield sizes and configurations for which g-function data are available, ranging from lines of a few boreholes to fully-populated rectangular fields with upwards of 100 boreholes. Figure 2-1 shows the non-dimensional "g-function" response against non-dimensionalized time for a few different borehole configurations.

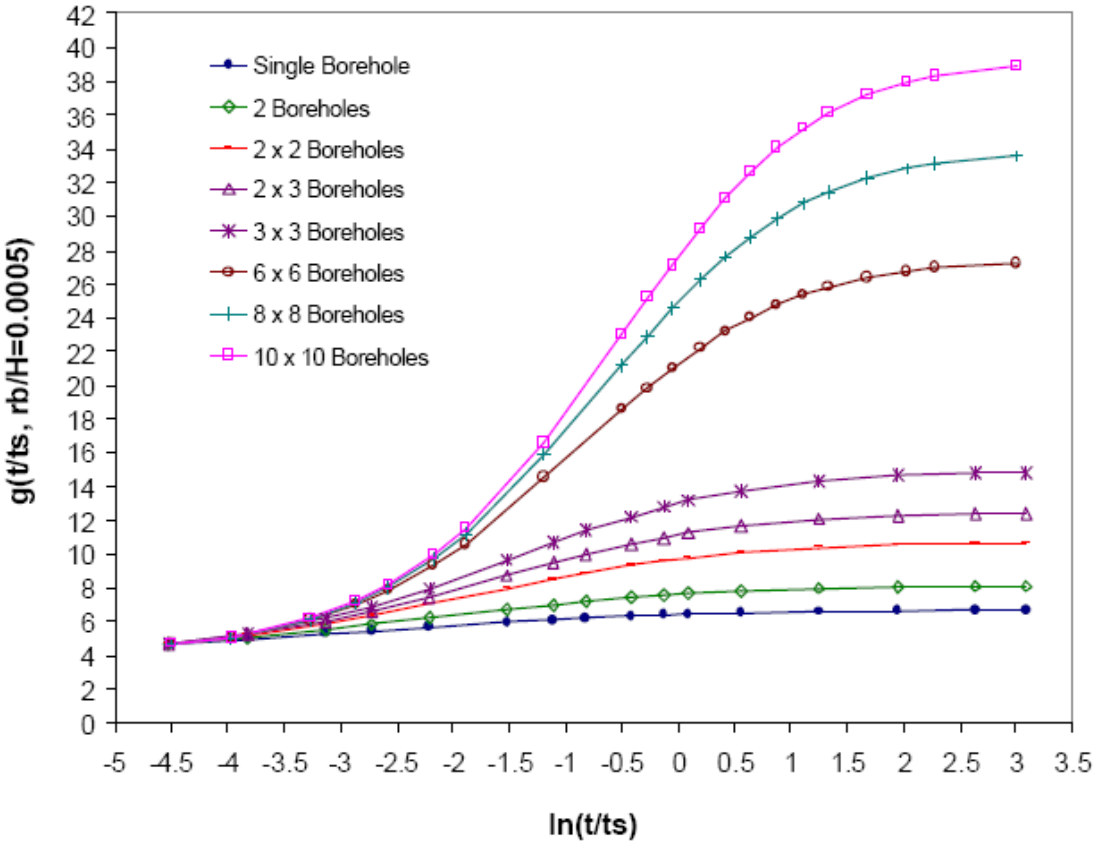

Figure 2-1: G-function temperature response factors for various borehole configurations (used with permission from Spitler [2000])

The determination of the g-function, as originally computed by Eskilson (1987), is restricted to time intervals greater than

$$t_s = \frac{H^2}{9\alpha} \tag{2-1}$$

Where t_s is the time scale, in s;

H is the depth of the borehole, in m; and

α is the thermal diffusivity of the soil, in m^2/s.

For practical depths and any reasonable soil, this time scale corresponds to anywhere from several hours to multiple days; for example, using a clay soil with diffusivity 1.24×10^{-4} m^2/s (Farouki, 1986) and a borehole 50 m deep, the time scale t_s is 2,250,000 s, or about 26 days. Obviously, many building simulations, including ground heat exchangers, are often performed on a daily or even an hourly basis, in order to account for peak load variations (Spitler 2000). Hellström and Sanner (1994) did expand Eskilson's g-function data, which was only for times longer than a couple of weeks, to shorter times using extrapolation of a line source solution, but this is still an insufficient level of detail to accurately determine the effects of single-hour peak loads.

For times shorter than Eskilson's time scale t_s, Xu and Spitler (2006) used a one-dimensional finite volume model to calculate responses for very short times that can be seamlessly combined with the longer time step g-function data. Using volumes carefully chosen so as to preserve both the thermal masses of grout and fluid, as well as the thermal resistance of the borehole, this method matches a more accurate two-dimensional borehole model while maintaining a high degree of computational efficiency, as shown by Xu (2007). Cullin (2008) used this short time

step technique to determine the best way to represent hourly loads on a VGHX when using a monthly simulation.

There are presently a wide variety of software design tools available, many of which utilize the g-function methodology. These tools include standalone programs such as GLHEPRO (Spitler, 2000; Cullin, 2008) and EED/Earth Energy Designer (Hellström and Sanner, 1994; Blomberg et al., 2008), as well as component models within larger building energy simulation programs such as EnergyPlus (Fisher et al., 2006).

2.1.3 Other Design Methods

Whilst the g-function approach is certainly a fairly common method for simulating vertical GHX systems, many other methods are also available. For example, the method currently promoted in official ASHRAE literature is that of Kavanaugh and Rafferty (1997), which itself was originally presented by Kavanaugh (1992). Kavanaugh and Rafferty base their design on the analytic solution for the temperature of a buried cylinder. This is used to determine the effective thermal resistance of the ground to heat pulses of varied durations ranging from hourly to annually. This equation-based method independently solves for two design lengths: one that satisfies the peak cooling load, and a second that satisfies the peak heating load; in other methods, the size is determined iteratively so that user-proscribed temperature limits are adhered to. Additionally, this method only models a single year, rather than a multi-year life cycle. To account for multiple years of operation, a temperature penalty is imposed based on a combination of load profile, borefield size, and borehole separation.

Fossa (2011) provides a thorough derivation of the temperature penalty term used in the Kavanaugh and Rafferty approach (1997). Using temporal superposition of hourly, monthly, and

yearly heat pulses, Fossa expressed the temperature penalty as a function of Fourier number, borehole length, and dimensionless response factors, thus demonstrating the iterative nature of the Kavanaugh and Rafferty scheme. Then, using spatial superposition and regression of previous finite line source solution data, Fossa generated a new expression for the average fluid temperature response that can be explicitly solved for the required ground heat exchanger length. However, recent work (Bernier et al. 2008) has called into question the accuracy of these tabulated penalties, as the authors were unable to reproduce the values in the table.

Hellström (1989) developed the duct ground heat storage model, commonly referred to as the DST model. The DST model uses three calculation domains and superimposes their solutions to determine soil temperatures. The local steady-flux heat transfer is computed analytically for the nearest pipe, while numerical models are used to compute both the short-time local heat transfer around the boreholes, as well as the global heat transfer between the soil "duct" volume and the far-field. This model has been implemented in the commercially-available TRNSYS simulation environment (SEL, 2012).

Bernier et al. (2004) calculated the temperature difference between the wall of the borehole and the ground for one borehole using the cylinder source model, with an equivalent steady state thermal resistance determined using the method of Zeng et al. (2003). Thermal response factors (Sheriff and Bernier, 2008), which are computed using the finite line source method, are then applied to account for the thermal interference between boreholes, in order to find the average temperature change at the borehole wall.

Cui et al. (2007) developed a two-part simulation of a vertical borehole heat exchanger. The borehole region, which includes the U-tube, working fluid, and grout, is modeled numerically with a quasi-3D approach that accounts for varying fluid temperature along the borehole depth,

including the upward- and downward-flowing sections of the U-tube. Outside the borehole, soil temperatures are modeled analytically with as a finite line source, and the two simulation domains are linked at the borehole wall. Cui et al. (2007) use superposition is space to account for multiple boreholes, and superposition in time to determine the effects of sequential load application.

Katsura et al. (2006) and Nagano et al. (2006) describe a design tool that approximates the cylinder source approach. This method may be capable of determining thermal interactions between boreholes of arbitrary configuration, even if they are not identical, so long as the boreholes are far enough apart. In this tool, the temperature of the fluid in the ground loop as a whole is determined with a flow rate weighted average of the individual boreholes. However, whether this tool is practically useful is unclear. Unlike many other simulation tools currently in use, this tool utilizes hourly loads; the authors quote a 40 second computation time for a two-year simulation of an unspecified number of boreholes (that may or may not have been identical). Since simulations of ground heat exchanger systems are frequently performed for at least 10, and sometimes more than 20, years, and iteration is often required to determine adequate sizing, it is easy to anticipate that computation times for practical applications to be unacceptable for a designer, though these methods are certainly still of research interest at the very least.

Picard and Helsen (2014) created a "hybrid step-response model" in the Modelica environment that is capable of analyzing both short- and long-term behavior of a borehole heat exchanger system, based on the analytical work of Classson and Javed (2011). This model is quoted as being much faster computationally than other methods within the Modelica environment. However, it loses accuracy in comparison to the g-function approach when the borefield becomes compatct.

2.1.4 Three-Dimensional Modeling

Although such techniques are computationally unsuitable for design purposes, three-dimensional modeling of borehole heat exchangers has been explored by several authors. He (2011) created a dynamic 3D finite volume model in a generalized multi-block solver to simulate the heat transfer in and around boreholes. Using a boundary-fitted mesh generation scheme to preserve the complex geometry of a borehole, this model provides an accurate result when compared to experimental data (He 2011; Rees and He 2013). Though computationally inefficient with a finer grid, this finite volume model can capture effects, such as the fluid transport delay in the piping, which are impossible to compute with a two-dimensional approach. As a means of improving computational time, the authors do, however, propose a two-dimensional approximation.

Kim et al. (2011) propose splitting the computation domain into three sub-regions: the working fluid, the near-borehole area, and the greater soil field. Each region experiences a different scale of transient behavior, depending upon the speed of reaction to a change in boundary conditions. Kim et al. decompose the soil volume bi-directionally—into concentric horizontal zones so as to apply different time steps when possible, and into equally-sized vertical slices to simplify boundary conditions in that direction. Then, the conduction equation for this system is converted to state form, and by identifying the dominant mode or modes of heat transfer in each sub-zone created by the decomposition step, the state model is reduced in complexity. This model was validated against experimental data, with results showing good matches in both fluid and borehole wall temperatures along the depth of the pipe, and a reduction in computation time by a factor of 27 over a non-reduced model for a single horizontal slice.

Overall, there are many methods available for simulating vertical ground heat exchangers. Often, they take advantage of phenomena such as superposition to make the solution more tractable and computationally feasible. While many of these methods have been experimentally validated to some extent, there has, to date, not been an extensive validation study performed on the simulation tools; such a study could lead to better understanding of how simulations perform in special cases such as low flow or long-term heat buildup (or drawdown) in the ground. This, in turn, could answer questions posed by some in the industry as to why GHX design tools often overpredict system requirements.

2.2 Validation and Testing of GHX Simulation Tools

The previous section shows that there are quite a few models and model variations used for the design of ground heat exchanger systems. There should, then, be some standard method of analysis and testing of these models in order to characterize their accuracy and performance. Testing GHX models can be broken down into two categories: experimental validation, and intermodel comparison. However, the composite of the validation and testing efforts available in current literature clearly shows the need for a standardized procedure for analyzing these models, and the need for models to be checked against multiple data sets with a range of behaviors.

2.2.1 Experimental Validation of GHX Models

Ground heat exchanger models presented in the literature are typically presented with some sort of experimental validation, based on data collected from some sort of test setup. Gentry (2007) compared the g-function model, using hourly and sub-hourly time steps, to experimental data collected from a hybrid ground-source heat pump test facility (Hern, 2004) located at Oklahoma State University. Cullin (2008) validated the same g-function model, integrated into a design tool

and using a monthly time step, against the same data set. Both authors found that the model performed reasonably well, although Gentry (2007) only analyzed one cooling season, and Cullin (2008) identified issues with prediction of peak values when the monthly time step is used.

Pertzborn et al. (2011) present a validation of the duct storage ("DST") model using experimental data from two separate facilities. The model predicted loop temperatures acceptably well for the first data set, but only after low flow data was discarded. Due to both the model itself and the experimental design, the DST model overpredicted the heat transfer to the GHX when flows were low. For the second field, the model failed to accurately predict loop temperatures using thermal property data measured prior to the start of the experiment. Since five years had passed prior to collection of the data, during which time the system was fully operational and running, ground properties changed substantially during this time. A better match was made when the soil conductivity and heat capacity were calibrated to provide a good fit.

2.2.2 Intermodel Comparison of GHX Models

A second method by which to analyze ground heat exchanger models is to compare them to one another, utilizing either a single experimental data set or a common theoretical test such as a constant heat pulse response. Shonder et al. compared five common design tools for both residential (1996) and commercial (2000) applications, each using a different core simulation algorithm. The authors found differences in recommended design length of 27% for a simulated residence (Shonder et al., 1996); using updated design tools for the commercial simulations, sizes were within 16% for a heating-dominated climate, and about half of that for a cooling-dominated climate. Spitler et al. (2009) found similar differences among common design tools in comparing results to experimental data from a three-borehole system, and to a simulated system consisting of

196 boreholes. In this case, however, several of the simulation tools had a common algorithm, yet still produced varied results.

2.2.3 Standardization of GHX Model Testing

Because of the varying conditions inherent in an experimental GHX facility—number, depth, and spacing of boreholes; climate; load balance; thermal properties; type and frequency of data gathered—it can be hard to draw specific conclusions from validation of one model against one set of experimental data. Yavuzturk and Spitler (2001) identify several key parameters of a high-quality experimental data set:

- In-situ measurement of ground thermal properties independent of the experiment. This ensures the best possible depiction of the borehole surroundings.
- Calibrated measurement of, at the very least, GHX entering and exiting fluid temperatures as well as borefield flow rate. This ensures an accurate representation of the heat extracted from or rejected to the ground.
- Continuous data collection, uninterrupted from the start of system operation. This ensures a continuous data set free from assumptions of behavior during times without measurements.
- An accurate characterization of the borehole, including geometry as well as grout and fluid properties. This ensures heat transfer inside the borehole wall can be correctly modeled.

While Yavuzturk and Spitler (2001) provide a sort of checklist for how the data is collected, as well as the parameters necessary for a successful comparison, Bertanoglio et al. (2012) propose several types of test cases. Testing of heat transfer local to the borehole can be done with, for instance a constant heat rejection case. This has the advantage of, at least for short durations,

being very similar to an analytical line source. Second, long-term effects should be tested with a cyclic loading. Ideally, this would include an appreciable heat buildup/drawdown over time; while this is not desirable for a real-world system, the simulation must be able to accurately predict the behavior of both good and bad designs. Finally, borehole interaction should be examined by testing the model's performance against data from a multiple-borehole system.

At present, there is a paucity of experimental data sets that meet the definition of high-quality established above. Coupled with the need to test the same model against multiple data sets to establish an overall picture of performance, there has consequently not been a thorough study of simulation tool results that takes all of this into account. This is further confounded by some of the behaviors that are neglected (or, worse, ignored completely) in the typical analysis of ground heat exchangers.

2.3 Typical Assumptions Made

In simulating (and therefore also, frequently, in designing) vertical ground heat exchangers, certain assumptions are made during the process. This may be by design—for instance, if an available simulation tool is incapable of modeling a particular phenomena, such as freezing or moisture transport, it is neglected. However, these assumptions may also be made implicitly and without realization, as the engineer selects a method of design with a set of assumptions that are either taken for granted or, perhaps, not made clear at all. At times, published sources occasionally give contradictory statements as to the impact of some of these effects.

To date, very little effort has been made in the literature to categorize and quantify these assumptions. What follows, then, are assumptions typically made, explicitly or implicitly, that

may potentially have an impact on the system performance, along with the methods that make these assumptions. It should be noted that, as a confounding issue, these assumptions may not even be stated in the literature that presents each individual method!

2.3.1 "Average" Fluid Temperature

A typical simulation of a ground heat exchanger will determine what is named the "average" fluid temperature in the loop at each time step; then, temperatures entering and exiting the ground loop are computed based on this value. The use of the term "average" can be a bit misleading, however, as it is frequently used in multiple connotations, often without clarification. This average can be a temporal value, representing the mean value over the entirety of the previous time step. It can also be a spatial average of the mass of fluid in the loop at a given instant (the end of a time step, usually).

The typical approach in computing the temperatures entering (T_{in}) and exiting (T_{out}) the ground loop is to assume that the mean fluid temperature (T_m) is halfway between the two; that is,

$$T_m = \frac{T_{in} + T_{out}}{2} \tag{2-2}$$

Knowing the value of the heat transfer rate across borehole, then, the GHX inlet and outlet temperatures may be computed simply. For the analysis of a single borehole, this phenomenon is perhaps less important, as that lone heat exchanger is the only heat source/sink impacting the ground. As more boreholes are added and they start to interact, assuming a linear temperature profile in this manner becomes unrealistic. The soil temperatures start to change near the boreholes, and since the inlet and outlet temperatures will not be equal, the radial temperature profile around any arbitrary borehole will not be symmetrical. Thus, it perhaps becomes necessary to find a more accurate way of analyzing the temperature of the fluid as it transits. Some work has been done in this regard for *in situ* thermal response testing of a single borehole

(Beier, 2011; Beier et al., 2012), where the vertical temperature profile is found as part of quasi-steady-state modeling of the borehole. However, this study was only for a single borehole, and the overall impact on a multiple borehole system over longer time scales has yet to be assessed. Additionally, assuming a linear temperature profile can be problematic for ground heat exchangers with long residence times, such as would be encountered with extremely large pipe lengths or low flow rates—it is numerically possible, though physically unrealistic, for the borehole return temperature to drop below the borehole wall temperature. Obviously this behavior may lead to inaccurate results in these circumstances, so another, more accurate formulation for the average fluid temperature may be necessary.

Marcotte and Pasquier (2008) assert that assuming a constant heat flux along the borehole wall in order to compute the inlet and exit temperatures will lead to an overestimation of the borehole thermal resistance when performing a thermal response test. They propose a power-based formulation for the average fluid temperature, namely

$$\left|\Delta T_m\right| = \lim_{p \to -1} \frac{p\left(\left|\Delta T_{in}\right|^{p+1} - \left|\Delta T_{out}\right|^{p+1}\right)}{(1+p)\left(\left|\Delta T_{in}\right|^{p} - \left|\Delta T_{out}\right|^{p}\right)} \tag{2-3}$$

The delta terms in the above equation are simply the differences between the given temperatures and the undisturbed ground temperature. Marcotte and Pasquier (2008) denote this the "*p*-linear" average; their value for $p \to -1$ was determined by best matching the borehole temperature profile from a 3D numerical model. Interestingly, this formula collapses to other familiar means for different values of *p*: it becomes the standard arithmetic mean for $p = 1$, the harmonic mean for $p = -2$, the geometric mean as $p \to -½$, and the logarithmic mean (the same used in the LMTD method in heat transfer applications) as $p \to 0$. While this *p*-linear average may improve determination of the borehole resistance in a thermal response test, problems may still arise under specific conditions as before.

2.3.2 Nonparticipating Horizontal Piping

In a vertical ground heat exchanger, particularly one with multiple boreholes, not all of the piping will be vertical. Some piping—connections between boreholes, header runs, etc.—will by necessity be horizontal. As this horizontal piping is placed in shallow depths below the ground surface, these pipes will likely have some interaction with the outside weather conditions. Since the total amount of horizontal piping may account for up to 10% of the total installed length, it is easy to see that this horizontal piping may be influential in both the short- and long-term performance of a VGHX. In the short term, particularly warm or cool days may increase or decrease, respectively, the temperature of the fluid in the loop, while for longer periods, it may be the case that the presence of horizontal piping serves to dampen long-term temperature change in the soil. Despite all of this, and that no existing published method considers this behavior, the influence of horizontal piping on a VGHX has not been quantified in the literature: The horizontal piping is assumed to be "nonparticipating", in terms of heat transfer.

2.3.3 Isothermal Ground Surface and Uniform Borehole Heat Flux

In computing the first sets of g-functions, Eskilson (1987) considered all boreholes to be identical. That is, each borehole had a uniform heat flux applied to it, and the boundary conditions for each were the same. In deriving the g-function approach, an isothermal ground surface boundary condition was applied; thus each borehole in a heat exchanger system consisting of multiple bores is essentially identical, with the only differences occurring due to spatial interference.

Malayappan and Spitler (2013) studied the potential effects, with regards to sizing error, of assuming a uniform heat flux between boreholes. They compared g-functions and resulting

borefield sizes between the numerically-derived g-functions of Eskilson (1987) and the analytically-derived g-functions determined by Claesson and Javed (2011). Malayappan and Spitler (2013) found that the analytical approach, with an explicit assumption of uniform heat flux, oversized systems by around 5-6%, though the exact figure is dependent on borehole spacing, depth, and configuration, as well as the building load profile.

To date, the impact of an isothermal upper boundary condition has so far not been quantified. While this assumption is probably not that significant, especially since the top layer of the borehole is considered inactive in the generation of the g-function, it may have some influence when coupled with other assumptions, particularly the neglect of horizontal piping.

2.3.4 Inactive Top Layer of Borehole

Eskilson (1987) considered a short portion of the vertical installation at the top of the borehole to be "inactive", *i.e.* not participating in heat transfer. The quoted borehole depth, then, extends below this distance. In deriving g-function data, Eskilson used typical Swedish geologic parameters, which include an upper soil layer of overburden with lower conductivity; this layer functions more or less as an insulator since the deeper soil has much higher conductivity, and so was neglected in Eskilson's analysis. This inactive top layer would, in an installed system, include any inter-borehole connective piping or runs to and from piping headers, which may or may not be insulated. Thus, the degree to which this layer is actually inactive cannot be readily assessed without further study. Practically, neglecting this distance mitigates the impact of outdoor weather conditions, such as solar radiation and convection due to wind, that may provide significant heat transfer at the surface. While this assumption was necessary as Eskilson developed the g-function expression based on what was then available, again, the degree to which it is accurate merits some investigation.

Since this assumption is used by Eskilson (1987), the methods that rely on the g-function will be affected by this assumption. This includes the VGHX component model within EnergyPlus (Fisher et al. 2006), as well as commonly-used standalone programs such as GLHEPRO (Spitler 2000; Cullin 2008) and EED/Earth Energy Designer (Hellström and Sanner 1994; Blomberg et al. 2008). Furthermore, since this assumption is very closely tied to the behavior of the heat exchanger at and near the ground surface, it will be strongly coupled to other surface-related assumptions, including the effect of horizontal connective piping and an isothermal ground surface.

2.3.5 Moisture Migration

The movement, or migration, of water through the soil could potentially initiate heat transfer via advection. This could occur in several ways: horizontal flow due to spatial differences in material properties in the soil, vertical flow due to differences in the height of the water table or presence of aquifers, and evaporation of moisture from the ground surface. Of all the typical assumptions made in simulating ground heat exchangers, the neglect of unsaturated moisture transport is perhaps the most commonly made, and one of the only assumptions to have some study in the published literature.

Chiasson et al. (2000) numerically investigated the effect of horizontal groundwater flow on the long-term behavior of ground heat exchangers, as well on the thermal response tests frequently used to measure ground thermal conductivity. Chiasson et al. found that for most systems, horizontal groundwater flow is not a significant factor; the only cases for which horizontal flow is likely to significantly affect fluid temperatures in boreholes is when the soil consists of mostly porous materials, such as sands, gravels, and karst limestones.

As for the effect of vertical groundwater flow, the literature provides perhaps contradictory viewpoints. In the ASHRAE design guide, Kavanaugh and Rafferty (1997) claim:

> "Groundwater movement has a large impact upon the long-term temperature change in a densely packed ground coil. The amount of impact has not been thoroughly studied."

That work cites Ingersoll et al. (1954), who themselves state:

> "When considering the influence of one pipe on another as in neighboring loops, the effect of moisture migration will be secondary."

Whether the effect of vertical flow is "large" or "secondary" is unclear from the literature, though a first-order assessment of the relevant physical parameters may prove insightful.

According to Ingersoll et al. (1954), the effect of moisture migration becomes significant—the heat transfer rate increases by at least 20%—when the groundwater velocity exceeds 0.01 ft/hr (0.073 m/day). From Darcy's Law,

$$v_{gw} = \frac{k_{hyd} \frac{\partial H_{gw}}{\partial s}}{\varphi} \tag{2-4}$$

Where:

v_{gw} is the groundwater velocity, in m/day;

k_{hyd} is the hydraulic conductivity, in m/day;

φ is the soil porosity, unitless; and

$\frac{\partial H_{gw}}{\partial s}$ is the rate of change of the height of the groundwater table with respect to distance along a line normal to the local elevation contour, in m/m.

Using typical ground porosities from Fetter (1994), and hydraulic conductivity values tabulated by Freeze and Cherry (1979), the necessary slopes of the water table for different soil conditions may be computed. These values are listed in Table 2-1. As the table shows, only for soils such as sand, gravel, or karst limestones does the slope resemble a value that could realistically be expected. For other soil types, vertical water flow is extremely unlikely to be a significant factor at all. This mirrors the results obtained by Chiasson et al. (2000) for horizontal groundwater flow.

Table 2-1: Vertical groundwater flow data

Soil type	Porosity	Hyd. Cond., m/day	Water table slope, m/m
Sand, gravel, etc.	30%	1E-02	2.196
Clay, silt, etc.	50%	1E-06	36600
Harder/rocky soils	15%	1E-03	10.98

A secondary means of moisture movement in a ground heat exchanger system is the evaporation of moisture at the ground surface. Moisture can be lost to the atmosphere as plants growing at the surface absorb it from the soil, transpire it to their leaves, and lose it to the air; this combined process is known as evapotranspiration. Evapotranspiration serves as a heat transfer mechanism as the latent heat of vaporization of water is transferred out of the soil, and also achieves a lesser, secondary effect as it changes the moisture content, and thus the thermal properties (*i.e.*, the conductivity and heat capacity) of the soil. Xing (2010) explored the effects of evapotranspiration in a foundation heat exchanger system—a horizontal ground heat exchanger placed in a building excavation such that it interacts with a basement space. For the foundation heat exchanger system, the inclusion of evapotranspiration can yield a difference in loop temperatures of as much as 20 °C; essentially, this corresponds to the difference between a ground surface covered in medium grass versus a paved concrete lot. Obviously, since the vast majority of the piping in a vertical ground heat exchanger system is far enough below the surface

to be insulated from this effect, the impact of evapotranspiration on a VGHX system will be lessened. Nevertheless, it may still be influential, and has not been explored in detail in the literature.

Xu and Spitler (2011) developed and experimentally validated a numerical ground temperature model that includes the effects of vertical unsaturated transport, soil freezing, and surface snow cover, and that utilizes hourly meteorological data. They concluded that, when hourly weather data is available for a non-urban site, modeling moisture effects produces a "slight" increase in the accuracy of temperature prediction, but increases computation time by an order of magnitude.

2.3.6 Other Assumptions

Several other assumptions may also merit some investigation to determine their exact effects on the accuracy in simulating borehole heat exchangers. First, the soil is almost universally considered to be a single, homogeneous layer; in reality, the soil profile around a vertical borehole will usually contain some combination of a layer of topsoil, one or more layers of finer-grained material perhaps interspersed with larger materials like gravel, and eventually bedrock. Sutton et al. (2002) implemented a multi-layer model based on the analytical solution to the infinite cylinder source; however, validation was only performed qualitatively as no suitable experimental data was available. With each layer of material having its own thermal properties, the degree to which this influences simulation results is still unknown.

In most locations, the temperature in the soil will vary with depth at a roughly constant rate below a depth sufficient enough to completely dampen surface effects. This is termed the geothermal gradient. When borehole heat exchangers are analyzed, either via analytical equations such as the line source—infinite or finite—or by numerical means such as tools based on the g-function

approach, the initial soil temperature profile around the borehole is assumed to be constant. Whether the geothermal gradient contributes any appreciable effect to the overall performance of a borehole system remains to be seen.

Another factor that may contribute to inaccuracies in results is the assumption of an instantaneous change in temperature along the entirety of the borehole heat exchanger in response to a heat input. In reality, only that region near the source will change immediately, as the working fluid will take some time to circulate through the system. How much time is a function of the size of the system and the circulating pump. Lee (2013) has done some exploratory work into the effects of this transport delay, but a fuller study may prove insightful.

Finally, while Xu and Spitler (2011) explored the possibility of simulating soil freezing in determining temperatures, the effects of freezing both in the soil and in/around the borehole have yet to be quantified.

2.4 Need for Further Analysis

Current models of vertical ground heat exchangers have their limitations, whether by design to narrow their focus or improve computation time, or by implicitly assuming certain conditions apply that are not completely accurate. Several of these limitations have been set forth by Spitler and Bernier (2011) as definite items for future study. While it is definitely possible that the quantitative impact of one or more of these assumptions negate each other, it is also feasible that, by making some of these assumptions, a systematic error could be introduced into designs that either overpredicts or underpredicts the long term behavior of the system. Therefore, it is clear that some fairly detailed study is warranted to analyze the influence that each of these

assumptions has on the performance of a VGHX-based system, in order to quantify the assumptions and determine whether or not they are actually warranted. Any model used to analyze a VGHX without these assumptions in place would by necessity be of sufficient complexity that it would not be desirable for designing these systems. Rather, checking the validity of these assumptions would be done in an effort to examine the accuracy of existing models, and to identify places where the existing models can improve.

Analyzing these assumptions will require a model with flexibility in both geometry and boundary conditions. To account for things like the variation of temperature along the depth of a borehole, the model will also need to have the capacity to analyze heat transfer in all three dimensions; this points to the need for a finite volume approach that is robust enough to handle the complexities of a borehole, while focusing the computational effort on the area around the borehole where the temperature gradients will be highest. In order to facilitate simple comparisons and possible future adaptation to existing models should the g-functions, as currently constructed, be found lacking, casting simulation results that include these phenomena in the same manner as the g-function—as responses to uniform heat flux pulses—may provide the greatest insight.

CHAPTER III

PRELIMINARY INVESTIGATION OF THE EFFECT OF HORIZONTAL PIPING ON THE PERFORMANCE OF A VERTICAL GROUND HEAT EXCHANGER SYSTEM

Note: This chapter has been presented as a technical paper (Cullin et al., 2013) at the 2013 ASHRAE Conference in Denver CO, 22-26 June 2013.

3.1 Introduction and Background

Ground source heat pump (GSHP) systems are utilized frequently in "sustainable" heating and cooling systems worldwide, with an estimated total heating capacity of 35 GW (118 billion BTU/hr) installed across at least 3.0 million units in residential, commercial, and industrial settings (Lund 2011). For any heating or cooling system design, it is important to have an accurate procedure for sizing the equipment, so that the system may be adequately sized. A system that is undersized may lead to equipment failure, while an oversized system is often inefficient and unnecessarily expensive. This is particularly critical for sizing vertical ground heat exchangers (VGHXs) used in GSHP systems, where the cost of the ground heat exchanger represents a significant increase in first cost compared to more conventional systems.

Also, unlike conventional systems that are often sized based on a peak cooling load and/or peak heating load, the very long time constant of the ground necessitates accounting for heat transfer to/from the ground over a period of many years. It is possible for maximum heat pump entering fluid temperatures (EFT) to rise from year to year over the life of the system, for buildings that annually reject more heat than they extract. Conversely, buildings that annually extract more heat than they reject have the possibility of minimum heat pump EFT falling from year to year. At least two approaches have been taken to account for this phenomenon. Kavanaugh and Rafferty (1997) describe a simple procedure that uses a table of empirical factors to estimate the long-term change in ground field temperature; the basis of these factors is not provided. The other approach is to use a simulation of the VGHX with ground thermal properties, building loads, heat pump performance characteristics, and ground heat exchanger design as inputs. The simulation predicts the evolution of temperature with time, and the size of the ground heat exchanger is adjusted automatically to meet user-specified minimum and maximum heat pump EFTs. The simulation of vertical ground heat exchangers is discussed in detail in the next section.

Regardless of which approach is used, there are certain approximations that are inherent in the approach. For the simulation approach, these approximations include pure conduction heat transfer (no groundwater flow or unsaturated moisture transport), uniform ground thermal properties, an upper surface boundary temperature equivalent to the annual average ground temperature, and consideration of heat transfer to/from the VGHX only—losses or gains from the horizontal distribution piping are neglected. Although the basis of the long-term temperature change factors is not clear, the simplified procedure of Kavanaugh and Rafferty (1997) is believed to be derived using all of the same assumptions.

In recent years, there has been some controversy within the cognizant ASHRAE Technical Committee–TC 6.8–Geothermal Heat Pump and Energy Recovery Applications, as to whether or

not some of these assumptions may lead to the simulation approach overpredicting long-term heat pump EFT rise or fall. In fact, this goes back some years; accompanying the long-term temperature change factor table in the Kavanaugh and Rafferty (1997) reference is this statement:

> "The values in this table represent worst-case scenarios, and the temperature change will usually be mitigated by groundwater recharge (vertical flow), groundwater movement (horizontal flow) and evaporation (and condensation) of water in the soil."

It is certainly the case that each of these phenomena, if present, will mitigate the long-term temperature change to some degree. Chiasson et al. (2000) numerically investigated the effect of horizontal groundwater flow on both the thermal response tests used to measure ground thermal conductivity, as well as on the long-term performance of ground heat exchangers. That work suggests that horizontal groundwater flow is only likely to significantly affect borehole temperatures in sands, gravels, and karst limestones. The other effects have not been quantified in the published literature.

This chapter, though, examines one of the other assumptions – namely, neglecting heat transfer to and from the horizontal piping. The effects of this assumption have not, to date, been reported in the literature, despite the fact that horizontal piping can amount to more than 10% of the total installed vertical length. Obviously, this could be expected to have some effect on system behavior. To examine this effect, this work analyzes, as a first approximation, a VGHX and a horizontal ground heat exchanger (HGHX) coupled in series, with no thermal interference (via conduction heat transfer) between them. This will provide an upper-end estimate for the effect of horizontal piping on the performance of a VGHX system.

3.2 Methodology

To determine the effect of horizontal piping on a vertical borehole system, simulations of both a VGHX and a HGHX are needed. Additionally, two different buildings, each placed in two locations, were chosen to get an idea of the influence of horizontal piping when considering system size and dominant mode of operation of the system.

3.2.1 Simulation of Vertical Ground Heat Exchangers

Numerical simulations of vertical boreholes have been performed since the work of Eskilson (1987), who computed response functions ("g-functions") for specific borefield geometries based on superposition of a two-dimensional, radial-axial simulation of a single borehole. This approach has been improved to account for behavior at short time steps (Yavuzturk and Spitler, 1999) and a variable convective resistance inside the pipe (Xu and Spitler, 2006). The general g-function method has since been utilized in a number of design tools (Hellström and Sanner, 2000; Spitler 2000), as well as more general energy simulation tools such as EnergyPlus (Fisher et al., 2006) and eQUEST (Liu, 2008). Key assumptions in this method include consideration of conduction as the sole method of heat transfer, no header piping, and no direct consideration of moisture transfer in the soil (Eskilson, 1987), although Kavanaugh and Rafferty (1997) propose shortening the sizing period in their equation-based design method when moisture transfer may become a factor.

The g-function model, as implemented in a design tool, has been validated by Cullin (2008) for a three-borehole system. Eighteen months of experimental data from a hybrid ground source heat pump test facility in Stillwater, Oklahoma, were used in the validation; using measured heat extraction/rejection rates, the predicted heat pump end-of-month entering fluid temperatures were

typically within 1°C (1.8°F) of the experimental values. Several sources of error were analyzed, including a mismatch between experimental operation and the constant behavior typically assumed in a simulation. In addition, for simulations using a monthly time step and monthly total/monthly peak load profiles, a single peak duration may not be appropriate for any given simulation. Shoulder seasons may also introduce some error as heat pumps switch between heating and cooling modes within a single month. Nevertheless, predictions of annual maximum and minimum heat pump EFTs were within 3°C (5°F) despite these issues, with the larger differences due to these reasons.

Other VGHX simulation techniques do not use the g-function approach. Hellström (1989) developed a "duct ground heat storage" (DST) model that superimposes numerically-computed transient heat transfer solutions between the storage volume and far-field, as well as around the boreholes on a short time scale, with the analytically-determined steady-flux heat transfer solution around the nearest pipe. Another simulation software combines a cylinder source model around a single borehole (Bernier et al., 2004) with thermal response factors generated with a finite line source method (Sheriff and Bernier, 2008). Cui et al. (2007) created a VGHX simulation coupling an analytical finite line source solution outside the borehole with a quasi-three-dimensional model inside the borehole to determine the temperature of each individual borehole.

For this work, the g-function approach as enhanced by Xu and Spitler (2006) is used. This model was selected for its computational accuracy, as the design tool (Spitler 2000) in which it is implemented has been validated against experimental data (Cullin 2008) as discussed above. The EnergyPlus model (Fisher et al., 2006) utilizes g-functions which can be generated by this design tool, and has itself been verified as part of general EnergyPlus development (U.S. Department of Energy, 2012).

3.2.2 Simulation of Horizontal Ground Heat Exchangers

Horizontal heat exchangers have been modeled with limited flexibility by Mei (1988) and Piechowski (1999). Mei (1988) utilized a radial coordinate system surrounding either one or two pipes in the domain to calculate the temperature response of the heat exchanger. The approach relies on a far-field boundary condition imposed at the radial coordinate system boundary, without a detailed surface heat balance. Piechowski (1999) utilized a dual coordinate system approach to create an efficient numerical mesh. A Cartesian mesh is employed in a 3-D soil region with specific cells containing a radial mesh within. The radial system consists of, from outside-in, a series of soil cells, then the pipe cross section, and finally the fluid cross section. This methodology requires an interface between the two coordinate systems, but results in an efficient approach to localize computational effort in the near-pipe region, where thermal activity is expected to be highest.

A new model for horizontal ground heat exchangers based on this dual coordinate system was developed by Spitler et al. (2011), and also described by Hughes and Im (2012). Enhancements to the original approach include the ability to include any number of pipes in the domain, and using a flow-wise solution algorithm to simulate entire piping circuits within the domain. In this way, since each pipe is represented by an individual radial coordinate region within the larger Cartesian domain, interaction between pipes is considered. Additional boundary conditions were implemented to allow the ground model to tightly integrate with the zone heat balance algorithms in the building simulation program EnergyPlus (U.S. Department of Energy 2012). The surface heat balance was modified to include all essential heat transfer mechanisms, including convection to the outdoor air, conduction to the soil, environmental radiation (both long- and short-wave), and evapotranspiration. The evapotranspiration model is based on the standardized equation

developed by Walter et al. (2005). In addition, freezing in the soil, both at the ground surface and, potentially, around the heat exchanger piping, is considered. The undisturbed ground temperature at any particular depth is set with the Kusuda and Achenbach (1965) model, which uses an exponentially decaying sinusoid to estimate the seasonal penetration of heat from the surface; this model is used to update the far-field boundary at each time step.

The HGHX model was validated analytically (Hughes and Im 2012) using idealized boundary conditions and constant thermal properties to evaluate the model using a line source technique. The numerical model agreed with a high degree of accuracy to this analytic solution. The model was then validated experimentally using data from a foundation heat exchanger test site near Oak Ridge, Tennessee; a foundation heat exchanger is simply an HGHX installed near a basement wall, typically laid in the excavated foundation during building construction. The model predicted system temperatures with an annual mean bias error of 1.3°C (2.3°F), and predicted basement wall heat flux with an annual mean bias error of 1.1 W/m^2 (0.35 $BTU/hr\text{-}ft^2$).

3.2.3 Buildings and Locations

Two buildings and two locations were chosen for a small-scale study. One building is a house, while the other is an office building; these particular buildings were chosen as they provide reasonable loads for both a small residential-scale borefield, as well as a rather large commercial-scale borefield.

3.2.3.1 House

The house used in this study is a single-family, $100m^2$ ($1076ft^2$) dwelling, modeled in EnergyPlus (Crawley et al. 2001). Glazing covers approximately 40% of the north and south walls, and 20%

of the east and west walls. The house operates on constant thermostatic set points of 21°C (70°F) in heating and 24°C (75°F) in cooling, with a deadband between.

3.2.3.2 Office

The office building used in this study is a three-story office building, 48.8m (160ft) in each of the plan dimensions and 9.1m (30ft) tall; this building, modeled by Gentry (2007), is a scaled-down version of a real, much taller building located in Tulsa, Oklahoma. Glazing occupies 65% of the building façade, and the building operates with a 0.5 ACH infiltration rate. The thermostat is set at 20°C (68°F) for heating and 24°C (75°F) for cooling from 7am-6pm Monday-Friday, with a night and weekend setback of 5°C (41°F) in heating and 30°C (86°F) in cooling, again with a deadband between in both instances.

3.2.3.3 Soil

For this work, a soil typical of a heavier, damp earth was selected. The soil has a thermal conductivity of 1.30 W/m-K (0.75 BTU/hr-ft-°F) and a volumetric heat capacity of 2019 kJ/m^3-K (30.1 BTU/ft^3-°F). For Duluth, the undisturbed ground temperature is 5.0°C (41°F), while for Tulsa it is 16.7°C (62°F).

3.2.3.4 Locations

Two locations—Duluth, Minnesota; and Tulsa, Oklahoma—were selected to provide both a warm and a cool locale. The locations are specified in the simulations by means of Typical Meteorological Year (TMY) weather files. Loads for each combination of building and location were generated with EnergyPlus (Crawley et al. 2001); this was done separately from the ground heat exchanger simulation, as only the temperature response of the ground is of interest at this time. Load profiles are shown in Figures 3-1 through 3-4. The Duluth house (Figure 3-1) is moderately heating-dominated, with a heating-to-cooling ratio of 1.47; while the Tulsa house

(Figure 3-2) is cooling-dominated, with a ratio of 0.28. The Duluth office building (Figure 3-3), however, is relatively balanced, with a heating-to-cooling ratio of 1.04; while the Tulsa office building (Figure 3-4) is substantially cooling-dominated with a ratio of 0.033. It should be noted that, while these buildings were operated with a thermostatic control for the purposes of these simulations, in reality (particularly for Duluth) "free" cooling using outdoor air would be utilized instead of the heat pump system.

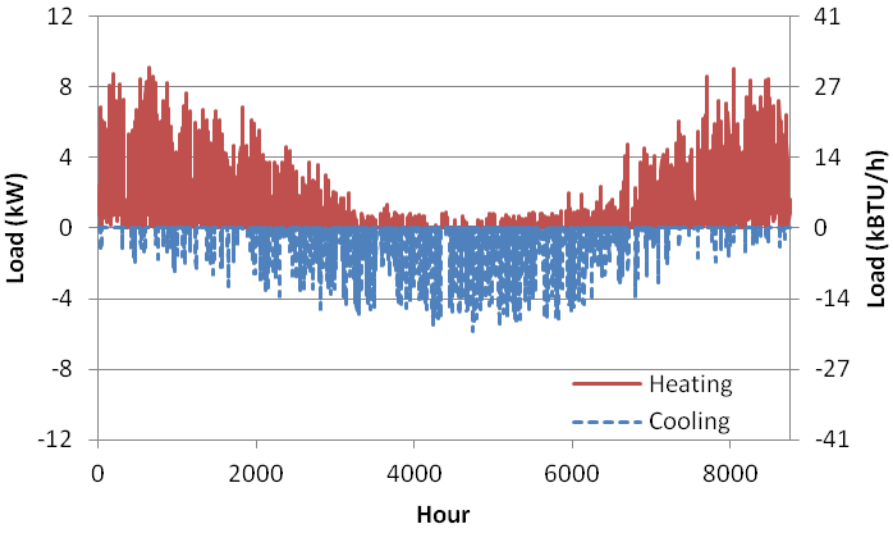

Figure 3-1: Load profile for Duluth MN house

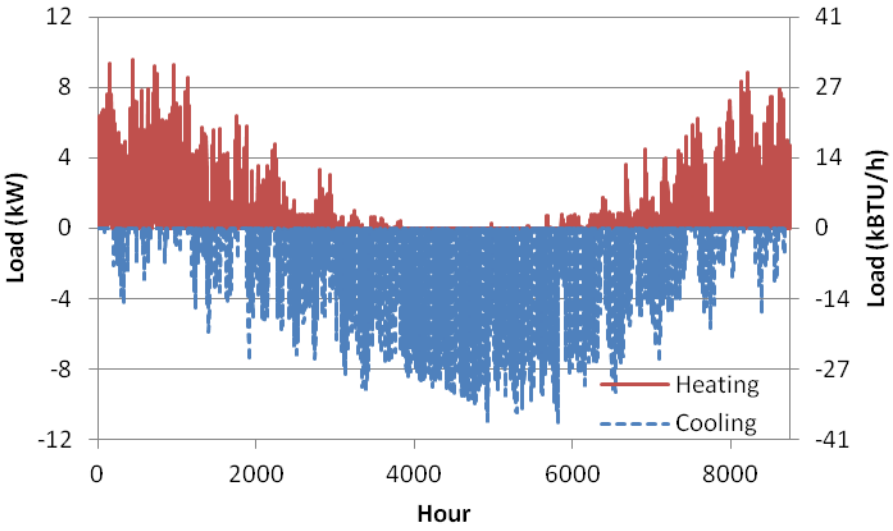

Figure 3-2: Load profile for Tulsa OK house

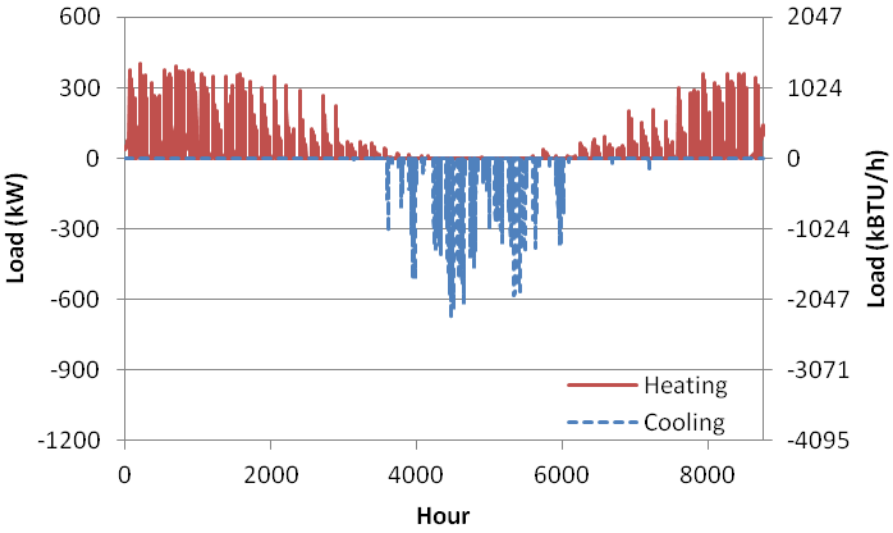

Figure 3-3: Load profile for Duluth MN office building

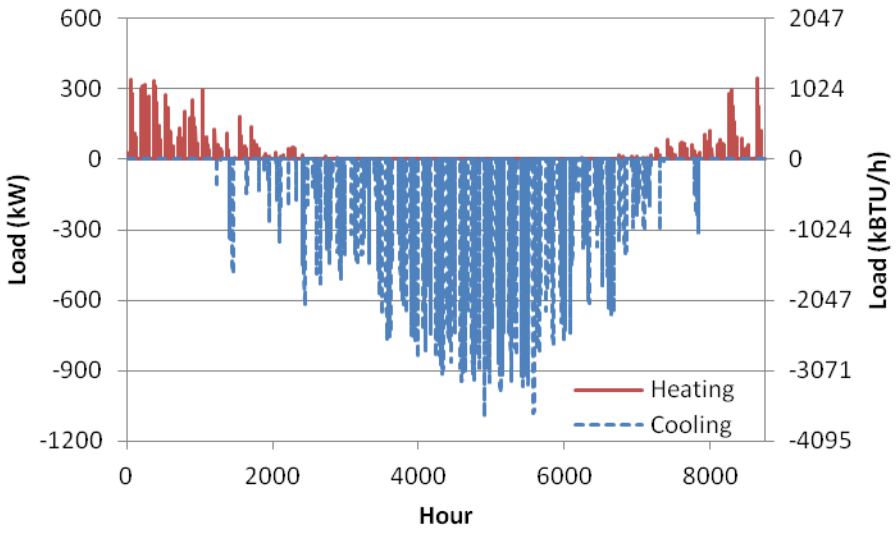

Figure 3-4: Load profile for Tulsa OK office building

3.3 Component Sizing

3.3.1 Vertical Ground Heat Exchangers

For this work, the vertical ground heat exchanger for each combination of building and location was sized using the software developed by Spitler (2000), which utilizes the same g-function approach as EnergyPlus. The individual borehole depth was set to 91.4m (300ft); the number of boreholes was adjusted so that the heat pump entering fluid temperature would be maintained between design constraints of approximately 1°C (34°F) and 30°C (86°F), with a 20% propylene glycol solution specified as the working fluid. For the two Duluth buildings, the design is constrained by the minimum allowable EFT, while the higher temperature constrains the two Tulsa buildings. So, if the Duluth buildings are under/oversized, that means that the simulated minimum EFT is lower/higher than the constraint, while the Tulsa buildings would be under/oversized if the simulated maximum EFT is higher/lower than the constraint.

3.3.2 Horizontal Ground Heat Exchangers

The horizontal piping in a vertical ground heat exchanger system consists of several parts: piping running between boreholes, piping to connect each borehole to the main fluid distribution pipe, and pipe to run from the borefield to the heat pump. Since, for the purposes of this work, the HGHX and VGHX are assumed not to interact with one another (i.e., their respective soil domains are isolated from one another and there is no conductive heat transfer between them), only one piping configuration was selected, with two pipes in the horizontal trench. The VGHX is piped in reverse-return configuration, and a simple equation was for the total horizontal length was developed based on the borehole configuration and spacing for a rectangular borefield.

A typical borefield is shown in Figure 3-5. For a borefield containing X-by-Y boreholes ($X \geq Y$) spaced s meters apart, there will be sX meters of horizontal piping in one run of boreholes, and Y such runs. Additionally, there will be $s(Y\text{-}1)$ meters of header piping connecting each of the parallel runs. For this work, a spacing of s = 5.0m (16.4ft) is used. To join each borehole to the main piping lines, there will be a short connecting pipe of length a; in this work, a is given a value of 0.20m (0.66ft). Finally, for a reverse-return piping scheme, this will be done once for supply and once for return, leading to Equation 3-1, which gives the total horizontal length, THL, for an arbitrary borefield configuration assuming that the distance to the building is very short.

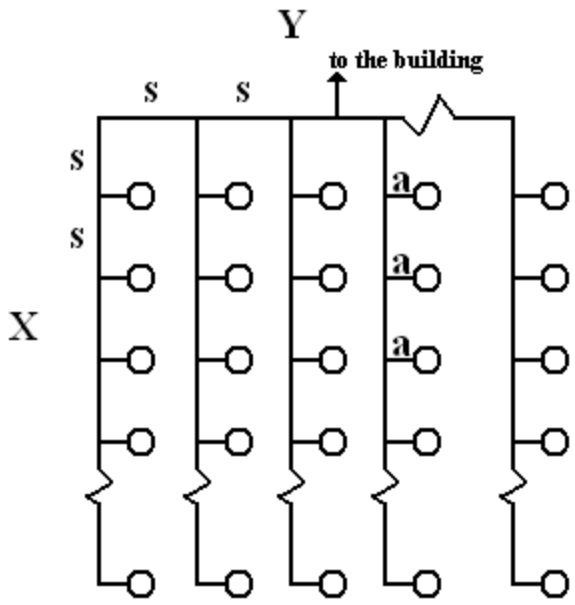

Figure 3-5: Borefield piping diagram

$$THL = 2\left[sXY + s(Y-1) + aXY\right] \tag{3-1}$$

Table 3-1 below shows the sizes of both the vertical and horizontal components for each combination of building and location. The horizontal length listed in the table only includes one pipe of the reverse-return configuration. Table 3-1 also shows two different ratios relating the horizontal and vertical installations. The H/V piping ratio is the ratio of the actual length of piping used; so, for a vertical borehole, it will be twice the design length as a U-tube has both downward and upward segments. The H/V length ratio, then, is simply the ratio of design lengths (horizontal trench length to total bore length), and is twice the piping ratio. Finally, to mirror the physical borefield using a reverse-return configuration, the simulated HGHX consists of two pipes, spaced 0.5m (1.6ft) apart.

Table 3-1: Heat exchanger sizes

Building, Location	Vertical configuration	Borehole depth, m (ft)	Total vertical length, m (ft)	Horizontal length, m (ft)	H/V piping ratio, %	H/V length ratio, %
House, Duluth	1x5	91.44 (300)	457 (1500)	52 (171)	5.7%	11.4%
House, Tulsa	1x3	91.44 (300)	274 (900)	32 (105)	5.8%	11.7%
Office, Duluth	13x16	91.44 (300)	19020 (62400)	2314 (7592)	6.1%	12.2%
Office, Tulsa	20x22	91.44 (300)	40234 (132000)	4766 (15636)	5.9%	11.8%

3.4 Results

3.4.1 Base Cases

For each of the two buildings in both locations, simulations were run in the EnergyPlus environment both with and without a HGHX. For the systems that include the HGHX, the horizontal piping is buried 3m (10ft) below the ground surface; while this is deeper than would be practically installed, this depth was chosen to isolate the additional heat transfer to the ground as a result of the horizontal piping from the heat transfer through the surface to outside conditions. Additionally, a 1m (3.3ft) deep HGHX was investigated, as this depth range should bracket the depths for which horizontal distribution piping would be installed, and therefore also bracket the net effect of the piping on the thermal performance of the system. Figure 3-6 shows the minimum monthly heat pump EFT (for Duluth buildings) and maximum monthly heat pump EFT (for Tulsa buildings) for the simulation containing both the VGHX and HGHX. The two Tulsa buildings, in particular, show evidence of heat buildup over time, while the heat pump EFT for the Duluth buildings remains relatively consistent on a year-to-year basis. The plots in Figures 3-7 through 3-10, then, will show the deviation from these values for a system that does not consider the system's horizontal piping.

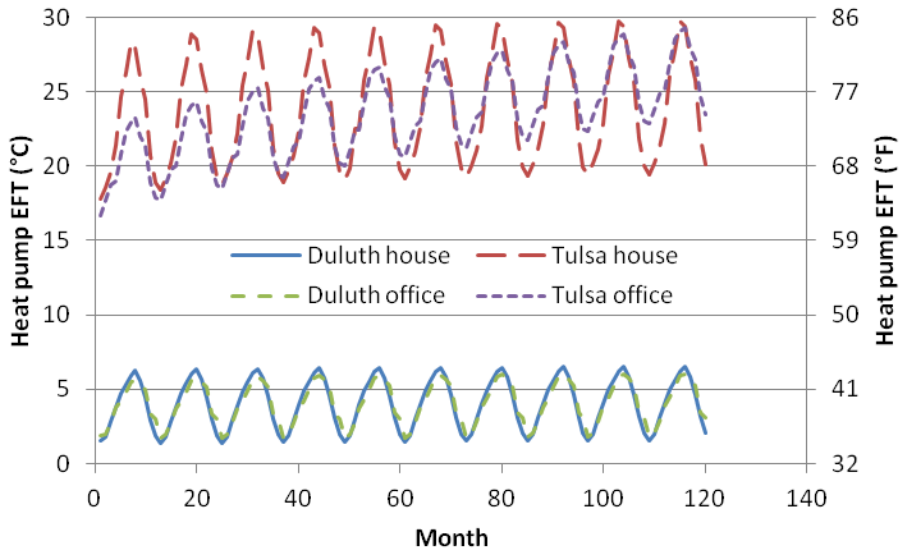

Figure 3-6: Base case maximum (for Tulsa) and minimum (for Duluth) monthly heat pump EFTs

For a heating-constrained system in Duluth, Minnesota, Figures 3-7 and 3-8 show the difference in heat pump entering fluid temperature (EFT) between a system with just a VGHX, and a system with a HGHX in addition to a VGHX. For the house in Duluth (Figure 3-7), the five borehole, heating-dominated system shows very little deviation in temperature due to the presence of the HGHX; overall, the effect averages about 0.05°C (0.09°F), and there is no appreciable increase or decrease over the course of ten years. For the office in Duluth (Figure 3-8), however, there is an obvious downward trend, which indicates that the system with the HGHX is predicting a higher temperature than the system with the VGHX alone. In ten years, the peak difference is about 0.5°C (0.9°F); while this could represent an opportunity to slightly reduce the size of the initial VGHX since the HGHX is supplying more heat to the system, it is important to note that this estimate is on the high end, as there is no calculated interaction between the two heat exchangers. Nevertheless, the question of whether it might be possible to take advantage of the horizontal piping by intentionally undersizing the VGHX will be addressed in the next section.

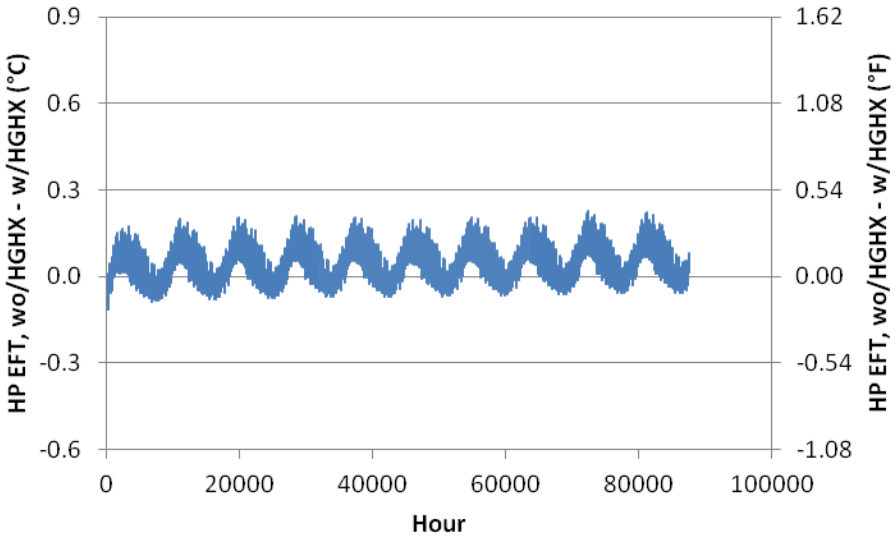

Figure 3-7: Effect of horizontal piping on a house in Duluth MN

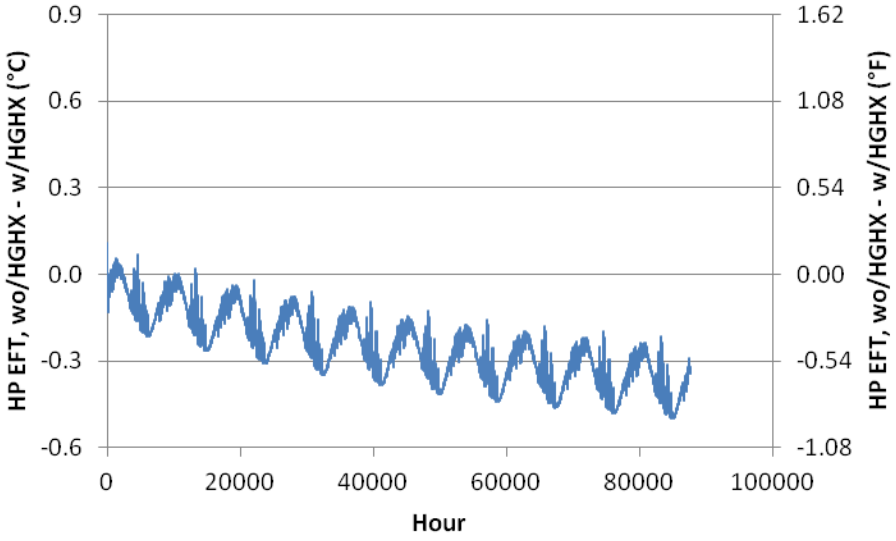

Figure 3-8: Effect of horizontal piping on an office building in Duluth MN

Figures 3-9 and 3-10, respectively, show the same difference in heat pump entering fluid temperature for a house and an office building in the cooling-dominated climate of Tulsa, Oklahoma. For the Tulsa house (Figure 3-9), the temperature difference is positive, indicating

that the HGHX is acting as an additional heat sink. Even for a VGHX with just three boreholes, the peak effect is about 0.6°C (1.1°F) after ten years. This is a much more pronounced effect than for the similarly-sized, heating-dominated system in Duluth. Peak fluid temperatures in the Tulsa house system are around 30°C (86°F) while the undisturbed ground temperature is 17°C (62°F); for the Duluth house system, however, the peak temperature is about 1°C (34°F) with an undisturbed ground temperature of only 5°C (41°F). Thus, there is a much greater temperature difference in the soil, and consequently higher secondary heat transfer from the horizontal piping.

For the Tulsa office building (Figure 3-10), the influence of horizontal piping is pronounced. Over the course of a ten year simulation, the system with the HGHX has a peak maximum heat pump EFT 0.8°C (1.4°F) lower than the base system with the VGHX alone. Additionally, after the first few years, the difference is growing on the order of 0.1°C (0.2°F) per year, and shows no indication of dampening after ten years. This indicates that, at least for a relatively large, cooling-dominated ground heat exchanger system, it may be possible to intentionally undersize the VGHX—at least based on current sizing techniques—and still meet the desired design constraints.

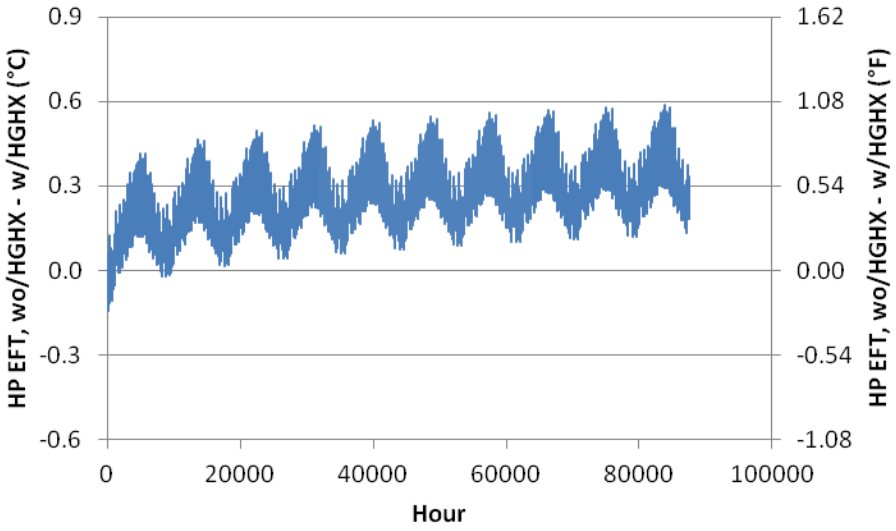

Figure 3-9: Effect of horizontal piping on a house in Tulsa OK

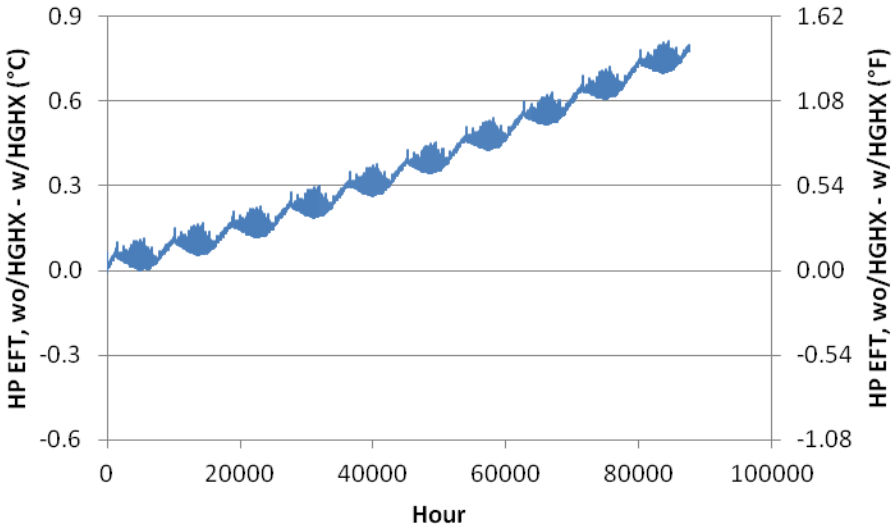

Figure 3-10: Effect of horizontal piping on an office building in Tulsa

3.4.2 Changing the Length of the VGHX

As the vertical ground heat exchanger is undersized, the horizontal piping becomes a greater fraction of the total length of heat exchanger in the soil. Thus, it would be expected to have a greater influence on the behavior of the system as a whole. In addition, the results from a system

sized through current simulation techniques suggest that, at least for a VGHX in a larger, cooling-dominated system, the presence of horizontal piping could make up for a slight undersizing of the vertical boreholes. For the house and office building in both Duluth and Tulsa, Table 3-2 shows the maximum difference in heat pump EFT between a system without a HGHX and one in which the HGHX is considered, when the VGHX is undersized. Since the HGHX length remains constant, this undersizing increases the ratio of horizontal to vertical design length from about 12% for a fully-sized VGHX to around 18% when the VGHX is reduced to 70% of the base size.

As Table 3-2 indicates, as the size of the VGHX decreases, the total effect of the horizontal piping increases. This is as anticipated, since there is now comparatively more horizontal piping for heat to transfer through. The effect is greater for the cooling-dominated buildings in Tulsa than the heating-dominated buildings in Duluth, since, again, there is a larger difference between the fluid temperature in the loop and the ground temperature, on average. The horizontal piping produces the most significant effect for the Tulsa office building, as there is an 0.81°C (1.47°F) difference between the two systems with a normally sized VGHX, and a 1.48°C (2.67°F) difference when the VGHX is reduced to 70% of its base size.

Table 3-2: Effect of horizontal piping at 3m (10ft) when VGHX is undersized

Building, Location	Maximum difference in heat pump EFT:wo/HGHX - w/HGHX, °C (°F)			
	100% VGHX size	90% VGHX size	80% VGHX size	70% VGHX size
House, Duluth	-0.11 (-0.20)	-0.12 (-0.23)	-0.18 (-0.32)	-0.21 (-0.38)
House, Tulsa	0.58 (1.06)	0.63 (1.13)	0.75 (1.35)	0.95 (1.70)
Office, Duluth	-0.50 (-0.90)	-0.54 (-0.97)	-0.58 (-1.05)	-0.63 (-1.13)
Office, Tulsa	0.81 (1.47)	1.12 (1.83)	1.26 (2.27)	1.48 (2.67)

A similar effect may be seen when the heat exchanger is oversized. Table 3-3 shows the effect of the horizontal piping on system performance when the VGHX length is increased up to 130% of

its base size. As the size of the VGHX increases, the fraction of total pipe length accounted for by the HGHX decreases; thus, as expected, the difference between the two systems drops as the horizontal piping has less of an impact.

Table 3-3: Effect of horizontal piping at 3m (10ft) when VGHX is oversized

Building, Location	Maximum difference in heat pump EFT:wo/HGHX - w/HGHX, °C (°F)			
	100% VGHX size	110% VGHX size	120% VGHX size	130% VGHX size
House, Duluth	-0.11 (-0.20)	-0.10 (-0.18)	-0.08 (-0.15)	-0.08 (-0.14)
House, Tulsa	0.58 (1.06)	0.51 (0.91)	0.44 (0.80)	0.40 (0.71)
Office, Duluth	-0.50 (-0.90)	-0.13 (-0.24)	-0.13 (0.23)	-0.12 (-0.22)
Office, Tulsa	0.81 (1.47)	0.65 (1.17)	0.61 (1.10)	0.56 (1.01)

3.4.3 Effect of HGHX Depth

While the horizontal piping effect shown so far indicates a practically significant, if not statistically significant, effect, the horizontal pipe for a VGHX is typically buried much closer to the surface than the 3m (10ft) considered thus far. So, to explore the effect of the depth of the horizontal piping, the simulations were repeated with the HGHX moved up to 1m (3.3ft) below the surface, which would be closer to what might be installed in an actual system. At this depth, the HGHX might also be expected to interact much more with outdoor weather conditions.

Table 3-4 shows the results of the same undersizing study, this time with the horizontal piping buried much closer to the surface. In each instance, the maximum temperature difference increases with the horizontal pipe closer to the surface. At just 1m (3.3ft) below ground, the piping has a much greater ability to interact with the top layers of the soil. In cold months, the fluid temperature will be around 1°C (34°F), while the average outdoor air temperature is higher than that; as a result, the top layers of soil will be warmed by convection and radiation, and the horizontal piping can absorb this heat. In contrast, during hot months, the temperature in the loop

will be closer to 30°C (86°F), and heat will be transferred from ground to air by means of convection and evapotranspiration, so the horizontal piping can reject extra heat and lower the temperature in the ground loop.

Table 3-4: Effect of horizontal piping at 1m (3.3ft) when VGHX is undersized

Building, Location	Maximum difference in heat pump EFT:wo/HGHX - w/HGHX, °C (°F)			
	100% VGHX size	90% VGHX size	80% VGHX size	70% VGHX size
House, Duluth	-0.36 (-0.65)	-0.38 (-0.68)	-0.41 (-0.74)	-0.43 (-0.77)
House, Tulsa	0.73 (1.31)	0.77 (1.39)	0.87 (1.56)	1.02 (1.84)
Office, Duluth	-0.60 (-1.08)	-0.63 (-1.13)	-0.65 (-1.17)	-0.71 (-1.29)
Office, Tulsa	1.14 (2.05)	1.39 (2.50)	1.68 (3.03)	2.01 (3.62)

3.4.3 Sensitivity in Design Length

The horizontal piping in a VGHX system has a noticeable effect on the temperatures entering the heat pump, as the HGHX can reject extra heat in summer and absorb it in cooler months. What, then, is the impact of this on design length? Can the horizontal piping be expressed in terms of an equivalent amount of vertical U-tube, assuming no HGHX influence? To explore this, a sensitivity analysis was performed to determine the influence of the horizontal piping on design length, as the VGHX is both undersized *and* oversized. Using a sensitivity coefficient approach (Spitler et al. 1989), the error in design length due to the error in heat pump EFT caused by neglecting the influence of the horizontal piping may be estimated as follows:

$$E_{length} \approx \frac{\partial L}{dEFT} \cdot E_{EFT} \approx \frac{\Delta L}{\Delta EFT} \cdot E_{EFT} \tag{3-2}$$

The partial derivative here is estimated from the change in design length and maximum (for cooling) or minimum (for heating) heat pump EFTs. For the Duluth house with the 3m (10ft) HGHX, the partial derivative is 31.2% per degree, so an error of 0.11°C (0.19°F) in the EFT

would lead to an error in the design length of approximately 3.4%. Similarly, errors for the Tulsa house, Duluth office, and Tulsa office, respectively, are 7.8%, 28.1%, and 6.2%.

Another way to explore how the horizontal piping affects the design length is to express the horizontal length as an equivalent length of vertical piping. Results so far have shown that considering the HGHX leads to a system that overperforms; i.e., the design limits are not reached because the HGHX compensates for additional heat extraction or rejection, depending on the season. For each system, curves can be generated that show the trend in maximum or minimum heat pump EFT when the VGHX design length changes. From these curves, the HGHX equivalent vertical length may be obtained by tracking back from the design point on this curve to the point at which the heat pump temperature constraint is identically met; the difference in lengths is due to the consideration of active horizontal piping, and represents the length of VGHX that the horizontal piping is equivalent to. Figure 3-11 below shows the EFT versus design length curves for the Duluth buildings, while Figure 3-12 shows the same for the Tulsa buildings. The 100% design lengths are the same used previously, targeted to 1° (34°F) for heating and 30°C (86°F) in cooling. Taking the Duluth house as an example, the minimum heat pump EFT using the design length is 1.35°C (34.4°F); following this curve back finds the 1°C (34°F) constraint at about 89% of the design length. Thus, for this system, the horizontal piping could be said to be equivalent to 11% of the total vertical length. Similarly, the equivalent vertical length of horizontal piping is around 9% of the total vertical length for the two Tulsa buildings, while it accounts for roughly 30% for the Duluth office. More study is definitely needed to examine the interactions between the horizontal and vertical components; since the interactions between horizontal and vertical piping were neglected, these values are only estimates, and are likely on the high end.

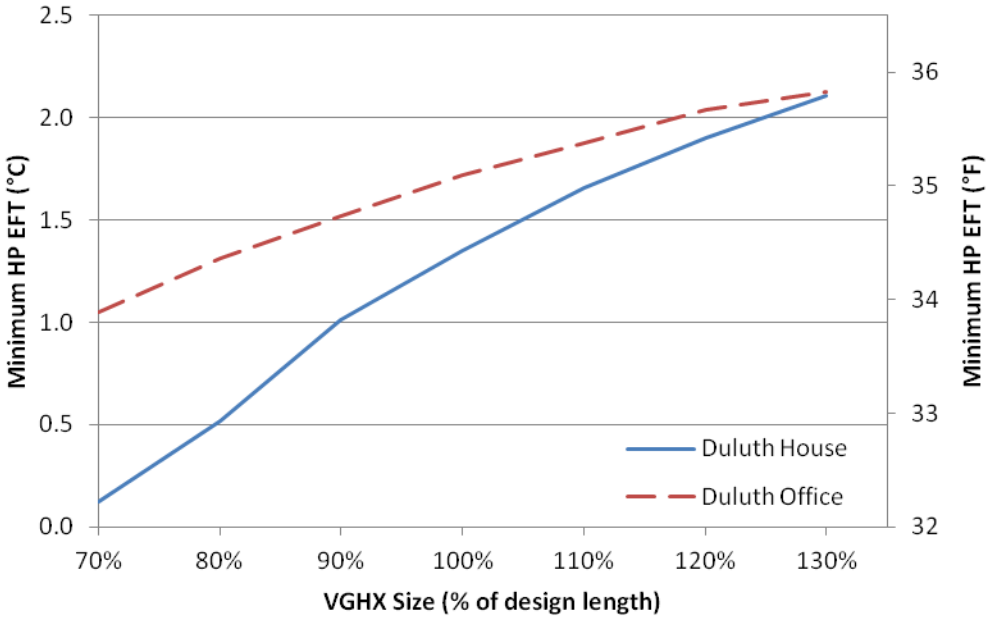

Figure 3-11: Minimum heat pump EFT vs. design length for Duluth buildings

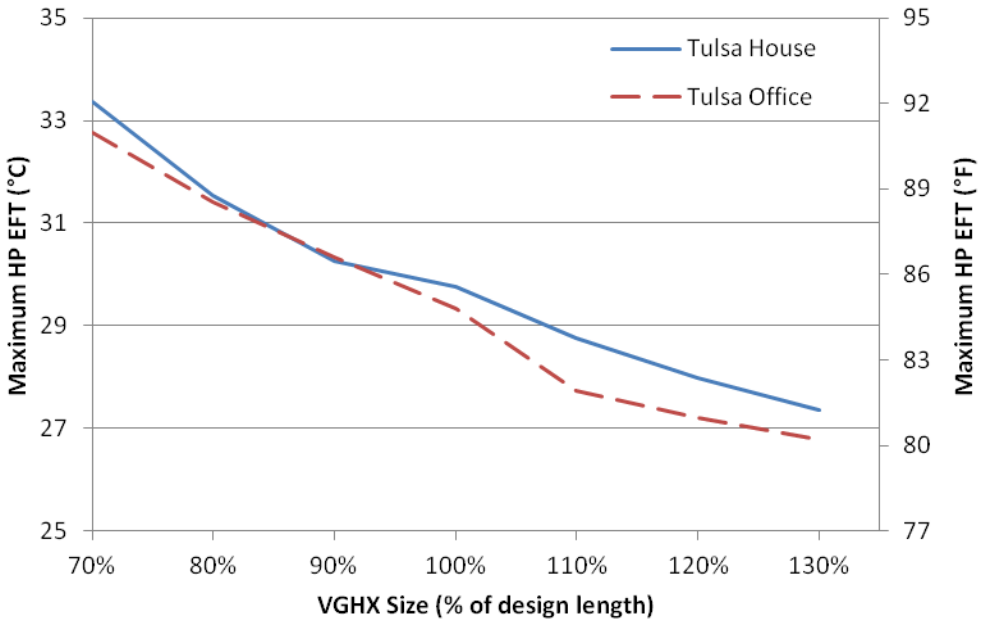

Figure 3-12: Maximum heat pump EFT vs. design length for Tulsa buildings

One important thing to note about Figures 3-11 and 3-12 is the effect of design temperature limits on the resulting heat exchanger size. If the design constraint is increased for cooling or decreased for heating, the required VGHX length will drop—sometimes significantly, as for the Duluth house, even for only a degree's change in the constraint. If a system is sized using less extreme limits, then the heat exchanger could end up being quite a bit oversized, particularly if the heat pump and other equipment are capable of handling those more extreme temperatures. In other words, the amount by which a system is oversized or undersized depends not only on the temperature response, but on the EFT constraints placed upon the design. In addition to being economically inefficient, this could certainly provide one explanation as to why some real systems do not exhibit the long-term temperature change frequently foreseen in simulation.

3.5 Conclusions

This chapter represents an initial exploration of the effect of horizontal piping on the performance of ground source heat pump systems that utilize vertical ground heat exchangers. In simulating two buildings in two different locations, a horizontal ground heat exchanger was added in series with a vertical ground heat exchanger, and the results were compared with a system consisting of the VGHX alone. Results for the base case, with the HGHX located 3m (10ft) below the ground surface, showed that the HGHX plays a role in the temperature response of the entire system, rejecting extra heat in summer months in the warmer location while extracting extra heat during winter months in the cooler location. When the horizontal piping is moved closer to the surface, the effect is amplified.

As the size of the VGHX shrinks, the horizontal piping becomes a greater proportion of the total pipe length of the system. As would be expected, the difference between a simulation with the

HGHX and one without grows as the VGHX is undersized, and decreases as it is oversized. Additionally, both a sensitivity analysis and an estimation of the equivalent length of VGHX for the horizontal piping were performed. The office in Duluth showed the highest sensitivity and influence of the horizontal piping, with values of about 30% of the VGHX design length for each.

This study has assumed no conductive interaction between the horizontal and vertical piping, while in reality there will be some interplay between the two. This should certainly be explored in future work. In addition, these results strongly suggest that the design temperature constraints play a very important role in the expected behavior of a ground heat exchanger system. A system designed with higher extreme temperatures will result in smaller design lengths, though this may result in a long-term change in ground temperatures if the design length is sufficiently low.

These effects have, to date, not been experimentally quantified. While it would, in theory, be possible to add temperature sensors at the inlet and outlet of each borehole of an already-installed system, it would be quite expensive to instrument, maintain, and monitor such a system over the length of time—several years, at least—required to generate a data set sufficiently large to use in any experimental comparison. As a result, it is impossible to anticipate such experimental data becoming available in the near future. Rather, this study has suggested one possible, partial explanation for why vertical ground heat exchanger design tools, which assume only pure conduction heat transfer to and from the VGHX, are thought to over-predict long-term temperature rise or fall.

CHAPTER IV

IMPLEMENTATION AND VALIDATION OF AN INTERMEDIATE-LEVEL GROUND HEAT EXCHANGER MODEL

[NOTE: A condensed version of the model description in this Chapter is included as part of the following paper:

Cullin, J.R., J.D. Spitler, C. Montagud, F. Ruiz-Calvo, J.M. Corberán, S.J. Rees, S.S. Naicker, and M. Mitchell. 2014. Experimental Validation of Two Short Time Step Ground Heat Exchanger Models Using Multiple Data Sources. (Submitted to HVAC&R Research.*)]*

This chapter describes a new ground heat exchanger model of greater complexity than many currently in use. This new model utilizes multiple coordinate systems within one numerical domain to focus computational efforts on the areas of greatest heat transfer—namely, very near to, and between, the boreholes. This VGHX model has been developed based on a similar existing model for shallow horizontal ground heat exchangers (Lee 2013), such as might be installed around a basement in a building's foundation excavation. In addition to adaptation for vertical pipes, a model of the interior borehole region (consisting of the U-tube, grouting, and immediately surrounding soil) has been integrated that can account for the often-ignored intra-borehole thermal short-circuiting. Preliminary validation of this model has been performed

against the line source, with results less than ideal. An enhanced version of the model, with improved consideration of thermal mass, significantly increases the accuracy of the model.

4.1 Overview of Existing GHX Simulation/Design Methods

Several methods currently exist for usage in the design and simulation of ground heat exchanger systems. As each of these are discussed in greater detail elsewhere, they will only be summarized in list form here, with references to the other sections in which the respective methods are discussed further.

4.1.1 Analytical Methods

- The line source method (Ingersoll et al., 1954) assumes a single line heat source (or sink) of infinite length. Using a known analytical solution, the temperature at a given radius (for example, the pipe radius) can be determined, and the fluid temperature may be backed out via a thermal resistance computation. More details about the history of the line source approximation are located in Section 2.1.1, while the implementation of the line source method is detailed in Section 4.2.1.

4.1.2 Design Methods

- The GLHEPRO design tool uses a simulation-based approach to size a vertical ground heat exchanger. Via an iterative approach, the length of the VGHX is adjusted until the heating and cooling loads are met while still maintaining the heat pump entering fluid temperatures within both maximum and minimum design constraints. The GLHEPRO tool has been described in the literature by Spitler (2000), with an updated version

presented by Cullin (2008), while the treatment of loads over time using a hybrid time step procedure is described by Cullin and Spitler (2011). Section 4.2.4.1 gives a brief overview of the design methodology.

- The ASHRAE Handbook method uses an equation-based approach described by Kavanaugh and Rafferty (1997), and presented for quick design calculations by ASHRAE (2011). A single equation gives the necessary length for heating, while a similar equation does the same for cooling. This method is set forth in detail in Section 4.2.4.1

4.1.3 Simulation Methods

- GLHEPRO uses the g-function simulation method (Eskilson, 1987) to determine the fluid temperatures in the system. A hybrid time step (Cullin and Spitler, 2011), consisting of a monthly period for average loads, plus multiple hours for peak loads, is utilized. The g-function method is described in Section 2.1.1, with implementation details in Section 4.2.4.1.
- HVACSIM+ is a generalized modular platform for simulation of HVAC systems. Gentry (2007) implemented the g-function model in this environment, which offers fast computation time but some restrictions on model connection; at present, the HVACSIM+ g-function model exists in a standalone fashion with a spreadsheet interface. The g-function method is described in Section 2.1.1, with implementation details in Section 4.2.4.1.
- EnergyPlus also uses the g-function method, as implemented by Fisher et al. (2006). The g-function method is described in Section 2.1.1, with implementation details in Section 4.2.4.1.

A new multi-coordinate method has now been developed for in-depth analysis of vertical ground heat exchanger systems. Based on the work of Lee et al. (2013), this method focuses computational efforts on a fine radial grid surrounding the borehole, with a more coarse rectangular grid farther afield. Development, implementation (in EnergyPlus), and validation of the multi-coordinate method are described in Section 4.3.

4.2 Development of a Multi-Coordinate Simulation Approach

Currently available simulation tools are restricted based on the assumptions they make: specific boundary conditions, interactions between components, etc. To completely explore the behavior of a borehole heat exchanger system, a new model is needed that applies none of these assumptions, so that the assumptions themselves can be analyzed.

4.2.1 Basis for New Simulation Approach

Lee et al. (2013) have developed a new method of simulating horizontal ground heat exchangers that uses a dual-coordinate system approach inside a finite volume formulation. This approach utilizes a Cartesian grid in the soil region to maximize computational efficiency. This grid is partitioned into regions of either coarse and fine spacing, depending on the placement of heat transfer pipes and any building foundation—areas nearer the ground surface, pipes, and foundation have closer spacing, with increased spacing farther afield. Heat exchanger pipes nest inside a single pipe cell, and utilize a fine radial grid inside which consists of cells representing the fluid, pipe, and surrounding soil. This approach, as first proposed by Piechowski (1996), focuses the computational effort nearest to the pipes—where the temperature gradient, and therefore the heat transfer rate, will be the highest.

Since the fluid is modeled as a lumped element in each segment, the radial grid is made axisymmetric to further increase computational efficiency. In the third dimension, the heat exchanger pipes are segmented with a specified flow direction, to capture the effect of changing temperatures as the fluid passes through the heat exchanger. The two coordinate systems are connected by careful consideration of an energy balance at the interchange between the radial and Cartesian meshes. The entire region—both rectangular and radial cells—is gridded automatically, with only the physical location of the pipes, domain dimensions, and grid density parameters needed as inputs to fully discretize the heat transfer domain.

The soil-plus-pipe(s) domain is then coupled to a whole-building simulation in the EnergyPlus environment. The soil domain is linked to a zonal heat balance by connecting the wall(s) or floor of the zone to a domain boundary. At each time step, the surfaces are lumped into an average floor and an average wall surface, and transient conditions within the floor/wall are handled by those surfaces' respective surface heat balance algorithms. The ground model takes the heat flux from these surfaces as the boundary condition for the proper cells at each time step; at the end of the time step, it determines an effective average temperature for the surfaces, which is paired with an extremely high convection coefficient and passed back to the surface.

Coupling to the whole-building simulation also occurs by means of the fluid passing through the ground heat exchanger. In this way, the working fluid can interact with heat pumps, circulating pumps, and even other heat exchangers to get a complete picture of the thermal performance and energy consumption of the system. The ability to link this ground heat exchanger model to other thermally-active components allows for a wide array of possibilities for system design.

4.2.2 Adaptation for Vertical Ground Heat Exchangers

To adapt the Lee et al. (2013) model for horizontal ground heat exchangers into something suitable to analyze vertical heat exchangers, several modifications were required. Since a HGHX only has a single pipe in each location, the innermost radial "pipe cell" had to be converted into a "borehole cell", consisting of fluid, U-tube, and grout. In addition, boundary condition adjustments were needed, since the flow direction is now vertical instead of horizontal. Finally, the heat transfer inside the borehole wall, being more complex than simple radial heat transfer, necessitates careful accounting. Appropriate thermal resistance terms must be computed, and suitable capacitances determined, in order for the results to be accurate.

4.2.2.1 Specifying the Borehole Cell

In the Lee et al. (2013) model for the horizontal ground heat exchanger, the main grid is in Cartesian coordinates, and is generated automatically using user-specified domain dimensions and mesh density parameters. Certain cells, based on their specified locations, are assigned as pipe cells, meaning that they contain a finer, radial coordinate system inside them. The innermost cell of this radial region, then, represents the inside of the pipe—the working fluid—while one or more cells depict the pipe, and one or more further cells corresponding to the soil immediately surrounding it. The interface between the inner cylindrical system and the remainder of the rectangular cell is handled by monitoring the heat balance at the interface. The Cartesian cell containing a pipe is used as the smallest such cell, with an expanding grid utilized moving away from the cell; when two or more pipes are present, the grid expands and contracts between them in order to reduce computation time.

For a vertical system using one or more borehole heat exchangers, the geometry inside the cylindrical region becomes more complex, as shown in Figure 4-13. Instead of a simple set of

radial regions, there are now two smaller cylindrical regions inside the innermost cylindrical cell. Nothing changes outside the borehole wall (the soil region, represented by the brown color in Figure 4-1). Inside the borehole, there are cylindrical cells consisting of grout (orange color); the thermal properties of this material must be provided, as they will typically be different than the surrounding soil. Similar to the way pipe cells were handled before in the dual-coordinate scheme of Lee et al. (2013), the pipe is now represented by the outer cell of both of two cylindrical sub-regions, one for each leg of the U-tube (red color). As before, the fluid still occupies the innermost cylindrical cell, but this time in the cylindrical sub-region. Handling the heat transfer between these sub-regions and the grouted area is a more complex matter due to the presence of multiple heat sources, namely the two legs of the U-tube.

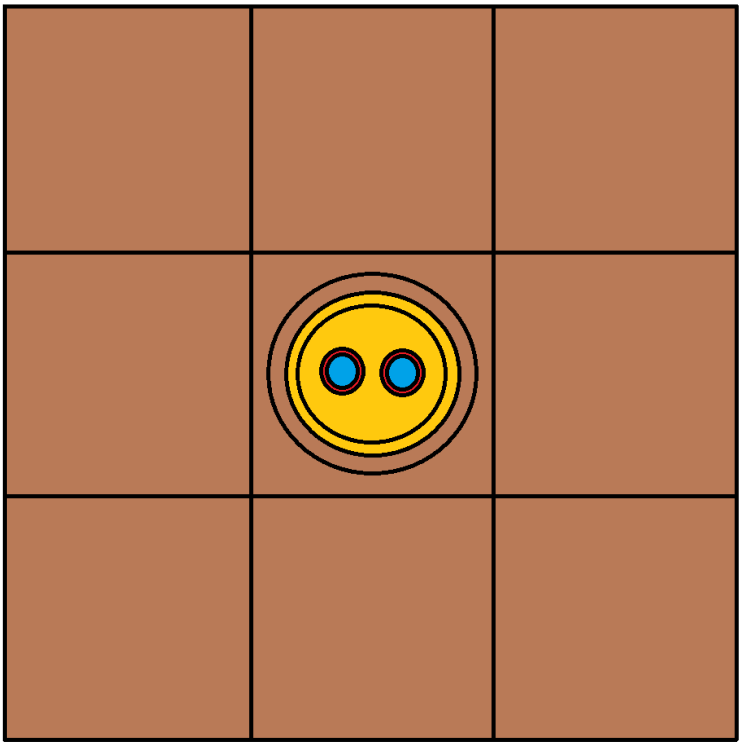

Figure 4-1: Cell schematic near borehole

4.2.2.2 Correctly Accounting for Intra-borehole Heat Transfer

The key difference between the horizontal ground heat exchanger model developed by Lee et al. (2013) and this model of the vertical ground heat exchanger is the complex geometry surrounding the pipes. Whereas the radial cells surrounding the pipe region in the HGHX model only need to accommodate a single pipe, this region in the VGHX model is a complete borehole, consisting of a U-tube with a region of grout surrounding the pipes. Consequently, the previous method of a straightforward cylindrical thermal resistance network is no longer applicable.

Lee (2013) showed that, for a backfilled horizontal heat exchanger, it is possible to achieve an accurate result by carefully controlling the thermal properties (*e.g.*, conductivity and heat capacity) of the cells in the radial region. Xu and Spitler (2011) showed similar results for a horizontal ground heat exchanger in the cases of moisture transport and soil freezing. For a borehole, similar steps can be taken; however, due to the complicated two-pipe geometry inside the borehole, a more complex thermal resistance/capacitance network has been implemented. Figure 4-2 shows the thermal resistance/capacitance network for a borehole heat exchanger, assuming only a single capacitance (associated with the grout). In addition to the convective resistance of the fluid and conductive resistance of the pipe (only shown on one pipe but present on both), there is a resistance R_{ptp} between the two pipes, and another resistance between each of the upward and downward U-tube legs and the pipe wall—$R_{up,ptw}$ and $R_{dn,ptw}$, respectively. Temperatures, including the borehole wall temperature, are assumed uniform in each horizontal plane, with temperature variations accounted for between vertical slices. For now, only the one thermal capacitance will be utilized, though this approach will be investigated later. The issue, then, becomes how to calculate these pipe-to-pipe and pipe-to-wall resistance values.

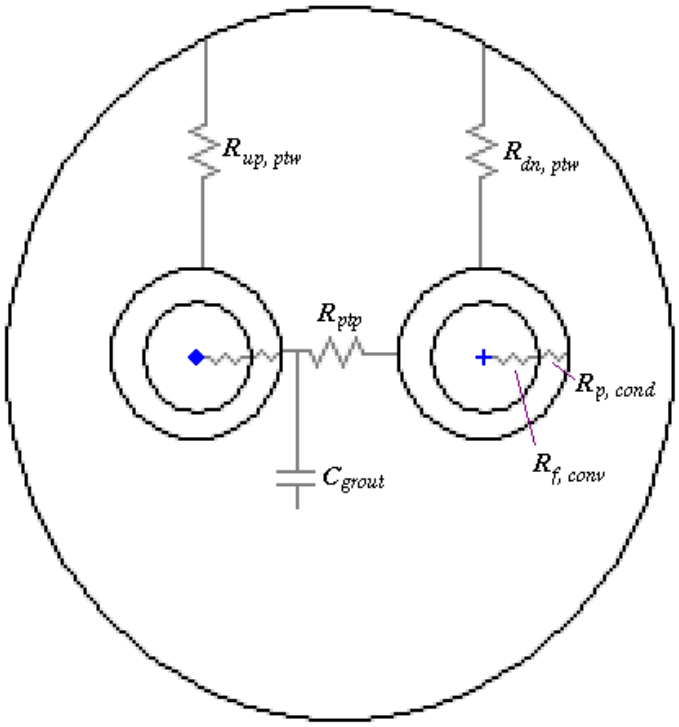

Figure 4-2: Borehole thermal resistance/capacitance network

An analytical approach is available to compute the resistances needed; this approach, based on complex Fourier analysis, is termed the "multipole" method (Bennet et al., 1987; Claesson and Bennet, 1987; Claesson and Hellström, 2011). This method uses a set of iterative equations based in the complex Fourier domain to determine the thermal influence of any number of arbitrarily-placed parallel "poles", or heat sources. Due to the complicated nature of the equations, this method is available as a computer code. For this work, the multipole computer code is used to generate the pipe-to-pipe and pipe-to-wall thermal resistance terms that are needed for the enhanced thermal resistance network in the borehole.

4.2.2.3 Boundary Conditions for the VGHX Domain

While the simulation principles are very similar between horizontal and vertical ground heat exchangers, the boundary conditions differ somewhat due to the difference in flow direction with respect to the ground. For the horizontal case, the ground surface (and respective energy balance) is parallel to the flow direction, with other faces having a time- and depth-variant temperature condition specified with the Kusuda and Achenbach (1965) expression. This expression utilizes an exponential sinusoid to compute the soil temperature at an arbitrary depth and time due to an imposed temperature at the ground surface. The Kusuda and Achenbach expression, then, leads to a couple of assumptions, namely that the ground surface temperature can be expressed by a composite sinusoid of annual, seasonal/monthly, and daily components; and that any effects of the geothermal gradient are neglected. For a closed-form boundary condition, the first assumption is adequate, though it may not account for other means of heat transfer or varying ground thermal properties. The second assumption seems clearly valid for a horizontal ground heat exchanger, with pipes only a few meters, at most, below the ground surface. However, for a vertical ground heat exchanger, this may need further refinement, particularly in the case of very deep (*e.g.*, on the order of hundreds of meters) boreholes.

For a vertical heat exchanger, the ground surface is perpendicular to the direction of fluid flow in the pipes. Thus, the pipe direction has been shifted to accommodate the change in system geometry. For the VGHX model, the upper boundary is still a full surface heat balance, consisting of conduction, convection due to wind, short- and long-wave radiation, and evapotranspiration through any plant cover. Evapotranspiration is modeled via the Walter et al. (2005) reference equation, which is governed by air thermal properties, wind speed, and a variable tabulated coefficient to account for different ground covers. In this work, the standard 5 cm grass reference is used. On the other domain boundaries, the Kusuda and Achenbach (1965) equation is again used; the geothermal gradient has been neglected for now. Finally, as a

holdover from the horizontal GHX model, it is possible to couple the exterior wall/floor of a basement zone to the soil domain; this zone, when used, is situated in one corner of the soil domain. At each time step, the heat flux through the basement wall and the average wall temperature are passed to the GHX model, and soil temperatures at the interface are returned. The soil model does not actually simulate any of the basement interaction; rather, that is handled within EnergyPlus by existing routines (such as conduction transfer functions). Figure 4-3 below shows a schematic of the boundary conditions used in the VGHX model.

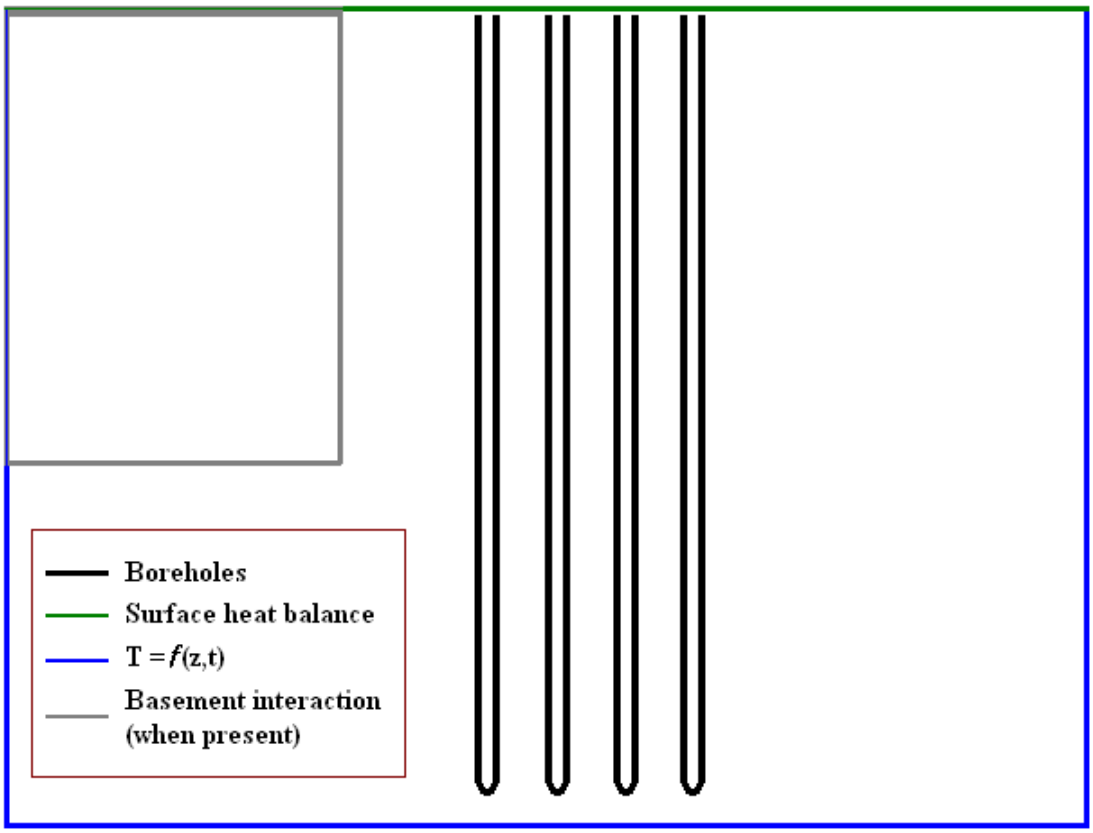

Figure 4-3: Boundary conditions for multi-coordinate VGHX model

4.2.2.4 Domain Grid Independence

With any finite difference or finite volume method, it is important to use a grid of sufficient density to attain the most accurate results possible, while at the same time not using a grid so large as to unduly increase computation time. For the multi-coordinate model, each Cartesian direction includes an associated mesh density parameter, reflecting the number of cells in that direction, and a geometric coefficient to dictate the rate of grid expansion. For the *x*- and *y*-directions, the mesh density governs the number of cells with a size equal to that of the borehole cell, before any expanding grid comes into consideration. In the *z*-direction (down the borehole), on the other hand, it is simply the number of cells in that direction.

For the single borehole "sandbox" test used in validating this model in the Section 4.2.3, a grid independence check was run. For low mesh densities (less than 4 in the field directions, and less than 5 vertically), temperature change between nodes was observed to be quite large—up to a degree or more difference between nodes in each time step, particularly vertically. Knowing that the temperature gradient will decrease further away from the borehole, more cells were added to fully capture this behavior. The final parameters settled on were a mesh density of 10 (so, 10 slices) in the vertical *z*-direction, and 6 (meaning 6 cells away from the borehole cell that are of identical size to the borehole cell) in the *x*- and *y*-directions. Expanding grid coefficients of 1.03 were utilized in each direction; this parameter had much less of an effect than the density parameters. Further increasing the values of the grid parameters served only to increase computation time, without additional refinement of the results.

4.2.3 Model Validation

As with any new mathematical model, validation is an important step. This model has been tested against data from the sandbox test, which will be discussed in detail in Section 5.1.1, in

addition to comparisons with the HVACSIM+ simulation. As shown in Figure 4-4, the multi-coordinate model does not perform as well as the HVACSIM+ model, with an RMSE of 0.66°C. (The other curves on this figure will be discussed in more detail in Chapter 5.) On this figure, the quasi-steady-state period appears as a straight line, when the temperature increase becomes roughly linear with the natural logarithm of time. The HVACSIM+ model more closely matches during this period.

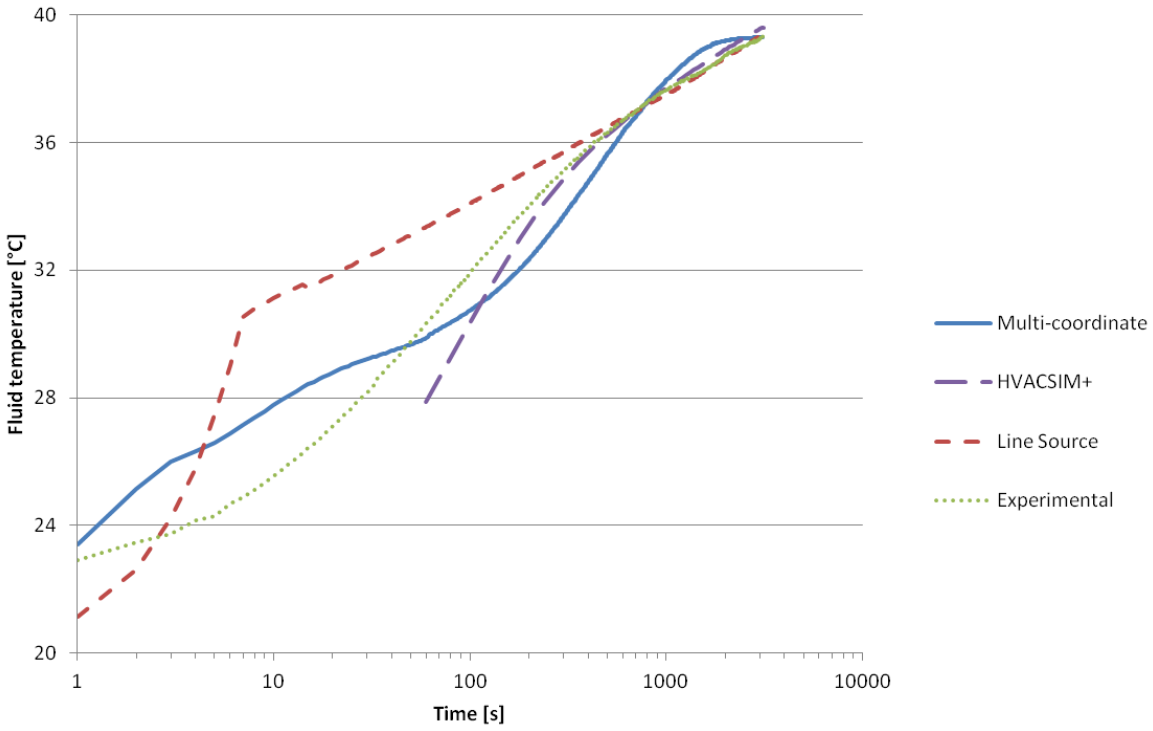

Figure 4-4: Model validation against sandbox experimental data

This test has shown that the model reacted more slowly than both the experiment and the HVACSIM+ model to changes in heat input, which suggests an insufficient accounting of thermal capacitance. Clearly, the thermal behavior of the multi-coordinate model can be greatly improved by refining the capacitances used in the model. At this stage, only a single lumped capacitance was utilized, so splitting this into multiple pieces should help results.

4.3 Refinement of the Multi-Coordinate Method

Development and preliminary validation of the multi-coordinate model shows promise as an intermediate-level model. It provides a higher level of detail than analytical solutions of simplified single boreholes, or of the numerical techniques such as the g-function approach, all of which require some set of assumptions about the behavior of boreholes and boundary conditions. Enhancement of the multi-coordinate model, particularly to make it more predictive on shorter time scales, would result in a more robust model capable of handling a wider variety of systems. This, coupled with the capability to link the model to other systems, including horizontal ground heat exchangers and full building models, could provide an extremely useful tool for assessing other GHX models.

4.3.1 Enhancement of the Model

Initially, the multi-coordinate model used a fairly basic thermal resistance network inside the borehole cell, with just a single lumped capacitance. While the validation efforts in the previous section have shown that this model produces a reasonable match to an experimental data set, there are obvious places for improvement, particularly in the short-term response characteristics of the model. This strongly suggests that a more detailed capacitance scheme is necessary to garner greater accuracy.

Xu (2007) investigated the short-term response of vertical boreholes with respect to the g-function approach, with the goal of creating a set of accurate g-function response values for shorter time steps (around one hour and shorter). Xu (2007) combined the two ends of the U-tube into one equivalent pipe and collected the pipe and grout regions together. One uniform, adjusted conductivity was used for this region, with different thermal masses for the pipe and grout cells.

A uniform distribution of the thermal mass along these cells was applied. For the multi-coordinate model, then, a similar approach will be taken in order to create a more accurate representation of the short-term behavior around the heat exchanger. However, the new model does not require combining the two pipes of the U-tube in this manner. The proposed resistance network for the revised multi-coordinate model is shown in Figure 4-5 below. Note that, for the grout and soil capacitances in particular, the thermal mass will be split among all the cells of that type in proportion to the cell volume, even though the cell type is only shown once in the diagram.

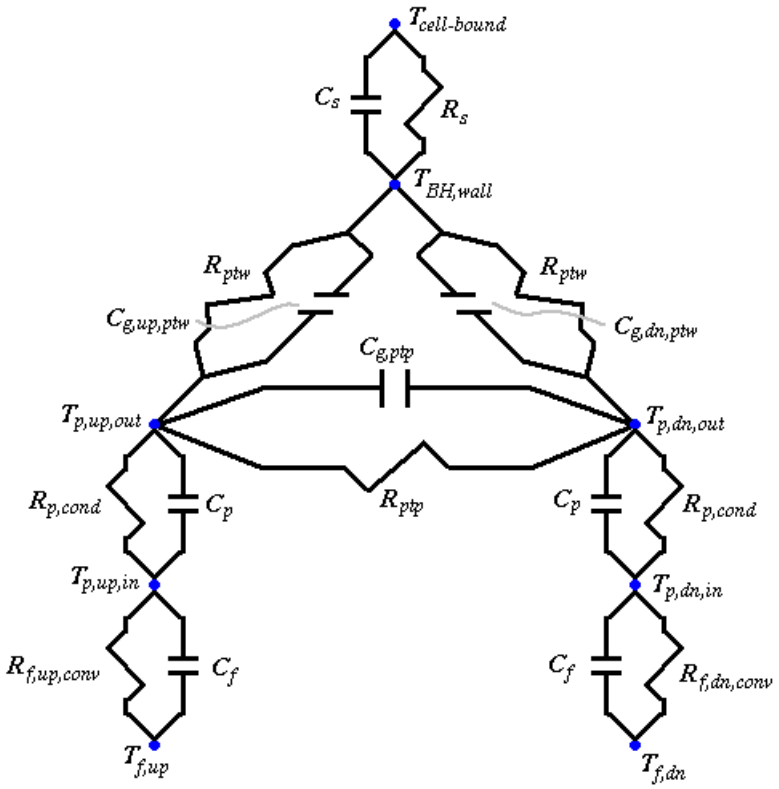

Figure 4-5: Improved borehole thermal resistance/capacitance network

One final exploration is the number of grout and soil cells needed to provide a sufficiently acceptable result. The thermal capacitance can be split between cells of the same type, so that the thermal mass is more evenly distributed. This will occur in the region between pipes, as well as

both sectors between a pipe segment and the borehole wall; additional cells may be added to the soil region, with an additional capacitance corresponding to each cell, as well. The next section validated the model with the enhanced resistance network from Figure 4-19, while assessing how many capacitance nodes give the best result.

4.3.2 Enhanced Model Validation

Figure 4-6 shows a comparison of the multi-coordinate model, enhanced to use the more detailed thermal resistance/capacitance network from Figure 4-5 and with multiple "lumps" of capacitance in each section. The figure shows the initial simple model, plus the enhanced model with three and five lumps of capacitance (Multi-coordinate, MCM-3, and MCM-5 in Figure 4-6, respectively) for each grouting section, with temperature responses plotted against time on a logarithmic scale. Three soil cells, each with its own capacitance, were used in the MCM-3 and MCM-5 runs; additional cells did not show significant changes in the response.

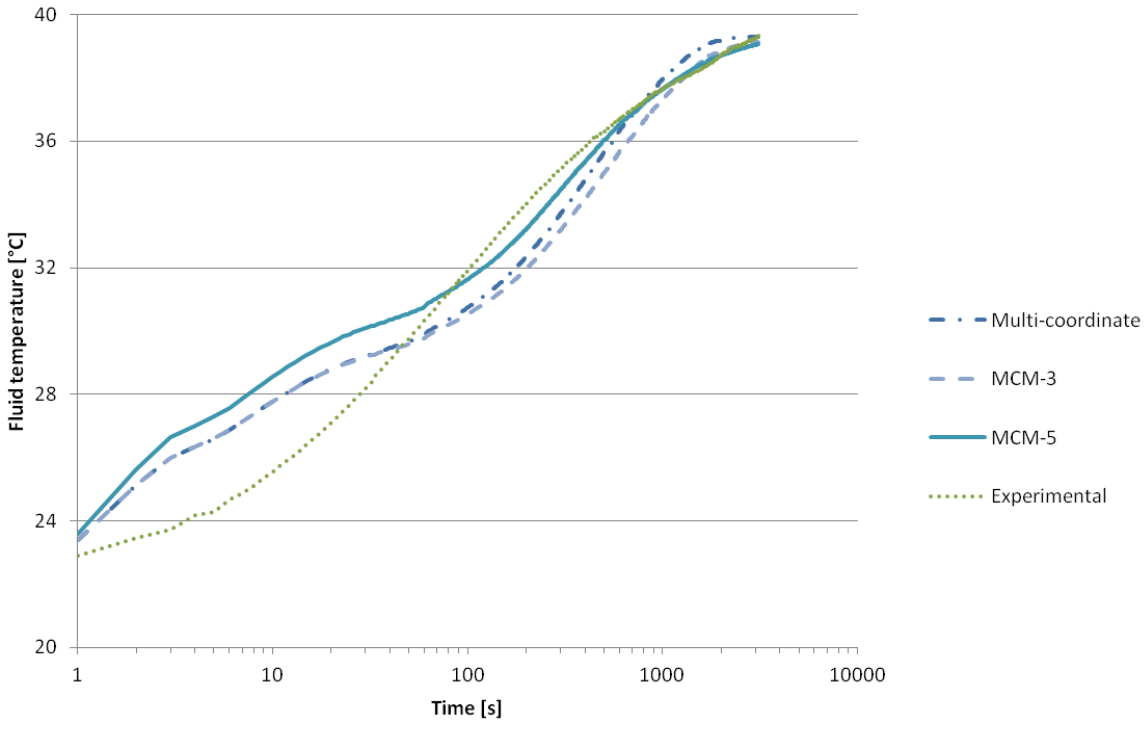

Figure 4-6: Enhanced MCM comparison to sandbox experimental data

For the original MCM, the RMSE was 0.66°C. For the three-lump enhanced model, the error actually increases to 0.78°C. However, the mismatch is most pronounced in the early period; from Figure 4-5, the experiment starts behaving in a very similar fashion to a line source after about 8 hours (log time ~9). Taking again an RMSE, only using the period after 8 hours, the RMSE drops to 0.37°C, as compared to 0.42°C for the original, unenhanced model. Increasing capacitance to five lumps, the overall RMSE drops to 0.39°C, with an RMSE of just 0.13°C after the eight-hour mark. Clearly, then, this is a substantial improvement in both the early and later behavior of the model, as Figure 4-6 confirms visually.

Further increasing of the number of capacitance nodes beyond five only served to increase computation time with no appreciable increase in accuracy. Changing to seven nodes only reduced the RMSE by a further hundredth of a degree. This came with a roughly 20% increase in computation time, while using the same one-minute time step.

4.4 Conclusions

This chapter has presented an overview of existing simulation/design methods for vertical ground heat exchangers. The drawback in using any of these models is that certain assumptions are inherent; a methodology that does not necessarily require making these assumptions could prove useful in further research. To that end, a multi-coordinate system model, with a coarse Cartesian grid away from the boreholes, a radial grid encompassing the borehole, and two smaller radial grids for each leg of the U-tube inside the borehole.

Initial validation of the model against experimental data from a sandbox test (Beier, 2011) showed that the model did not respond well in the early period after initiation of the test heat pulse. As this suggested an issue with the thermal mass of the system, the *RC* network for the model was enhanced to utilize multiple thermal capacitances in the soil and grout regions. Validation of this enhanced model showed improvement after five capacitance components were included, with additional lumps providing little extra improvement particularly when weighted against the added computation time. The recommendation, then, is to utilize the multi-coordinate model with five capacitance nodes in the grout region, plus three radial soil cells outside the borehole, in future simulations.

Further testing of the multi-coordinate VGHX model could prove very useful in understanding the conditions under which it performs well. The next chapter includes validation against several other data sets, in comparison with other models. This may provide some insight into the workings of each of these models.

CHAPTER V

VALIDATION OF MULTIPLE GROUND HEAT EXCHANGER MODELS

[NOTE: Much of this chapter is compiled from two papers:

1. *Cullin, J.R., C. Montagud, F. Ruiz-Calvo, and J.D. Spitler. 2014. Experimental validation of ground heat exchanger design methodologies using real monitored data.* ASHRAE Transactions *120(2): pages pending. {To be presented at ASHRAE Summer Conference 2014 in Seattle WA.}*
2. *Cullin, J.R., J.D. Spitler, C. Montagud, F. Ruiz-Calvo, J.M. Corberán, S.J. Rees, S.S. Naicker, and M. Mitchell. 2014. Experimental Validation of Two Short Time Step Ground Heat Exchanger Models Using Multiple Data Sources. (To be submitted to* HVAC&R Research.*)*

System descriptions (Section 5.1) are used in each paper, and are integrated into the paper stemming from Chapter 6. Paper 1 comprises Subsections 5.2.3.1-5.2.3.4; Paper 2 comprises Subsections 5.2.2, 5.2.4, and all of Sections 5.3 and 5.4.]

As discussed in Chapter 2 and Chapter 4, there are multiple models commonly used in the simulation and design of vertical ground heat exchanger systems. Validation of these current methodologies is done several ways. Judkoff (1988) described three different techniques for

validating energy analysis simulations; each of these will be used to some degree in this work. First, analytical verification may be used to check model performance against a standard analytical model; however, this is limited to cases for which an analytical solution may be derived. Second, empirical/experimental validation provides a greater level of scrutiny for the models, in that a real system can be simulated and results compared to actual measured data. The simulated and physical systems are in this case equivalent, at least to the extent that measured physical parameters and experimental data are precisely measured. Third, intermodel comparison may be utilized to explore the relative performance of two or more simulation methodologies. This technique has the advantage of being able to simulate anything from simple systems to extremely complex ones. Though there is no external source for comparing the results, this type of comparison is often useful in finding a model's limitations, as well as problems with its implementation.

This work uses a mix of all three techniques in validating existing GHX simulation methodologies. To begin, multiple potential experimental data sets are identified and evaluated in Section 5.1. Since data from a simple thermal response test, built for the purpose of validating test analysis procedures, is available (Beier et al., 2011), models may be compared to this experimental data; since this thermal response test situation approximates a line source, analytical verification against the line source solution (Ingersoll et al., 1954) is also performed, and the relative performance of different simulation methods with respect to one another is compared. For other data sets, those of actual installed heating/cooling systems, hourly simulation results may be used to validate the short-term performance of the models; at the same time, validation of design methods, which are typically concerned with just the extreme temperatures seen during operation, may also be performed, though this is the explicit focus of Chapter 6. The overarching goal is an *en masse* validation of multiple short time step simulations and design procedures

against multiple data sets, as the literature is short on large-scope ground heat exchanger validations, particularly with regard to design procedures.

5.1 Data Sets for Experimental Validation

At present, there is very little large-scale validation of ground heat exchanger models in the literature; models are typically only validated against a single data set, which may not be best suited for experimental validation due to reasons such as those set forth by Yavuzturk and Spitler (2001) or Bertagnolio et al. (2012). Spitler et al. (2009) presented a round-robin intermodel comparison of several different models against one data set, with mixed results: Although most methods did perform acceptably well, some differences between models of similar genesis could not (and as yet have not) been explained due to the round-robin nature of the work. However, there is little other work in the literature regarding intermodel comparison of ground heat exchanger models. This section details the validation of several different simulation methods and design procedures against a range of experimental data sets.

Multiple experimental data sets exist that can be used for validation purposes. The essential features of an acceptable data set for usage in validation of simulations, as discussed in Chapter 2, are long-term measurements of temperatures—at a minimum, the temperatures entering and exiting the heat exchanger—as well as either the loop fluid flow rate or loading on the ground. Some of these sets have hourly (or sub-hourly) data available, while others only have daily data. Each data set will be presented here with a short summary of the relevant experimental parameters, followed by a discussion of the validation efforts that make use of each set.

5.1.1 Thermal Response Test "Sandbox"

Beier et al. (2011) constructed a horizontal borehole inside a laboratory, with the purpose of validating thermal response test analysis procedures. The results and data were later made publicly available for analysis projects such as experimental validation of system simulation. The single borehole, 18 m in length, is situated in a sand-filled box 1.8 m square. The sand is kept saturated by means of five perforated water lines interspersed throughout the box. The exterior walls of the box are maintained at uniform temperature (to resemble an "undisturbed" ground condition) by means of conditioned air circulated around the box; the initial undisturbed temperature was roughly 21 °C. The borehole itself is 126 mm in diameter, encased by a 0.2mm aluminum tube. The U-tube consists of 1" SDR-11 HDPE piping, and the borehole is filled with a bentonite grout consisting of 20% solids.

The thermal conductivity of the grout was measured, using a non-steady state probe, as 0.73 W/m-K, while the same technique was used at multiple points inside the box to determine an approximate soil thermal conductivity of 2.82 W/m-K. Fluid was circulated through the borehole for 52 hours at an average rate of 0.197 L/s, while heat was added by means of an electric resistance unit at a rate of 1056 W. Supply and return temperatures, as well as temperatures elsewhere in the sand and flow data, were recorded every minute. Figure 4-1 shows the supply and return temperatures for the 52-hour test. After the initial warm-up period has ended (roughly 10 hours, or 720 minutes), the calculated heat transfer rate based on the difference between the temperatures differs from the power supplied by the heater by an average of only 4 W, showing that this system has been adequately isolated and does indeed behave very similarly to a typical thermal response test.

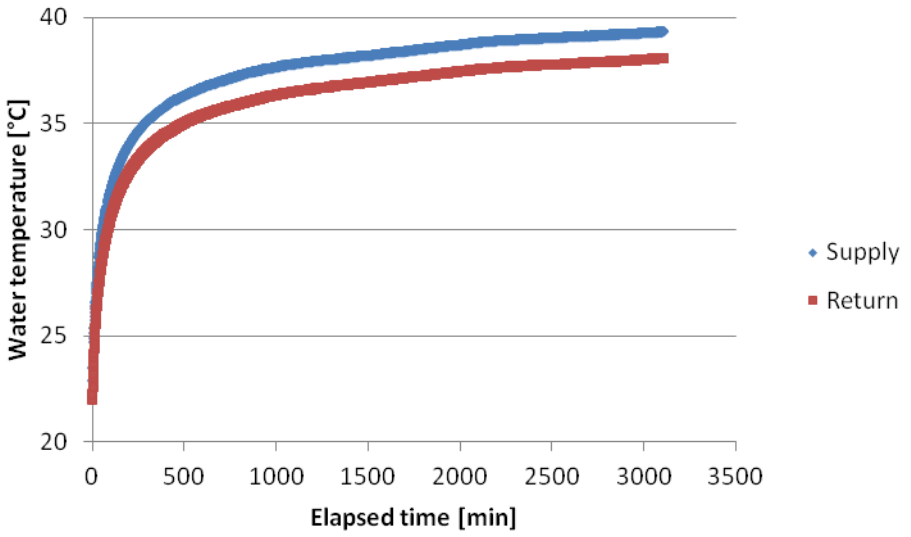

Figure 5-1: Sandbox test results

5.1.2 Hybrid Ground Source Heat Pump Test Facility

Hern (2004) designed and constructed a hybrid ground source heat pump test facility at Oklahoma State University in Stillwater OK. The ground heat exchanger consists of four vertical as well as one horizontal borehole, each 114 mm in diameter and averaging about 75 m in length, spaced 6 m apart; however, only three of the vertical boreholes were in use during the time in which the experimental data used here was taken. The cooling capacity of the ground loop is supplemented by a three-ton evaporative cooling tower, connected to the loop via a plate heat exchanger in order to maintain a closed-loop system. Additional supplemental cooling was available via a pond loop heat exchanger, although this was not used for this particular experiment. Two three-ton water-to-water heat pumps are used in the facility; one is configured to operate in cooling mode, while the other operates only in heating mode. For the majority of the experiment, only one heat pump is in operation; later in the experiment, the two are run simultaneously for a short time.

Hern (2004) measured the thermal properties in each borehole, finding a narrow range of values for each parameter. On average, the conductivity of the soil around the boreholes was 2.55 W/m-K (1.473 Btu/hr-ft-°F), with an average borehole thermal resistance of 0.162 m-K/W (0.280 hr-ft-°F/Btu); the mean undisturbed ground temperature for the three boreholes was 17.3°C (63.1°F). The fluid flow rate, for times when the system was on and operational, was roughly 0.63 L/s (10 GPM). The system was instrumented with flow meters and thermocouples at a many locations within the system, including at both the inlet and outlet of each borehole. Data were recorded at one minute intervals for the eighteen-month period from March 2005 through August 2006, and then automatically post-processed into averages of 10-minute duration. The experiment was run continuously except for very brief periods of computer downtime and regular system maintenance; for this analysis, the first twelve months of data were used, as this preceded the beginning of simultaneous heating and cooling loads with two heat pumps in operation. Figure 5-2 below shows the heat pump entering and exiting (or the GHX exiting and entering) fluid temperatures loads on the ground heat exchanger for the first 12 months of operation, plotted as daily averages, while Figure 5-3 shows the total heat extracted from the ground on a daily basis, in kWh/day. These loads were computed based on the measured temperature difference across the three boreholes in operation. There are two distinct splits in the data, one in late March and the other at the end of November, which coincide with the transition between heating and cooling modes. Times with zero load, such as early December and parts of February, are incidents with no data, meaning the system was temporarily down for computer upkeep or routine system maintenance. Additionally, since the ground loads were computed based off of the system flow rate and the temperature difference across the ground heat exchanger, regardless of whether the heat pump was actually in operation, there are some hours with a "heating" load during cooling season or a "cooling" load in heating season. These are preserved in the data to allow for a complete description of the ground thermal behavior.

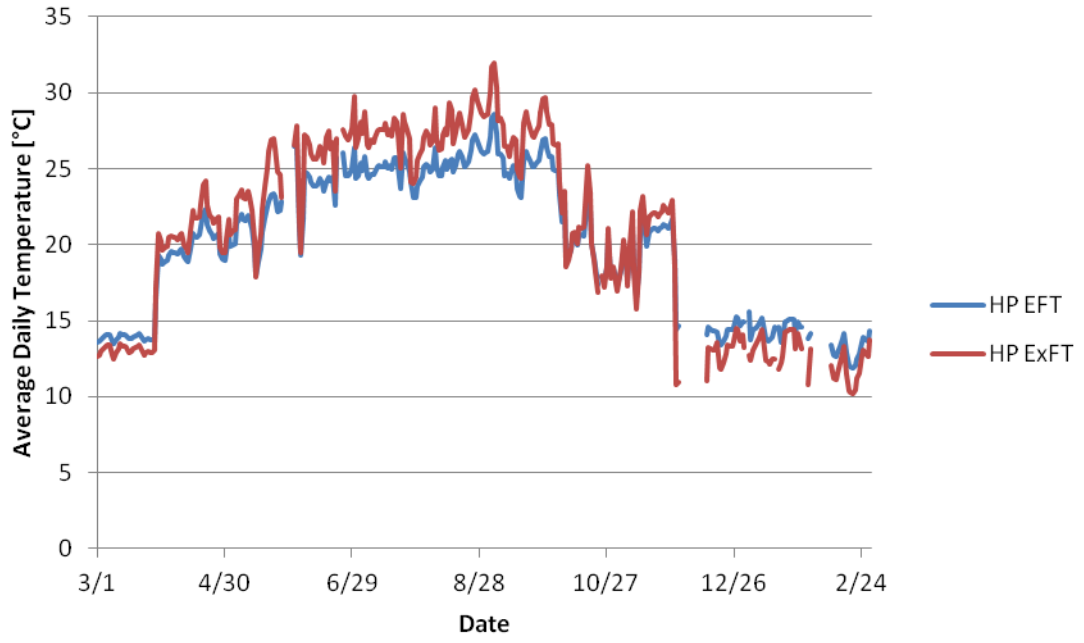

Figure 5-2: Stillwater experimental daily average temperatures

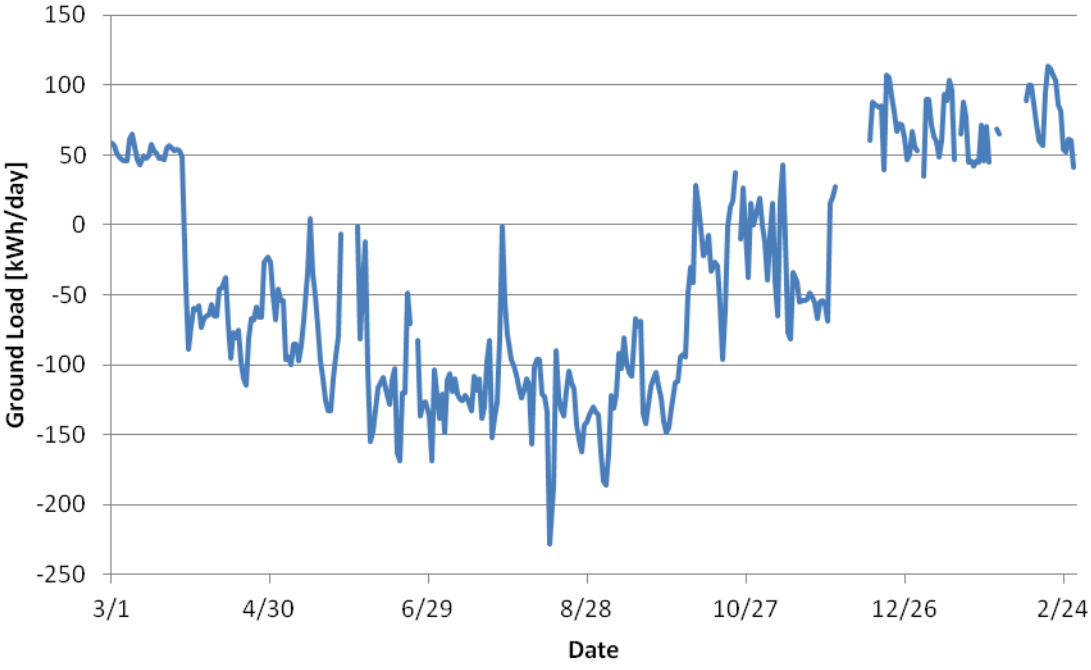

Figure 5-3: Stillwater experimental daily total ground heat extraction

5.1.3 Small University Monitored Borehole System

In 2005, the Universidad Politéchnica de Valencia installed a six-borehole ground heat exchanger system as part of their research in energy-efficient buildings (Montagud et al., 2011). Specifically, the system was designed to facilitate comparison of an actual ground-source heat pump system to a standard air-source system. The Valencia system consists of six boreholes, each 50 m deep, in a 2x3 rectangular formation spaced 3 m apart. The boreholes were backfilled with the same type of soil surrounding the borefield, which possessed a measured conductivity of 1.6 W/m-K. With its location near the Mediterranean coast of Spain, the undisturbed ground temperature at the site is 19.5 °C. The nominal system flow rate is 0.76 L/s, or about 2 GPM per borehole.

For this system, temperatures were measured at both the inlet and outlet of each borehole, as well as the heat pump, at ten-minute increments for six years of weekday daytime operation. The flow rate going out to the borefield and the power consumption of both heat pump and circulating pump were also measured. Figure 5-4 shows the heat exchanger inlet and outlet temperatures for 2010, the fifth full year of operation, averaged to give daily values. Figure 5-5 shows the total heat extracted from the ground on a daily basis, in kWh/day. The system operates in heating mode from January through April, and again from late October until the end of the year. In this analysis, the first three years of operation are stop-and-start, with 15 of the 36 months, including eight consecutive, not running or recording data. As described in Cullin et al. (2014), only the final three years of data, when the system is in continuous operation and shows a typical cyclical load profile, are used in this analysis.

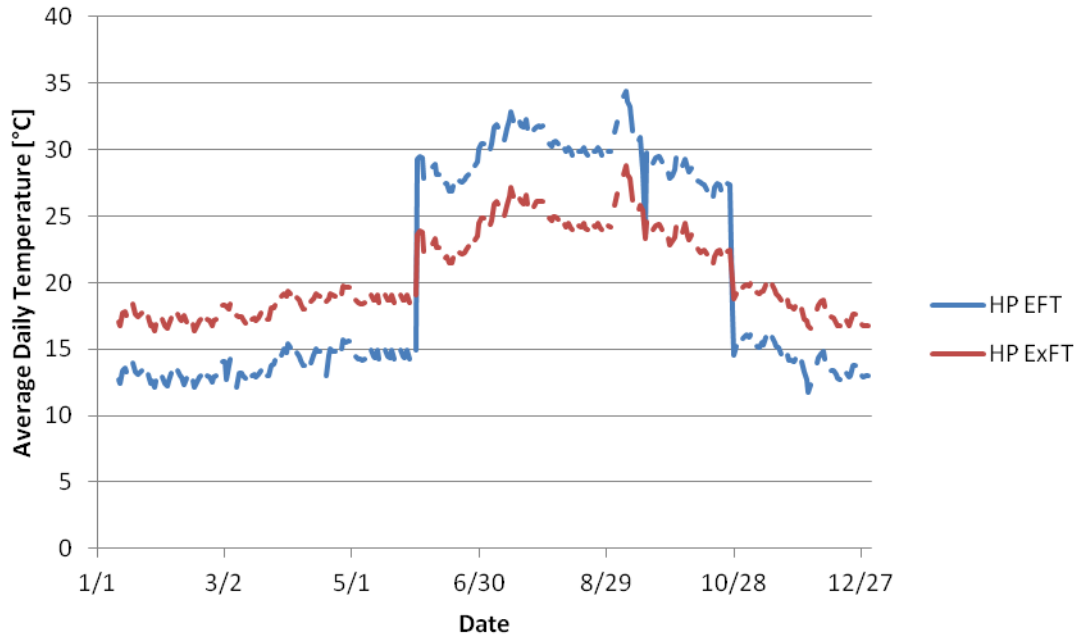

Figure 5-4: Valencia experimental daily average temperatures

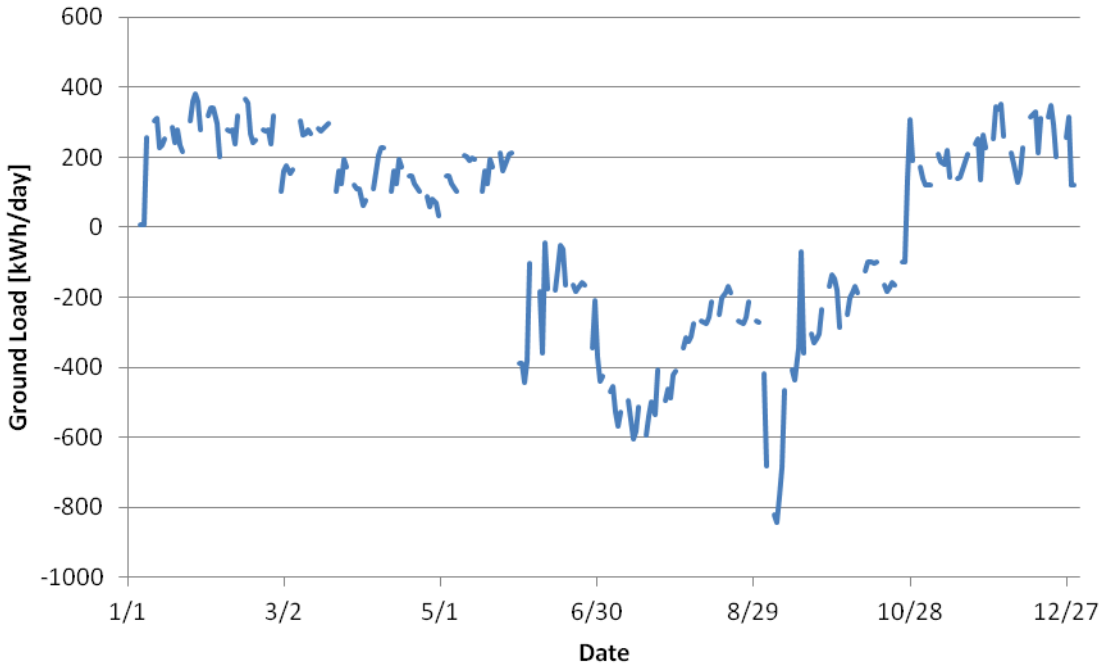

Figure 5-5: Valencia experimental daily total ground heat extraction

5.1.4 Large University Monitored Borehole System

Researchers at De Montfort University in Leicester, United Kingdom, have designed and installed a large-scale domestic GSHP system to provide data for performance evaluation, control strategy assessment, and model validation (Naicker and Rees, 2011). The GHX consists of 56 boreholes, each 100m (328ft) deep; the borefield is split into two arrays with 37 below the building's courtyard and the remaining 19 outside the building. Thermal conductivity testing gave an average value of 3.2 W/m-K (1.85 Btu/hr-ft-°F), with a specified grout thermal conductivity of 2.0 W/m-K (1.16 Btu/hr-ft-°F); this latter value is representative of the entire borehole, as only the top 25% of each borehole was grouted, with the rest being backfilled by cuttings produced during the drilling process. The borefield is served by a variable speed pump with a maximum flow rate of 30 L/s (476 GPM); the operating fluid is a 20% propylene glycol mixture.

Operation and monitoring of the system began in December 2009. However, measurements of system flow rate were not available until March 2010. For those first months, then, flow data were filled in based off of similar patterns later in the experiment. Figures 5-6 and 5-7 below show the heat pump entering and exiting fluid temperatures, as well as the daily heat rejected to the ground (negative numbers indicate rejection), for the first year of operation.

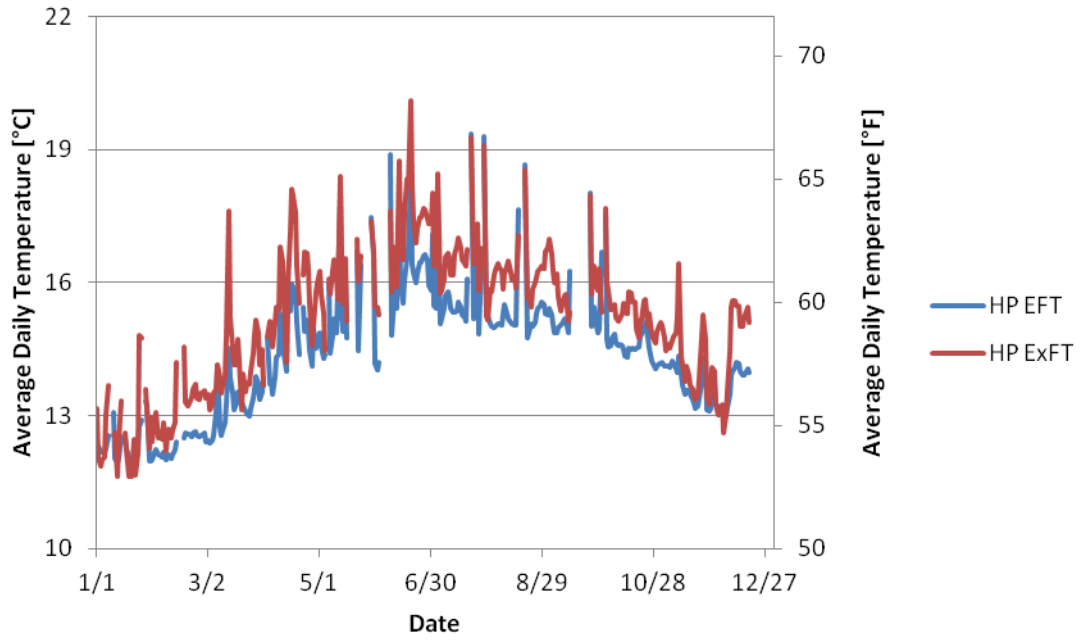

Figure 5-6: Leicester experimental daily average temperatures

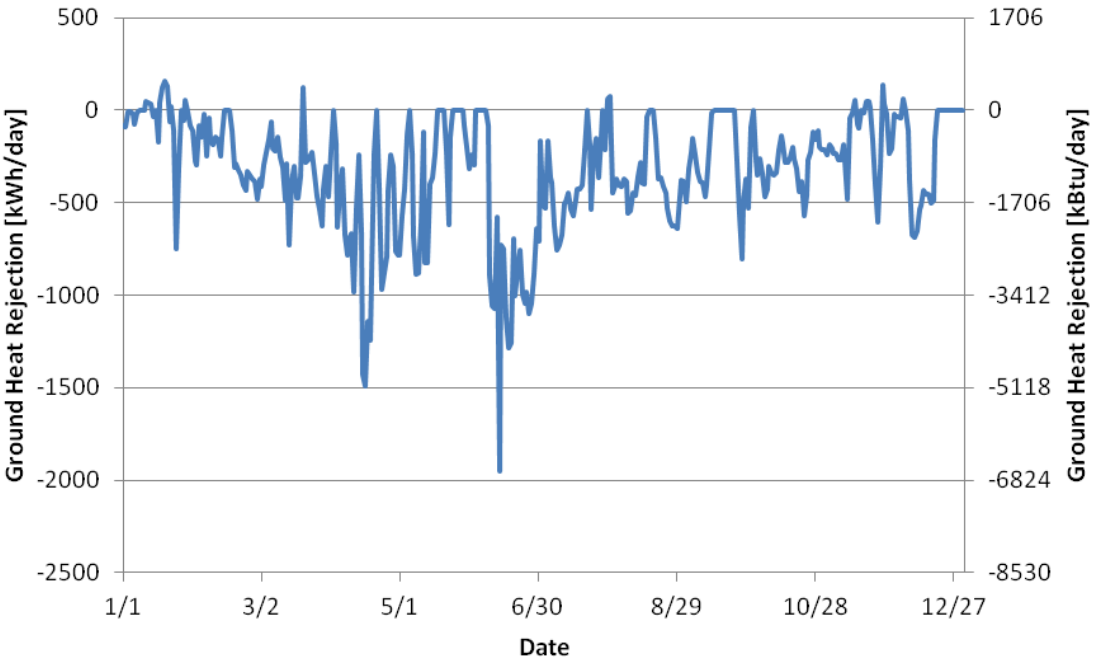

Figure 5-7: Leicester experimental daily total heat rejection

5.2 Experimental Validation

Each data set presented in Section 5.1 has been used to validate one or more of the simulation methods discussed in Chapter 4, including the newly-developed multi-coordinate model.

5.2.1 Validation Using Sandbox Data

The "sandbox" experiment by Beier et al. (2011) utilizes only a single borehole, and can be readily modeled as a line source. However, it can also be used to test a number of models, including the new multi-coordinate model described in Section 4.2. This model can be compared to both the line source and the experimental data; since the line source assumes an infinite length—that is, no end effects—there will likely be some difference between the experiment and the analytical equation. Additionally, the multi-coordinate model will be compared with the g-function model as implemented in the HVACSIM+ environment; this g-function model has been previously validated against the OSU HGSHP experimental data set (Gentry, 2007).

For this validation, the Ingersoll et al. (1954) formulation of the line source solution is used to find the temperature *T* of interest at a distance *r* from the source:

$$T(r) = T_0 - \frac{q}{4\pi k}\int_x^\infty \frac{e^{-x}}{x}\,dx \tag{5-1}$$

with

$$x = \frac{r^2}{4\alpha t} \tag{5-2}$$

where:

r is the radial distance from the heat source, in m;

T_0 is the initial uniform soil temperature, in °C;

q is the source heat transfer rate per unit length, in W/m;

k is the soil thermal conductivity, in W/m-K;

α is the soil thermal diffusivity, in m^2/s; and

t is the time elapsed from the instantiation of the heat source, in s.

The values of the integral were taken from a pre-computed table in the Ingersoll et al. (1954) work.

Since the thermal properties of the sandbox borehole bear some experimental uncertainty that is sure to translate to any potential match to the line source, and Beier et al. (2011) give a range of values for the borehole thermal resistance in particular, a parameter estimation was performed on the experimental data to determine the best values for the soil thermal conductivity and borehole thermal resistance. After discarding the warmup period of the first eight hours, values of 2.826 W/m-K for soil conductivity and 0.1515 K/(W/m) for the borehole resistance were found to provide the best match. The estimated conductivity matches almost exactly with the quoted value of 2.822 W/m-K, and is certainly within experimental uncertainty. Beier et al. (2011) give a range of 0.164-0.187 K/(W/m) for the borehole thermal resistance; as a comparison, the multipole method (Bennet et al., 1987; Claesson and Hellström, 2011) gives an analytical value of 0.2055 K/(W/m). It is not clear how this lower resistance value occurred, although one possibility is that the borehole receives a fin-like performance boost from the aluminum borehole wall. Additionally, the multipole resistance was computed using the average measured value for thermal conductivity; if the real value is a bit higher, then the borehole resistance will decrease. Since the multi-coordinate model only has a soil region and a grout region radial from the borehole centroid, it does not have the capability at present to handle any additional components such as a borehole casing.

The results of the comparison between the three methods and the experimental data are shown below in Figure 5-8. After roughly 8-10 hours, the experiment does indeed behave very much like a line source (RMSE = 0.76 °C overall), as shown by the nearly identical values after this point (RMSE = 0.08 °C after the first 8 hours); this close match is due to the tuning of the soil conductivity and borehole resistance described above. However, the beginning hours do not warm as quickly in the experiment as a pure line source would suggest; this is perhaps a consequence of the thermal mass of the fluid, which delays the transmission of the heat from the fluid to the soil.

HVACSIM+, using an hourly time step and assuming a borehole resistance that is the midpoint of the experimental range (0.175 K/(W/m)), follows the experimental data the closest (RMSE = 0.44 °C), although it begins to overpredict the fluid temperature toward the end of the simulation. The multi-coordinate model, using the five capacitance lumps identified in Chapter 4, predicts the temperatures fairly closely as well (RMSE = 0.13 °C after the first eight hours), although the initial behavior of the MCM for this test is fairly dissimilar to the experimental data. The MCM jumps to a higher temperature initially, but increases more slowly than the experimental data; in contrast, the HVACSIM+ g-function model takes longer to show a temperature change since it is an hourly simulation, but increases rapidly before slightly overshooting the experimental results.

This suggests that, for both models, the thermal resistance (and, in the case of the MCM, capacitance as well) could be further refined for a better match.

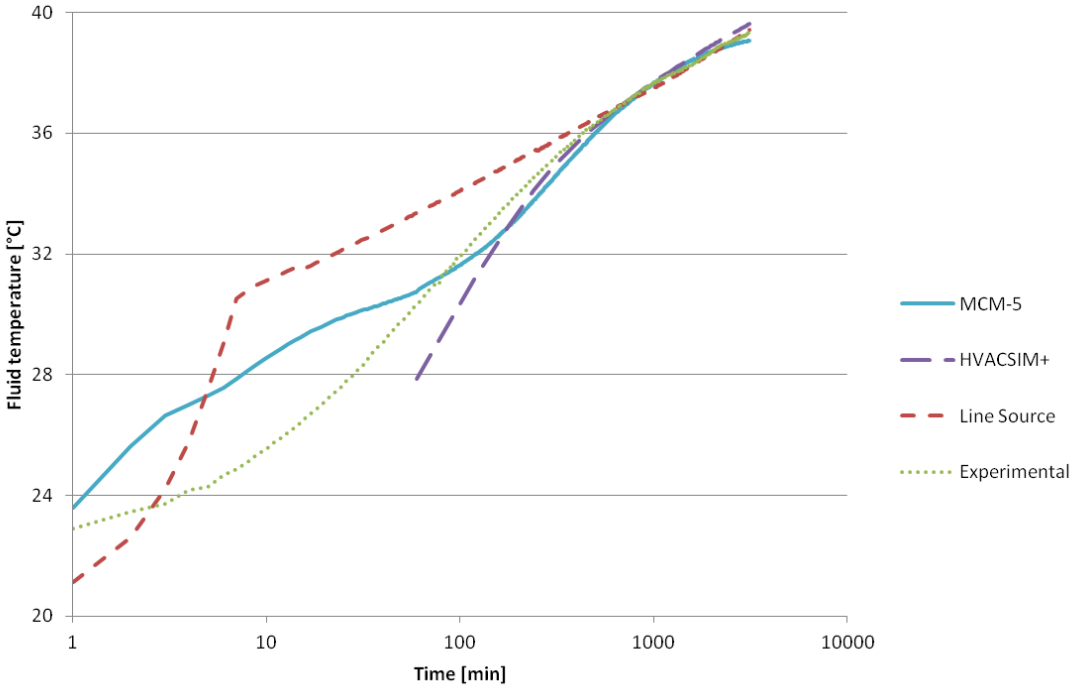

Figure 5-8: Model validation against sandbox experimental data

5.2.2 Validation Using OSU HGSHP Data

In order to test the multi-coordinate model described in Chapter for a more typical application, it will be validated against hourly experimental data from the hybrid ground source heat pump facility. Simulations were performed in the EnergyPlus environment using a 15-minute time step, with the g-function approach as implemented by Fisher et al. (2006).

Figure 5-9 shows the heat pump entering fluid temperature as determined with each simulation methodologies, in addition to the experimental values, on a daily average basis. To isolate the behavior of the heat exchanger itself, the loads input into EnergyPlus were computed based only on the flow rate and temperature difference across the borefield; heat pumps and other equipment

were neglected for this exercise. In addition, although 18 months of experimental data are available, only the first 12 months were utilized, as EnergyPlus restricts hourly input data from an external file to 8760 or 8784 hours.

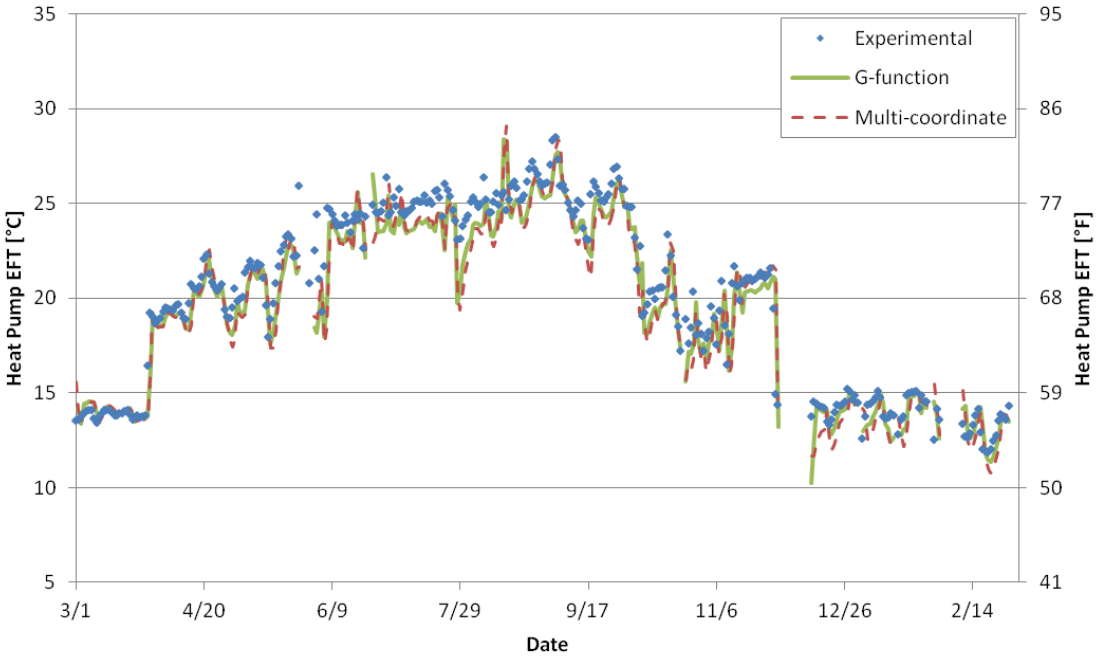

Figure 5-9: Validation of HVACSIM+ and MCM with Stillwater data – Daily averages

Figure 5-9 shows that both models follow the experimental data fairly closely, with RMSEs of 1.8 °C (3.3 °F) for the g-function model and 2.0 °C (3.5°F) for the multi-coordinate model. These values were computed only for hours with nonzero flow; periods with no flow but with measured temperature data, such as near the end of May, are not included in the RMSE calculation. Qualitatively, the g-function model follows the hourly variations more closely than does the multi-coordinate model; the multi-coordinate scheme, while following the overall EFT trend, tends to respond with a less pronounced peak magnitude, than either the g-function model or the actual experiment. This can be seen in the two sample days plotted in Figure 5-10; while the multi-coordinate model follows the same trends as the g-function model, the temperature swings are somewhat dampened. This is likely due to a difference in how the borehole

resistances are handled; the g-function model uses a single resistance between a representative single pipe and the borehole wall, while the multi-coordinate model utilizes separate resistances between the actual legs of the U-tube and the borehole wall as well as between U-tube legs; both, however, use the mutlipole method (Claesson and Hellström, 2011) to compute these resistances.

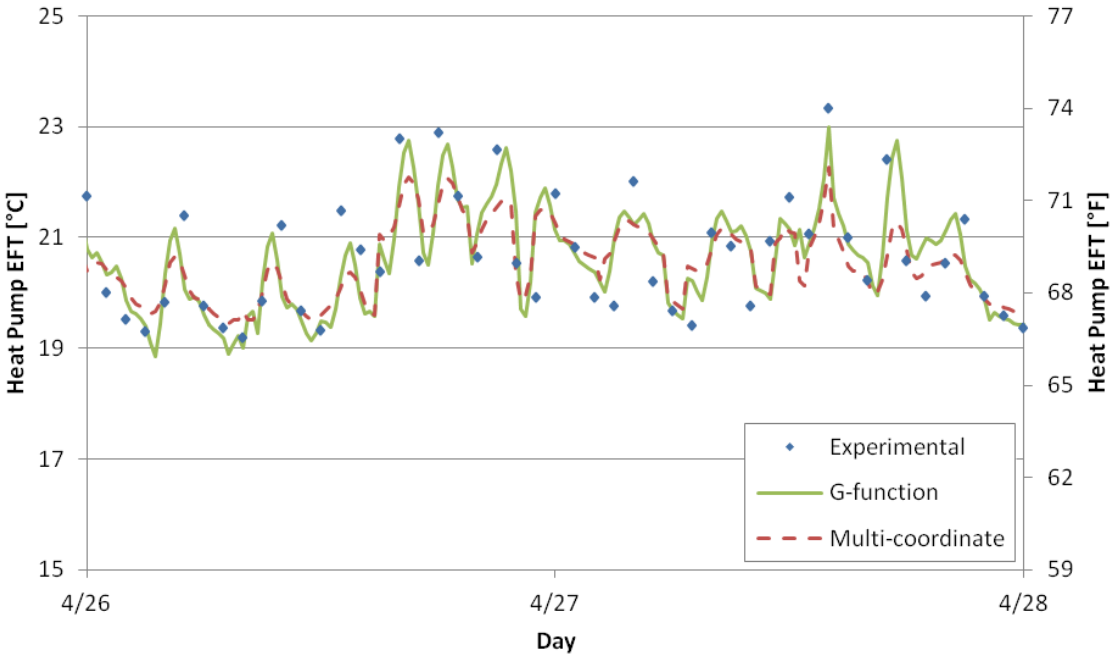

Figure 5-10: OSU HGSHP facility experimental validation - Sample days

5.2.3 Validation Using Small University System Data

The data for the university borehole system in Valencia has been used to validate both design procedures and shorter time step simulations. First, the simulation used in the design tool developed by Spitler (2000) and improved by Cullin (2009) was validated based on monthly values. Validation of the simulation in the design tool has been previously performed by Cullin (2009), but this provides another data set for comparison. Then, the design procedure in the tool itself, as well as the ASHRAE design equation, was validated against the Valencia data; this procedure is used with multiple data sets in an expanded test of these methods in Chapter 6.

Finally, the Valencia data is used in a validation of shorter time step simulations, namely the g-function method in HVACSIM+ and the multi-coordinate model (detailed in Chapter 4) in EnergyPlus.

5.2.3.1 Validation of Simulation Used in Design Tool

Before exploring the accuracy of the design procedures, it is first necessary to compare the underlying monthly simulation to actual experimental results. A comparison of the monthly simulation to data from the Valencia GHX facility is given in Figures 5-11 through 5-14. For all six years of observation, the average monthly heat injection rate to the borefield is plotted in Figure 5-11, with positive values indicating heat rejection from the system into the ground (i.e., a cooling load on the system, versus a heating load for negative values). The heat injection rates are fairly low for the first year of operation, before a period of one and a half years wherein the experiment was only running for two months, as previously explained. After resumption, the heat extraction rates began to stabilize into a fairly consistent annual cycle.

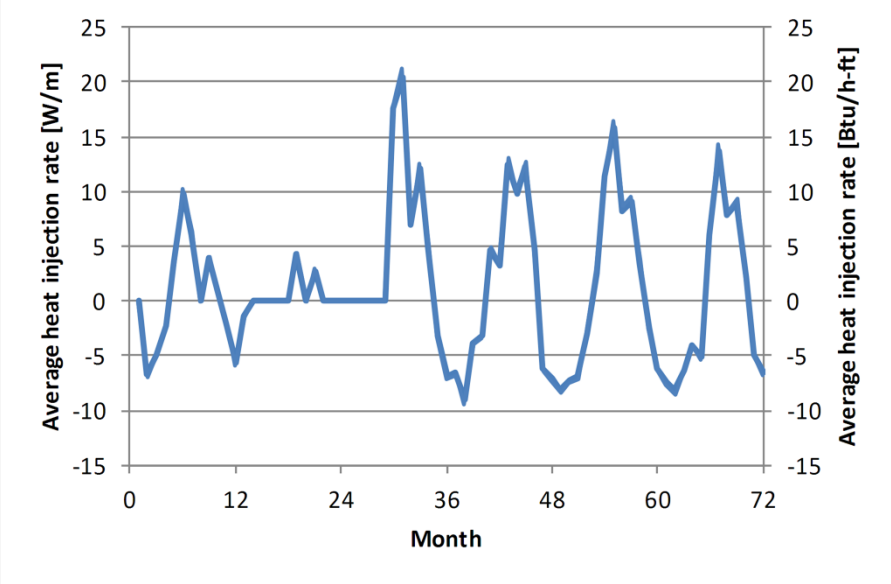

Figure 5-11: Valencia monthly experimental average heat extraction rate

Figure 5-12 shows the heat pump entering fluid temperature at the end of each month for both the experiment as well as the simulated results. The simulation tool reports the "average" heat pump EFT as the temperature at the end of the month due to the average heat extraction rate for that month. In processing the experimental data, the "average" heat pump EFT was taken to be the average value over the last two days of operation during that month (so, discounting weekends, holidays, and other off-periods), which was then weighted by runtime. The temperature used during this weighting procedure for the non-running periods was the minimum reported temperature (if in cooling mode) or the maximum reported temperature (if in heating mode), with the active mode being dictated by the net heat extracted from the ground during that particular month. The RMSE in the simulation results is quite reasonable, at 1.3°C (2.3°F), including only those months when the heat pump is operating—in other words, when the average heat extraction rate is nonzero. The match could be improved, particularly during the months in the middle of each heating/cooling cycle, by improving the weighting procedure used to determine a representative "average" heat pump EFT for the experimental data.

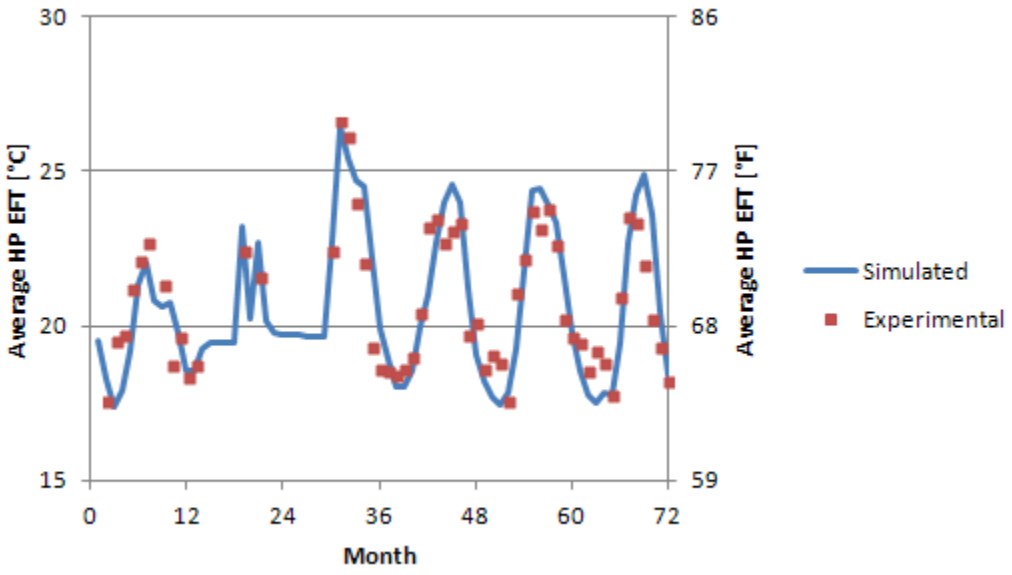

Figure 5-12: Valencia month-end heat pump EFT comparison

Figures 5-13 and 5-14 show, respectively, the maximum and minimum heat pump EFTs for each month, taken from the one-minute data. For the peak temperatures, RMSEs are less useful as a measure of simulation validity due to the fact that the simulation by its nature can predict neither a maximum temperature when there is no cooling load, nor a minimum temperature without a heating load. Due to factors such as on/off cycling and environmental influence, the maximum and minimum peak temperatures are not expected to match in winter and summer months, respectively. For the maximum EFTs during cooling months, as well as minimum EFTs during heating months, the values do indeed match quite well.

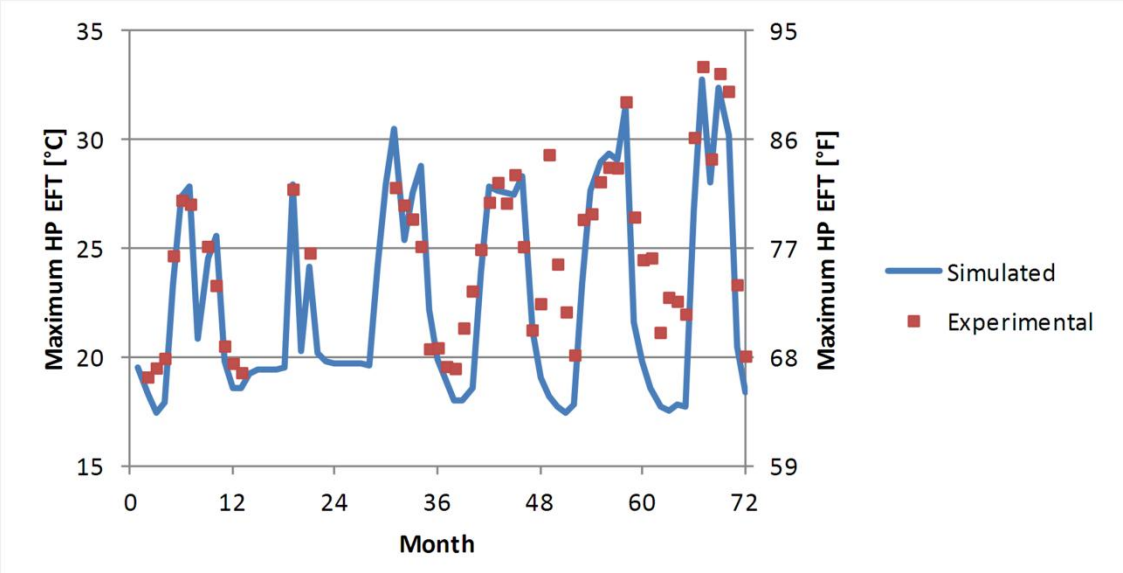

Figure 5-13: Valencia maximum heat pump EFT comparison

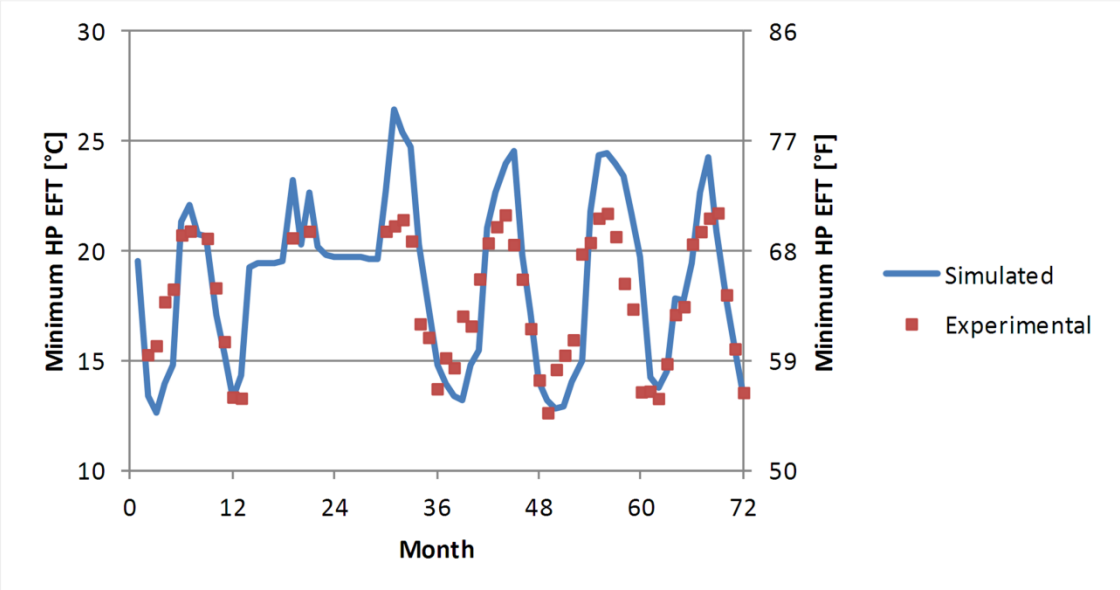

Figure 5-14: Valencia minimum heat pump EFT comparison

As mentioned above, these data are taken from the one-minute data. In month 49, which corresponds to January 2009, Figure 11 shows a high temperature of 29.3°C (84.8°F). This seems rather high for January, but a check of the one-minute results shows that this temperature is measured only once, when there is a sudden upward anomaly for a few minutes at about 6 a.m. on January 2nd. The heat pump is actually in heating mode at that moment, but there were cooling loads during January, and we have simply taken the maximum heat pump entering fluid temperature regardless of operation mode. For months with both modes of operation, perhaps it would be better to report maximum heat pump EFT only for cooling operation.

Discounting the month after the restart of operation in the third year, the simulation only misses the absolute maximum heat pump entering fluid temperature over the six years of operation by 0.6°C (1.1ºF), and the minimum by 0.3°C (0.5ºF). Overall, this is quite acceptable for a design tool that utilizes a monthly simulation, especially considering some of the issues in determining the peak loads themselves. However, in June of 2007, after the system has been off for some

months, the heat pump entering fluid temperature hits 35.9°C (96.6°F) on the 5th day of operation. On that day, the flow rate was about half of the normal flow rate, presumably causing a decrease in the pipe interior convection coefficient and an increase in the borehole thermal resistance, leading to the high heat pump entering fluid temperature.

For the peak heating and cooling loads, there is a noticeable mismatch in the timing of the peak loads between experiment (where they may occur any time during the month) and the simulation (where they are assumed to occur at the end of the month.). As detailed by Cullin and Spitler (2011), this can have a moderate impact on the accuracy of the simulated temperatures. While the simulation tool always assesses the peak load at the end of the month, based on the heat pump EFT at the end of said month, for this facility the peak load is frequently in the middle of the month. Since an entire month's worth of heating or cooling load has not yet been applied in actuality, one would expect the experimental values to differ from the simulated values. This behavior could be accounted for, as Cullin (2008) described, by utilizing an hourly simulation, but at the cost of a substantial computation time increase.

5.2.3.2 Validation of Simulation-Based Design Tool

Design methods typically assume the same loads to occur year after year. So, for purposes of validating the design methods, the average loads from the last three years of operation (2008-2010), when the monthly heating and cooling loads had stabilized to something approaching steady periodic conditions, were used. These loads, listed later in Table 6-4, were then applied these for a six-year period, with a maximum heat pump entering fluid temperature of 30°C (86°F) as the design condition. For the design tool, this yielded a total borehole length of 314 m (1030 ft.), which is an overprediction of 4.7%. This level of overprediction is quite acceptable for a simplified design tool. We also investigated the effects of uncertainty in the heat

extraction/rejection rates (±3%) and soil conductivity (±20%). These are summarized in Table 5-1, which gives estimates of the minimum and maximum overprediction, taking into account the uncertainties in the inputs. Accounting for these uncertainties suggests the simulation-based design tool could underpredict by about 2% and overpredict by as much as 12%.

Table 5-1: Sensitivity of simulation-based design tool to uncertainty in input parameters

Input parameter varied	Minimum uncertainty	Maximum Uncertainty
Regular inputs	4.7%	
Heat transfer rate	1.7%	7.7%
Thermal conductivity	0.4%	9.0%
Both HTR and TC	-2.3%	12.0%

The simulation tool provides a maximum heat pump entering fluid temperature 0.64°C (1.15°F) lower than the experimentally measured maximum over the nearly six years of operation. To explore the impact of this error on the design length of the GHX, a sensitivity coefficient approach (Spitler et al., 1999) may be used. With this approach, the error in GHX size may be estimated from the error in peak heat pump EFT by approximating partial derivatives:

$$E_{size} \approx \frac{\partial H}{\partial (EFT_{peak})} \cdot E_{EFT_{peak}} \approx \frac{\Delta H}{\Delta (EFT_{peak})} \cdot E_{EFT_{peak}} \tag{5-3}$$

For the Valencia system, the partial derivative is $\frac{\Delta H}{\Delta (EFT_{peak})} = 18.8 \frac{m}{°C} = 34.2 \frac{ft}{°F}$. Therefore, the error in the design length due to a 0.64°C (1.15°F) error in the heat pump EFT is 12.0m (39.4ft), or 4% of the total size of the GHX.

When using a simulation tool, however, it is frequently the case that a representative load profile, repeating annually, is used, instead of the sequence of individual monthly loads used here. To check the sensitivity of the design tool to the load profile, the analysis was repeated, using the 2009 load data as representative of a typical year. (The 2009 year was selected since it contains the highest single monthly average heat injection rate, apart from the two months immediately after the long off-period.) In this instance, the partial derivative is $\frac{\Delta H}{\Delta(EFT_{peak})} = 22.2\frac{m}{°C} = 39.6\frac{ft}{°F}$. For the same 0.64°C (1.15°F) error in the heat pump EFT, the corresponding sizing error is 14.2m (46.7ft), or 5% of the total size of the GHX. As this shows, the added error due to approximating the load as one representative year repeating cyclically, instead of distinct monthly values, is just an additional one percent.

One other potentially significant source of error in the simulation results is due to the uncertainty in the reported ground thermal conductivity. Laboratory analysis reported a 20% uncertainty in thermal conductivity, with a mean value of 1.43 W/m-K (0.826 Btu/hr-ft-°F). The sensitivity coefficient for the conductivity is $\frac{\Delta H}{\Delta(k_{ground})} = -45.4\frac{m}{W/m \cdot K} = -43.7\frac{ft}{Btu/hr \cdot ft \cdot °F}$. The negative value here indicates that the GHX size will decrease with increasing ground thermal conductivity, which agrees with fundamental engineering principles. Thus, an uncertainty of 20% in the value of the ground thermal conductivity used in the simulation tool would lead to an error in the GHX size of 13.0m (42.7ft), or roughly 4% of the total size of the GHX. Note that this value is very close to the error in design length initially seen; the uncertainty in the conductivity measurement could certainly explain some, if not most, of the error in the GHX sizing.

This approach may be repeated to analyze whether the choice of loads (specifically, using an average of the last three years over actual loads) makes any significant difference. However, the conclusion is that the errors shown in Table 2 are about the same whether or not the actual monthly loads are used instead of the average of the last three years. Furthermore, the impact of using one typical year instead of the actual monthly loads is only about 1%. This strongly suggests that the approach of using the average loads for the last three years is appropriate.

5.2.3.3 Validation of ASHRAE Handbook Method

The handbook method was validated in a similar way – the annual net heat transfer rate to the ground was again estimated based on the last three years of operation. This method is summarized in greater detail in Chapter 6, including Table 6-6 which summarizes the parameters that were used in the design equation. The design equation returns a GHX length of 610 m (2000 ft) for the facility in Valencia. In actuality, the installed system is 300 m (980 ft). For the Valencia GHX, then, the value produced from the design equation is 103% greater than the actual installed system length—that is, the method overpredicts the required size by a factor of two. Certainly, some of this error could be attributable to inaccuracies in the input variables. However, a quick parametric study demonstrates that, at most, only about 9% of the discrepancy could be due to inaccurate input parameters, as shown in Table 5-2. Values not listed in Table 5-2, such as the short-circuiting loss factor, only had an impact of less than 0.5% and therefore were not included in the table. Furthermore, as described in the next section, the method has surprisingly little sensitivity to the length of the design period. In repeating this validation exercise with other data sets, Chapter 6 examines why exactly there is such a marked deviation between the handbook method and the actual experimental results.

Table 5-2: Sensitivity of handbook method to uncertainty in input parameters

Input parameter varied	Minimum uncertainty	Maximum Uncertainty
Regular inputs	102.9%	
Heat transfer rate	101.1%	104.7%
Thermal conductivity	102.5%	104.5%
Both HTR and TC	99.1%	107.3%

5.2.3.4 Design Methods' Sensitivity to Design Period

Because the design period can be very important for buildings with unbalanced heat rejection and extraction, and because we had to make some simplifications ot the loads, which were not constant from year-to-year, we thought it would be desirable to investigate the sensitivty to the design period. Figure 5-15 shows the design lengths for both the simulation-based design tool ("SBDT") and the handbook method ("Handbook"). Neither method in this case shows much sensitivity to the duration of the design period, suggesting that the simplification of the loads to a single repeating annual profile is a reasonable approximation in this case. Evidently, the six borehole configuration coupled with relatively balanced heat rejection/extraction rates is relatively insensitive to the design period. (Borehole fields with small numbers of boreholes tend to be less affected by heat buildup than borehole fields with large numbers of boreholes.) Furthermore, the length of the design period offers no explanation for the discrepancy between the two methods.

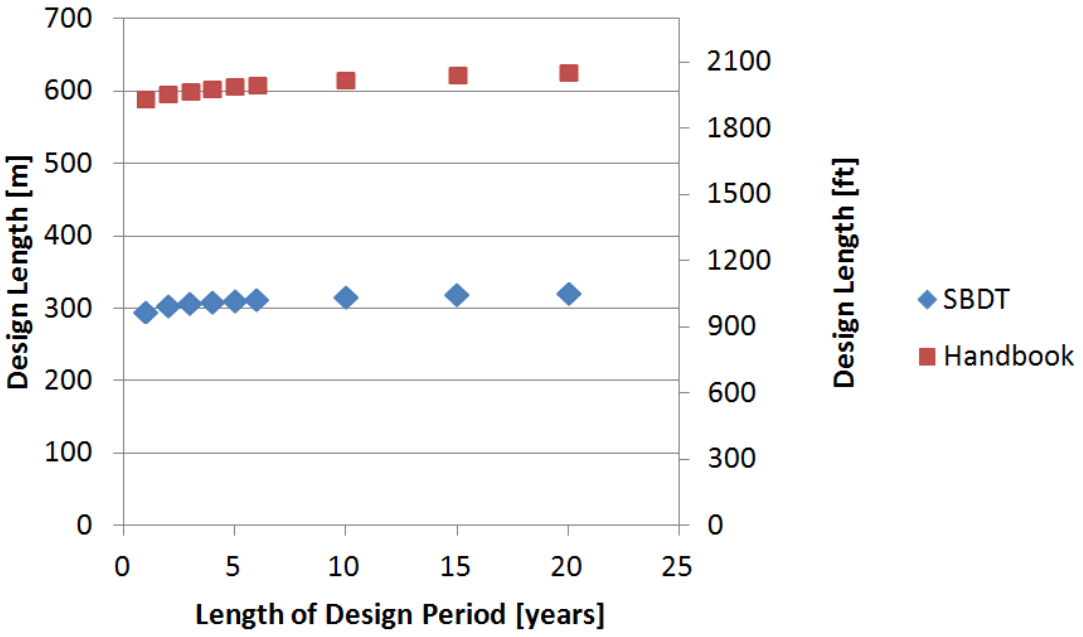

Figure 5-15: Exploration of design period for simulation-based design tool and handbook method

5.2.3.5 Validation of Shorter Time Step Models

The data from the Valencia GHX system has also been used in a validation of two models that run on shorter time steps, namely the g-function model in HVACSIM+ and the multi-coordinate model in EnergyPlus. G-function values were computed based on the analytical method of Malayappan and Spitler (2013). The enhanced multi-coordinate model, with its improved resistance/capacitance network, uses five capacitance lumps in the grout region, with three radial soil nodes, as discussed in Chapter 4. Other values for both models were based directly on experimental parameters. As the experimental data is provided in the form of load data, these loads were applied directly on the GHX on an hourly basis. The HVACSIM+ model uses an hourly time step, while the MCM runs on a 15-minute time step within the EnergyPlus environment.

Figure 5-16 shows the results of each simulation, plotted in comparison to the experimental value. The results are shown on the basis of average daily heat pump exiting (GHX entering) fluid temperature. Daily averaging was used because the actual system only runs from 6am-9pm on working days, and data were only reported during times when the heat pumps were running. Therefore, even though the models have no loads on the GHX during off hours, any comparison of hourly values would not mean much.

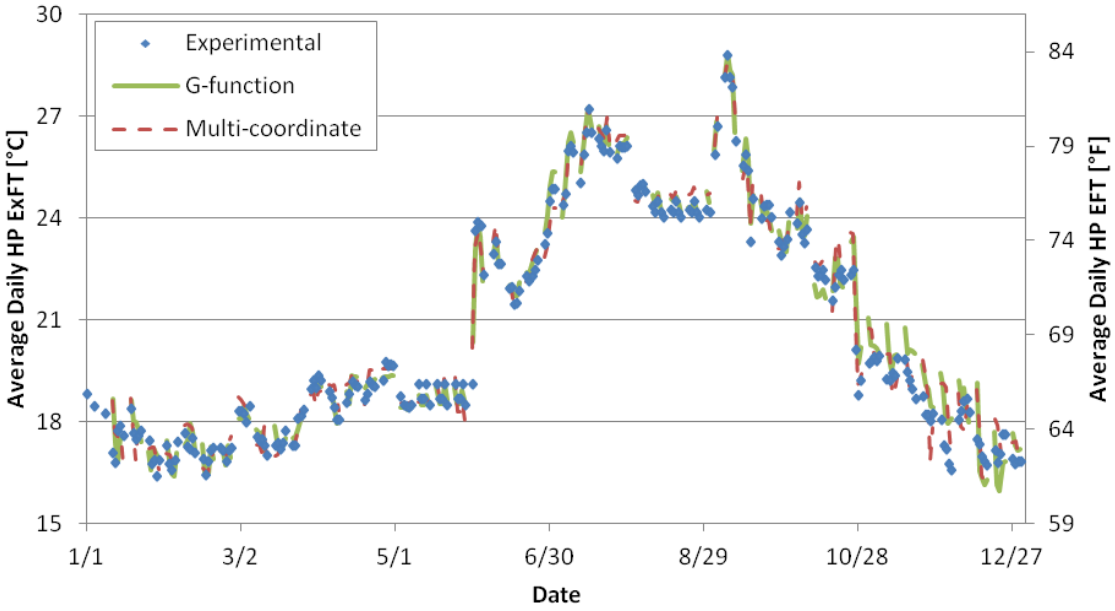

Figure 5-16: Validation of HVACSIM+ and MCM with Valencia data - Daily averages

For the HVACSIM+ simulation, the RMSE is 0.61°C (1.10°F), while for the MCM it is 0.75°C (1.35°F). The two models typically agree fairly well, although the multi-coordinate model shows several instances when it predicts a more gradual temperature change than the HVACSIM+ model, or than the experimental data. This can be seen more clearly in Figure 5-17, which shows the same daily average heat pump entering fluid temperature, zoomed in around the switch from heating mode to cooling mode. Particularly in the first and third weeks in the plot, the temperature slope between days is less than the HVACSIM+ model. In the context of the entire

year's data, there are multiple weeks, such as the second and third weeks in Figure 5-17, where the MCM starts the week with a more inaccurate initial EFT, and overcorrects in terms of the total heat transfer in a day or two. Coupled with the decreased day-to-day variation, this actually causes the RMSE to decrease as it pulls subsequent EFTs closer to the experimental values, even though the overall picture shows more difference between the two models than the RMSE perhaps suggests.

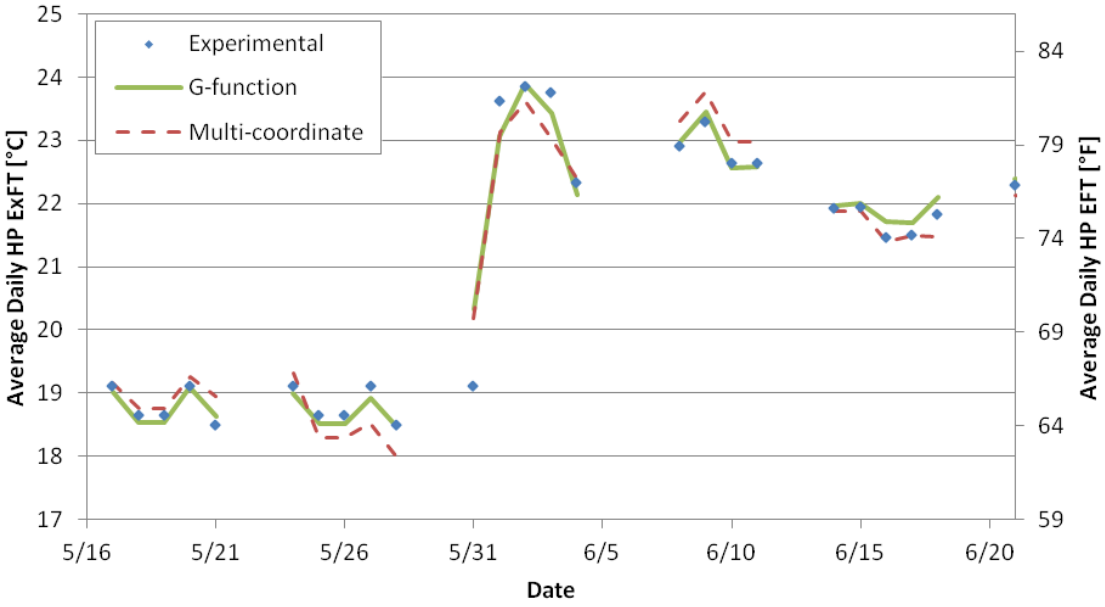

Figure 5-17: Valencia validation - Daily averages, zoomed around mode change

Figure 5-18 shows an hourly heat pump EFT comparison for two sample cooling days in May, corresponding to the first two days plotted in Figure 5-17. During this period, both simulations match quite well; for these two days, the RMSE of the g-function model is 0.09°C (0.16°F), and that of the multi-coordinate model is 0.12°C (0.22°F). Both models follow the trend of the experimental data well, though there are some small but noticeable differences. Primarily, the g-function model tends to match the temperature change from hour to hour (in other words, the slope of the plotted curve), even if the temperature values are a bit lower than the measured data.

The systematic difference could be attributable to a gradual shift in ground thermal properties over time, particularly the thermal conductivity (which could change due to, for example, a variation in moisture content). The multi-coordinate model shows, at times, a somewhat different slope, for example in the afternoon of the first day; there are hours where it predicts more rapid temperature change than the experiment, and hours where it predicts a smaller value. This suggests that some fine-tuning of the resistance-capacitance network might produce a more accurate result. In the off-cycles, when there is no load, the simulated temperatures slowly decrease toward the undisturbed ground temperature as expected (there is no experimental data when there is no load on the system).

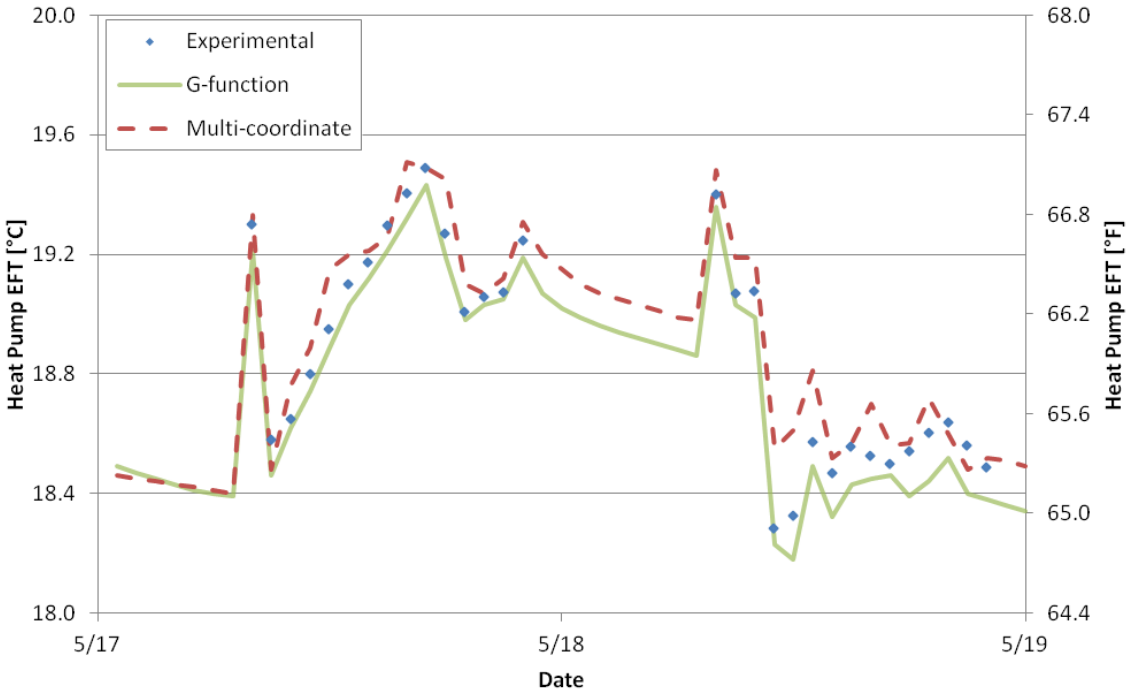

Figure 5-18: Valencia experimental validation - Sample days

5.2.4 Validation Using Large University System Data

The results of the HVACSIM+ simulation with the Leicester data are shown below in Figure 5-19. The overall match is reasonably good, with an RMSE of 0.57°C (1.03°F). The largest

differences can be seen in the summer period, where the simulation overpredicts the daily heat pump EFT by about 1°C (2°F); this could perhaps be attributable to changing physical parameters over the course of the year. This overprediction extends to the maximum daily average temperature, with a simulated value of 20.3°C (68.5°F), as opposed to an actual value of 19.3°C (66.8°F). Though daily averages are not necessarily indicative of individual hourly peaks, they are used here because of the design of the system: The system was designed to serve all of the cooling needs of the building, and a portion of the heating. There are many hours where there are significant heating and cooling loads within the same hour, so while there is a high level of confidence in the net amount of heat entering or leaving the ground on a longer time scale, assessment of individual hours with an hourly time step may not necessarily should not be expected to show the same response as the experimental data. A reasonable simulation of this minute-by-minute behavior would require the HVACSIM+ model to operate on a 60 second time step; as this is less than the transit time of the system, inaccuracies would be anticipated because the model at present does not account for fluid transit time.

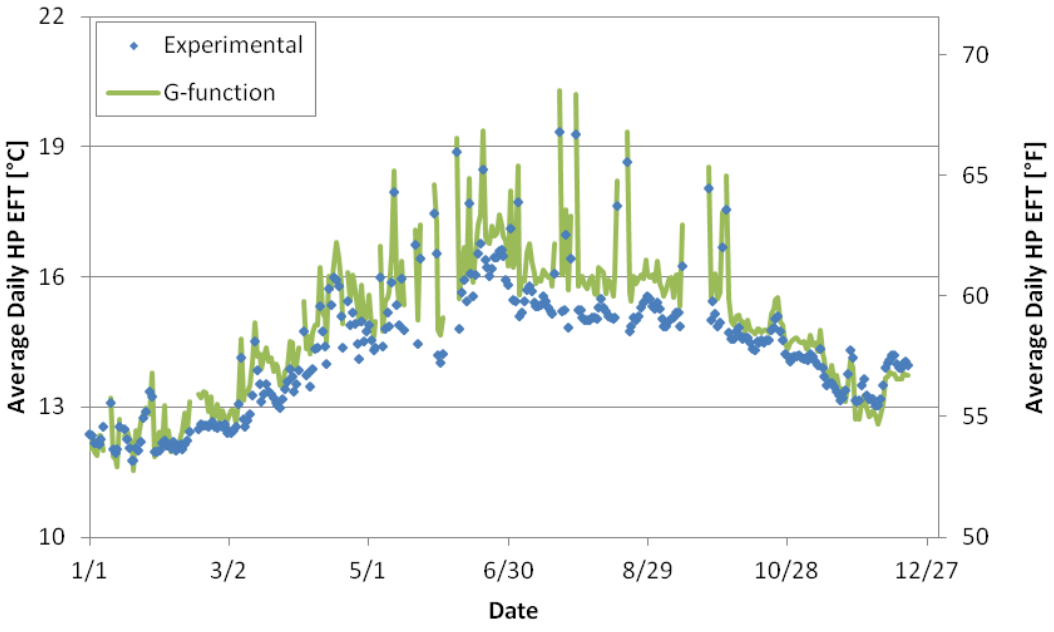

Figure 5-19: Validation of HVACSIM+ with Leicester data - Daily averages

In any case, Figure 5-20 shows the heat pump EFTs for both the experiment as well as the g-function simulation, for two sample days at the beginning of November. Noting the scale on the graph, the g-function simulation is consistently about 0.3°C (0.5°F) higher than the experimental data. However, the model mirrors the hour-by-hour change in temperature very closely indeed. The RMSE of the g-function model, for these two days, is 0.33°C (0.60°F); however, accounting for the 0.3°C (0.5°F) bias error, the remaining variance between the two is merely 0.06°C (0.12°F). This latter value represents what might be categorized as the "true" error in the model, due to the modeling process itself, while the 0.3°C (0.5°F) offset is most likely due to a shift in the borehole thermal resistance as time went on. One potential cause of that change would be a change in thermal conductivity; seasonal variations in moisture content could result in a varying conductivity, for example.

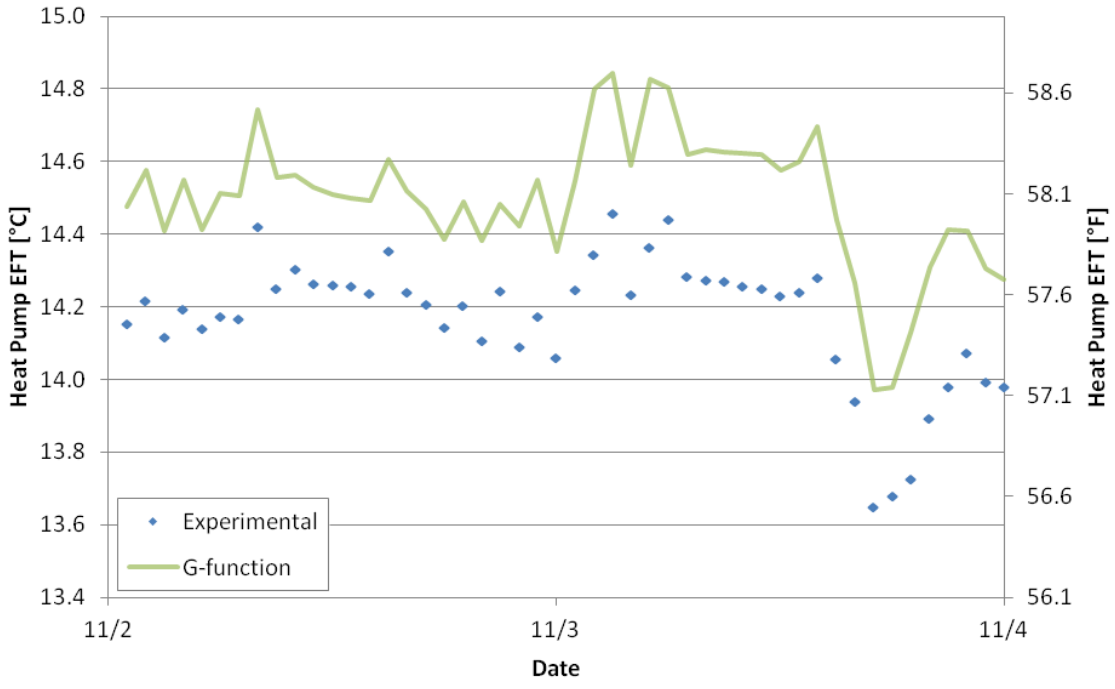

Figure 5-20: Leicester validation - Sample days

Attempts to validate the multi-coordinate model with the Leicester data proved unsuccessful. Because of the substantial computational burden required by a model discretized into three dimensions, there appears to be a functional limit on the size of system that the MCM can handle. With 56 boreholes, there are simply too many cells for this model to deal with; running the model for 24 hours showed no progress forward through time. This, then, is a major limitation of the multi-coordinate model.

5.3 Thermal Short-Circuiting

One issue with the current g-function model (HVACSIM+, EnergyPlus, etc.) is its behavior for systems with long residences times, either from low flow rates or extremely deep boreholes, as will now be demonstrated. Some systems may not require a significant heat extraction or rejection rate, and so, to keep the temperature difference across the heat pump large enough for efficient performance, a low flow rate will be used. In other cases, deep boreholes may be required due to space limitations.

Historically, the g-function method has essentially neglected thermal short-circuiting within the borehole. Practically, though, there will be some resistance between the upward and downward legs of the U-tube, with heat transfer occurring because the two are at slightly different temperatures. In the g-function model, there is only a single thermal resistance term, and this term does not consider the short-circuiting. For many cases, such as the three previous in this chapter, there is no evidence in the results of short-circuiting, which would appear as a persistent upward or downward shift in temperature when (for example) flow conditions change. However, for lower flow rates or extremely deep boreholes, the residence time of the fluid is long enough that thermal short-circuiting may have a significant impact. As Hellström (1991) described, the

borehole thermal resistance term can be modified into an effective value that includes this short-circuiting effect, but again, the g-function model currently does not explicitly account for this.

5.3.1 Description of Low-Flow Test System

To test the low-flow performance of the g-function model, data from a second borehole facility at Oklahoma State University in Stillwater OK (Smith and Perry, 1997) were used for validation purposes. The 77 m (252 ft) deep borehole, configured to run in-situ thermal property testing under variable flow conditions, was intended to be 114mm (4.5in) in diameter using standard 3/4" HDPE U-tube piping; however, upon grouting the borehole, a quantity of grout equivalent to the volume of a 125mm (4.9in) diameter borehole was required to fill the borehole completely. Thermal conductivity testing indicated a soil thermal conductivity of 2.77 W/m-K (1.60 Btu/hr-ft-°F); the thermally enhanced grout has a conductivity of 1.47 W/m-K (0.85 Btu/hr-ft-°F), and the overall thermal resistance of the borehole is 0.137 K/W-m (0.237 hr-ft-°F/Btu). The undisturbed ground temperature was determined to be 17.4°C (63.3°F), consistent with the value used found by Hern (2004) for the nearby OSU HGSHP facility.

This borehole has recently been used for testing under low-flow conditions. For a roughly constant heat injection rate of 3750 ± 200W, mass flow rates from 0.025-0.292 kg/s (0.41-4.63 GPM) were tested, as shown in Figure 5-21; this range corresponds to Reynolds numbers in the range of 2400-28,000. For the applied heat rate, temperature differences between the inlet and outlet of the borehole heat exchanger of about 35°C (63°F) for the lowest flow, down to around 5°C (9°F) for the greatest, were obtained.

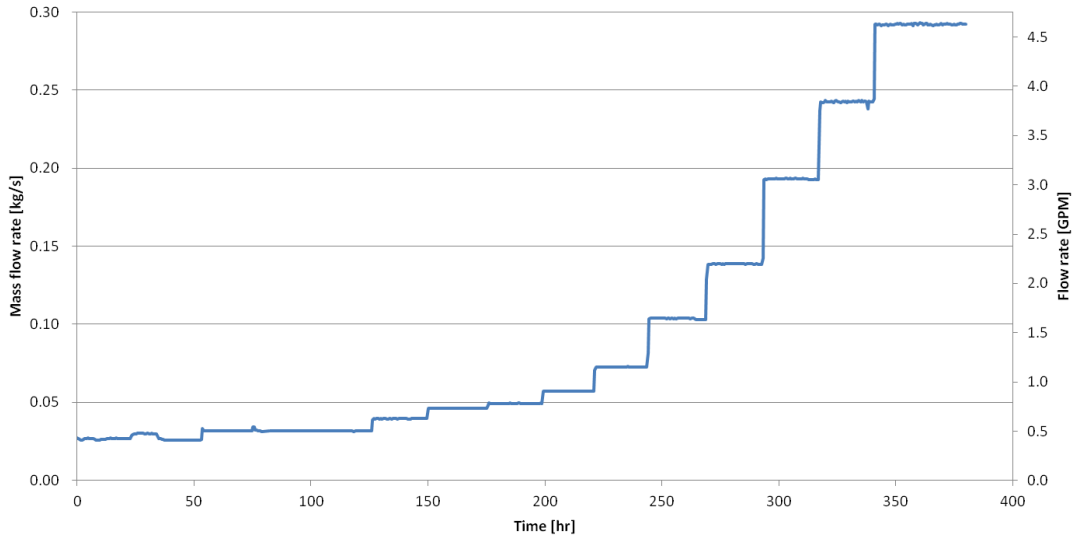

Figure 5-21: Low-flow borehole flow rates

5.3.2 Simulation with G-function Method

For an hourly simulation with the g-function method in HVACSIM+, Figure 5-22 shows the borehole entering and exiting (heat pump exiting and entering) fluid temperatures, over the variety of flow rates from Figure 5-21. These results are problematic. Aside from several hours in the first interval before the heat applied was adjusted slightly, the GHX inlet temperatures at the start of the experiment match fairly well, including the time around hours 70-80 corresponding to a heater failure. Even so, the exiting fluid temperature is substantially different. Perhaps more puzzling, though, is the sudden drop in GHX outlet temperature when the flow rate is first changed around hour 120. Heat is being added constantly, at approximately the same rate, so the exit temperature should continue to climb even as the entering temperature drops. After 250 hours or so, when the flow rate has increased above about 0.1 kg/s (1.6 GPM), the g-function model begins predicting both the inlet and outlet temperatures reasonably well. This, in total, suggests an issue with the thermal resistance. The convective component of the thermal resistance is updated hourly, based on changing flow rate; however, any effect of short-circuiting is not adjusted from one time step to the next. Thus, toward the end of the experiment when the flow

rate is comparatively high, short-circuiting ceases to be significant. Earlier, when the flow rate changes, the magnitude of the short-circuiting resistance will also change; since the overall effective thermal resistance is no longer correct, the simulated temperatures are shifted (downward, in this case, as short-circuiting will decrease with increasing flow) from their true values.

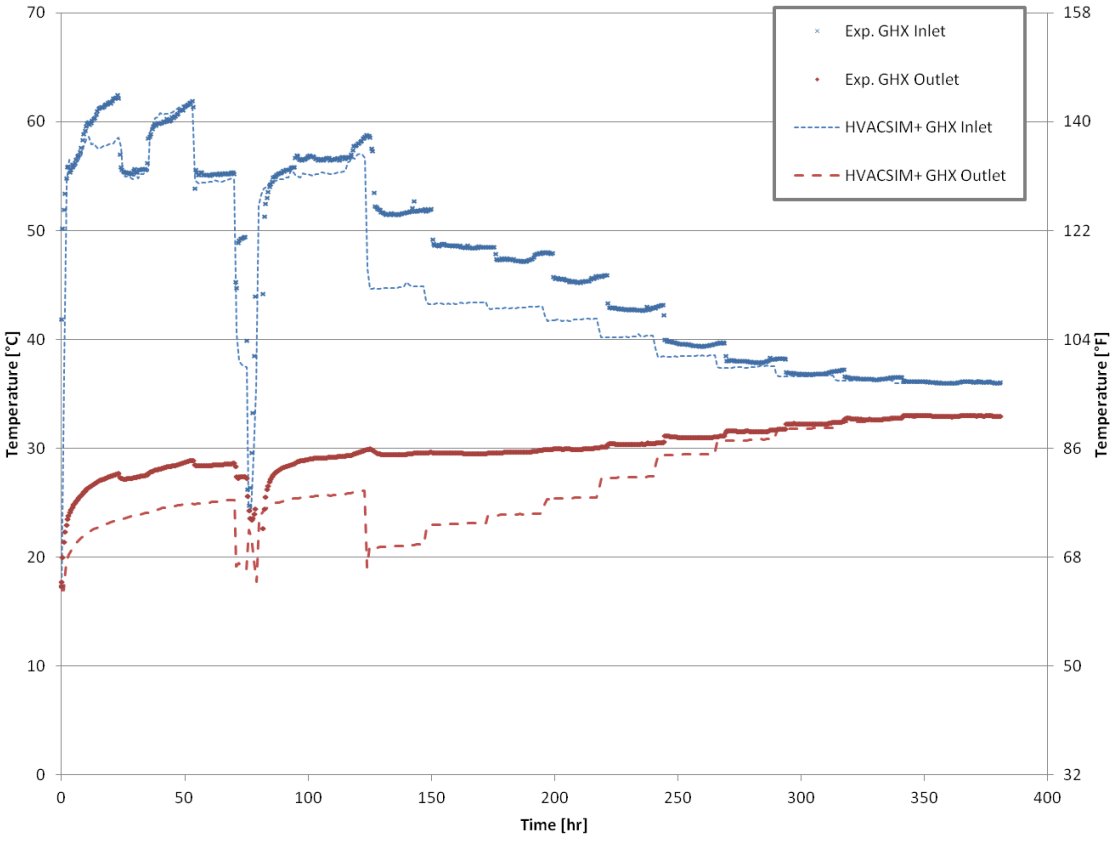

Figure 5-22: Simulation of low-flow system with g-function method

To demonstrate the potential effect that accounting for the changing thermal resistance, via consideration of short-circuiting at each time step, consider the revised HVACSIM+ results in Figure 5-23. Here, the overall borehole thermal resistance has been increased by 25% to account for greater short-circuiting than the base (higher flow) assumption. This causes an upward shift

in the temperature results of about 1.5°C (2.7°F), depending on the exact magnitude of the applied load. While the earlier and later hours are now less accurate than before, the time from roughly 230-270 hours now matches much better. It may become necessary, then, for systems with very high residence times—either very low flow rates, or extremely deep boreholes—to consider a time-varying borehole thermal resistance to account for a changing short-circuiting resistance.

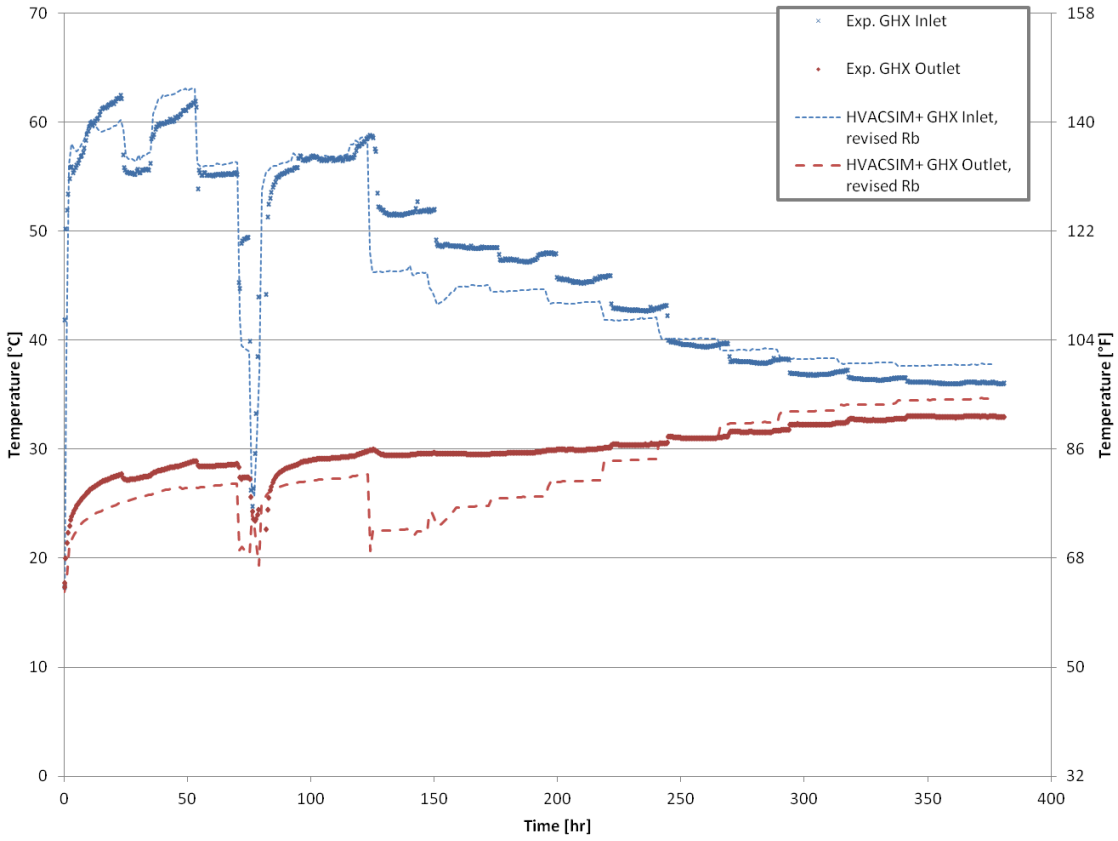

Figure 5-23: Simulation of low-flow system with g-function method, revised borehole resistance

5.3.3 Simulation with Multi-Coordinate Method

The same system was simulated with the more detailed multi-coordinate model in EnergyPlus, using a 15-minute time step. The heat pump entering and exiting GHX fluid temperatures are

shown in Figure 5-24. Immediately, a difference can be seen in how the two simulation methods behave. The MCM follows the inlet and outlet temperatures very well, including at the low flow rates. For this model, instead of a single resistance term, there are two resistances inside the borehole. The resistance between each U-tube leg and the borehole wall, as well as the resistance between legs of the U-tube, are both computed in advance with the multipole method (Claesson and Hellström, 2011). With a more detailed accounting of the behavior inside the borehole, there is no need for a time-varying resistance term to correct the results. Still, the results are not perfect, as there is a slight underprediction of the temperatures, about 1-2°C (2-4°F) for the first 100-150 hours, and a slight overprediction of about the same magnitude near the end of the experimental data. This could be due to a mismatch in thermal properties, which is understandable given the uncertainty in the grouting, in particular, for this borehole.

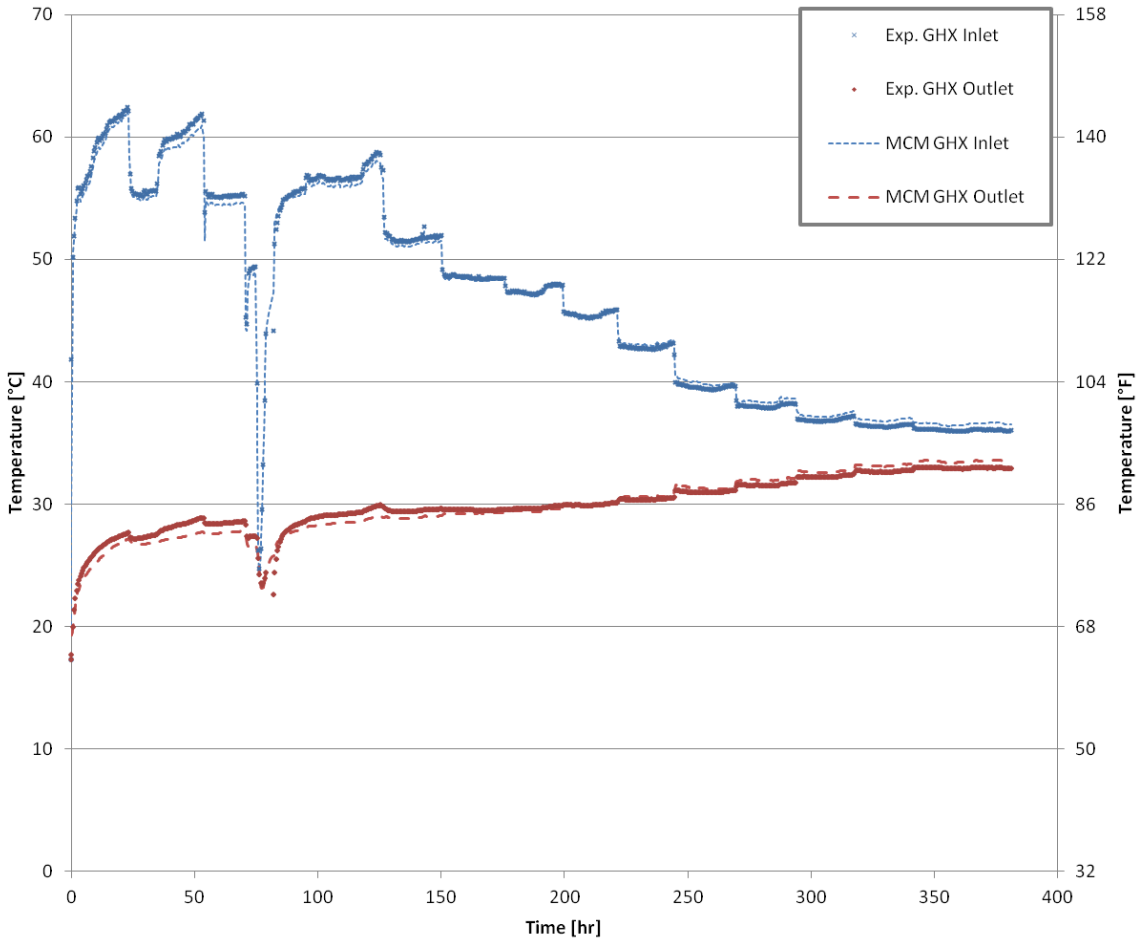

Figure 5-24: Simulation of low-flow system with multi-coordinate model

5.3.4 Accounting for Short-Circuiting

A more detailed study of the low-flow accuracy issues in the g-function method in HVACSIM+ is presently ongoing. As described above, a possible solution is to integrate an adjustment to the thermal resistance, so that short-circuiting could be somewhat accounted for in cases in which it becomes significant. This is not completely realistic, particularly since the single borehole thermal resistance term is computed by combining both legs of the U-tube into an equivalent single heat source for the mutlipole computation. A better approach might be to implement an analytical solution to the resistance network inside the borehole as derived by Hellström (1991),

which would explicitly model the short-circuiting resistance. This would require a slight modification of typical thermal response test analysis techniques; presently, response test data is used to fit thermal conductivity and borehole resistance, so a second short-circuiting resistance would need to be found as well. Regardless of the approach that corrects the issue, the end result will be a highly desirable, computationally efficient, more robust g-function model.

5.4 Experimental Uncertainty

Simulation models and design methods should, obviously, be as accurate as possible. The question, though, is: How accurate can they possibly be? To answer this question, the experimental uncertainty must be analyzed; the accuracy of any model will be strictly limited by the uncertainty in the experimental data.

Section 5.2.3 addressed the uncertainty propagated through to the design lengths found by both the simulation-based design tool and the equation-based Handbook method for the Valencia system, and found that the sensitivity of the design length to inputs in the design tool was +7.3%/-7.0%, while that of the Handbook equation was +4.4%/-3.8%. This accounted for uncertainties in the heat transfer rate and thermal conductivity. Overall, this addresses the issue of how closely the design length could be predicted until experimental "noise" means that the one value could not be considered more or less correct than another. These uncertainties, corresponding to 3% uncertainty in heat transfer rate and 20% in thermal conductivity, are likely similar to those of the other experimental systems; uncertainty parameters were not available for each system, though an error propagation analysis by Hern (2004) shows similar ranges for the Stillwater data, which also had an approximate accuracy of ±0.1°C in temperatures measurements and a slightly larger ±0.5% in flow readings.

Using this ±0.1°C uncertainty in temperature measurements as a typical guideline, Figure 5-18 (hourly results for two sample days of the Valencia system) is replotted below as Figure 5-25, this time including ±0.1°C error bars on the experimental values. The g-function results fall within the bounds of experimental uncertainty in 21/30 of the hours (70%) in which there is experimental data—when the facility is operating—while the multi-coordinate results are within this range in 18/30 hours (60%). The MCM has a larger error for a couple of hours in the afternoon of the first day, and in the second day after the largest single hourly temperature drop; however, it does recover to match reasonably well, and within the bounds of uncertainty, after the initial underprediction of the temperature change on the second day. The g-function method, on the other hand, generally matches very well except during the second evening, when temperatures are somewhat underpredicted. For these two days, though, both simulations are within experimental uncertainty (to say nothing of any additional error introduced by uncertainties in input parameters such as thermal conductivity) more than half of the time.

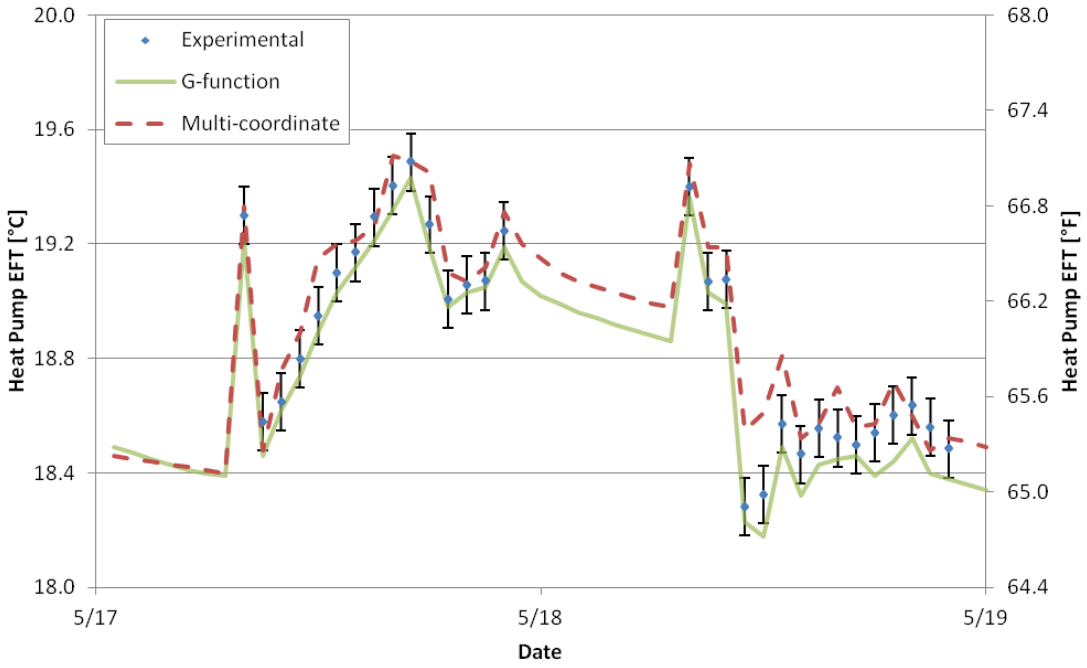

Figure 5-25: Valencia experimental validation - Sample days, with experimental uncertainty

5.5 Computation Time

One final important note is that the multi-coordinate model, in its current form, will probably never be satisfactory for design purposes as a single simulation. Due to longer computation times, it will be more suitable for research interests. For this validation, an annual simulation using 15-minute time steps required substantially more computation time—eight hours versus two minutes—for the multi-coordinate model than the g-function approach for the three borehole Stillwater system. The Valencia system required about twelve hours for the MCM, and roughly the same two minutes for HVACSIM+. Most notably, the MCM, given 24 hours, did not make any noticeable computational progress for the Leicester system, while the HVACSIM+ model required, again, around two minutes.

This difference in computation time for the MCM is in part due to the grid density required to generate accurate results, as the number of cells required helps to drive the computation time to a level unacceptable for a design tool. For the Leicester system, with 56 boreholes and 10 vertical slices, there are approximately 70,000 cells in the domain. In itself, this may not necessarily be prohibitive from a computational standpoint. However, each cell includes more than just the nodal temperature—it consists of geometric data for the centroid, plus material properties for each cell. As a result, the memory requirements grow. In tandem with this, the EnergyPlus solution algorithm may not be best suited to this type of approach, as there is doubtless some computational overhead involved in integrating a model such as this with the existing EnergyPlus framework. Optimizing this scheme, or perhaps investigating a way to separate the majority of

the computation from EnergyPlus, while at the same time reducing the number of cells needed, may enhance the performance of the multi-coordinate model.

Despite this limitation, the multi-coordinate model is still useful in comparing different design methodologies due to its inherent lack of simplifying assumptions, and capability to handle specialized systems such as the low-flow case. Additionally, the possibility exists to utilize the multi-coordinate model in a hybrid time step type of approach (Cullin and Spitler, 2011), to provide detail about peak performance while the core simulation uses a computationally faster approach.

5.6 Conclusions

This chapter details experimental validation of multiple design/simulation methodologies, including two design procedures (a simulation-based design tool and an equation-based design equation), and two hourly/subhourly simulations. The experimental data used for the validation come from four separate facilities, including a test borehole with low, variable flow.

The validation of the two models against experimental data from facilities in Stillwater, OK, and Valencia, Spain, showed good agreement. The RMSEs for the g-function HVACSIM+ model were 1.8°C (3.3°F) and 0.6°C (1.1°F) for the Stillwater and Valencia systems, respectively, while the RMSEs for the multi-coordinate model in EnergyPlus were slightly higher, at 2.0°C (3.5°F) and 0.8°C (1.4°F). The main difference between the two models is the use of pre-computed response factors for the g-function model, versus a detailed three-dimensional domain for the multi-coordinate model.

The g-function model in HVACSIM+ also performed well when validated against the Leicester data set, with an RMSE of 0.6°C (1.0°F). The simulation did, however, show a notable systematic error in the summer, perhaps due to a change in one or more system parameters that cannot be handled when assuming that these parameters are always constant. The multi-coordinate model was not able to handle the extremely large nature of the Leicester borefield, unable to make noticeable computational progress even after 24 hours (using a 3GHz CPU with 8GB RAM).

For the low-flow case, the g-function model showed incorrect results, due to the lack of consideration of thermal short-circuiting behavior at low flow rates. In comparison, the multi-coordinate model behaves much more in line with realistic expectations, with no unfeasible temperatures encountered, due to the explicit usage of a short-circuiting resistance in the intra-borehole analysis. The g-function model does recover, though, matching fairly well after the flow rate increases above a value of about 0.1 kg/s (1.6 GPM), when short-circuiting becomes less significant. Clearly, the g-function model needs to be enhanced to account for low-flow cases; other researchers are currently exploring this problem by perhaps implementing a flow-dependent correction on the overall borehole thermal resistance to account for short-circuiting, or—better still—implementing an improved resistance model that will eliminate the need for concern over low flow rates entirely.

The multi-coordinate model requires a great deal more computation time than the g-function model. While some of this is due to overhead with the EnergyPlus engine, the vast majority of the time increase occurs because of the sheer volume of cells required to achieve accurate results. This is understandable, as the multi-coordinate model is essentially a simple three-dimensional finite difference model, while the g-function method is based on pre-computed response factors.

However, the multi-coordinate model does serve some benefit, as it can show—as it has done for the low-flow case—where other methods are lacking. The issue of computation time could perhaps be addressed by utilizing the multi-coordinate model for only short time steps, such as around peak load periods, or under particular circumstances such as when flow rates are very low.

CHAPTER VI

VALIDATION OF VERTICAL GROUND HEAT EXCHANGER DESIGN METHODOLOGIES

[NOTE: This chapter has been developed into the following paper:

Cullin, J.R., J.D. Spitler, C. Montagud, F. Ruiz-Calvo, S.J. Rees, S.S. Naicker, P. Konečný, and L. Southard. 2014. Validation of Vertical Ground Heat Exchanger Design Methodologies. (Submitted to HVAC&R Research.*)]*

At present, there are perhaps three types of methods for sizing the ground heat exchanger for a GSHP system design. The first method is to use some type of rule-of-thumb relating peak cooling capacity or peak cooling capacity to a required depth. Particularly for non-residential systems, however, the ratio of capacity to depth varies widely (Underwood and Spitler, 2007; Spitler and Cullin, 2008). Therefore reduction of the sizing algorithm to a fixed borehole length per unit of peak capacity is unlikely to give satisfactory results, and the rule-of-thumb approach will not be further considered here.

The second type of method is based on computer simulation of the ground heat exchanger (Eskilson, 1987; Hellström et al., 1997; Spitler, 2000; Cullin and Spitler, 2011), whereby the

necessary system parameters (borefield geometry, borehole completion, thermal properties, etc.) are used as inputs to a simulation tool that generates loop temperatures as a function of time. These temperatures can then be compared to the desired temperature constraints—usually placed on the heat pump entering fluid temperature (HP EFT)—and the GHX depth iteratively adjusted until those constraints are met, a process which is typically done all at once by the software. Many design and energy analysis tools (*e.g.*, Hellström et al., 1997; Fisher et al., 2006; Liu and Hellström, 2006) rely on the g-function approach first developed by Eskilson (1987); one of these tools (Spitler, 2000) will be analyzed here. This tool, also described in some detail by Cullin (2008), is a ground heat exchanger simulation tool that operates on a monthly time step, and is widely used for system design due to its quick computations compared to other hourly simulation methods.

The other method for GHX system design, and the method currently presented by ASHRAE (2011), is that of Kavanaugh and Rafferty (1997). They give an equation derived from a cylinder-source model to compute a required heat exchanger length for both heating and for cooling (with the larger value, obviously, being the one required for the design). This method also utilizes tables of correction factors to adjust for both borehole-to-borehole interference and thermal short-circuiting; however, the development of these factors is unclear, and other researchers (Bernier et al., 2008) have failed to reproduce the tabulated borehole resistances and short-circuiting factors with any sort of accuracy. This method has also been integrated into a software tool that automates much of the computation (Kavanaugh, 1995).

To assess the performance of both of these methods, they will be validated against data from several monitored GHX facilities, as described in the next section. Traditional validation efforts typically involve using a simulation to determine fluid temperatures, which are then checked against experimental values. However, for this work, the design tools are used to *size* the GHX

for the system, with the measured peak heat pump entering fluid temperatures serving as the design constraints. This approach, then will provide insight into the accuracy of two commonly-used design approaches.

To check the suitability of the equation-based method, relevant information including total and peak load values, as well as maximum temperatures, will be entered into the design equation. The resulting "design length" can then be compared to the actual installed GHX length, to see how well the equation can predict loop length requirements. This value can also be compared to the length obtained with the simulation-based design tool, so that the relative performance of the two techniques can be assessed. Cullin et al. (2014) performed an initial analysis of this nature for the Valencia data set (see Section 5.2.3); this analysis has been extended here to include three other data sets, as well as a more thorough exploration of the reasons behind the differences in the two methods' design lengths.

6.1 Data Sources

As discussed in Section 2.2.3, Yavuzturk and Spitler (2001) identified criteria for field tests that would be ideal for use in experimental validation of ground heat exchanger simulations: (1) independent measurement of ground thermal properties (2) carefully calibrated and monitored data acquisition including, at least, measurement of entering and exiting fluid temperatures and flow rates (3) continuous data collection from the beginning of the ground heat exchanger operation, and (4) well characterized borehole geometry, backfill material properties, and heat transfer fluid properties. These same criteria apply for validation of ground heat exchanger design methods. To these criteria, we might also add that it is desirable to have multiple years of continuous data—the more the better—and, if possible, it would also be ideal to have a range of

system sizes and climates as well as a range of system parameters such as number of boreholes, borehole spacing, borehole depths, backfill materials, etc. Such data sets have been in remarkably short supply.

This chapter brings together results from four different GSHP facilities, selected to meet the above criteria as closely as possible. Two are located in the United States: one in Stillwater, OK, and the other at the ASHRAE Headquarters in Atlanta, GA. The remaining two are in Europe: one in Valencia, Spain, and one in Leicester, United Kingdom. With the exception of the Atlanta data set, each of these has previously been detailed in Section 5.1. For each data set, though, a critical detail is the way that the loads were selected, and how the design period was chosen. Following is a description of this process, as well as a full description of the Atlanta facility.

6.1.1 Stillwater OK

Hern (2004) designed and constructed a hybrid ground source heat pump test facility at Oklahoma State University in Stillwater OK. The ground heat exchanger consists of three vertical boreholes, as described in Section 5.1. Hourly ground loads were computed based on the measured system flow rate and temperature difference across the heat exchanger. For use in the design methodologies, the first year of data was utilized since the maximum loop temperatures were encountered during this period. Exploration with the simulation-based design tool showed that, even if the entire 19 months were utilized, the resulting design length is equivalent. Therefore, a single year design period was selected for both the simulation-based design tool as well as the Handbook design equation.

6.1.2 Valencia, Spain

The Valencia data set consists of six years of experimental data from a six-borehole GHX installed at the Universitat Politècnica de València in Spain (Montagud et al., 2011). For this system, temperatures were measured at both the inlet and outlet of each borehole at sixty-second increments for six years of weekday operation. The first three years of operation are stop-and-start, with 15 of the 36 months, including eight consecutive, not running or recording data. As described in Cullin et al. (2014), only the final three years of data, when the system is in continuous operation and shows a typical cyclical load profile, are used in this analysis. This was done because the system experienced stop-and-start operation over the first three years, including a span of 16 months during which only two months featured any actual operation. So, for the purposes of validating the design procedures, the average of years 4-6, when the system operated under conditions approaching steady periodic (*i.e.*, the condition typically assumed for designing a VGHX), were used in the analysis. Furthermore, since the initial three years only had sparse and irregular loading, they were ignored for the purposes of this analysis; three years was chosen as the system duration when sizing the GHX. Subsequent testing with a six years of design period (but still using the same cyclic load profile from years 4-6 as before) gave only a 1% increase in the size of the system when sized by the SBDT , and only a 3% increase when sized by the design equation.

6.1.3 Atlanta GA

The ASHRAE Headquarters building in Atlanta GA (Parsons, 2008) is an office building with a floor area of around 3250m^2 (35,000ft^2), with the heating and cooling for the second floor *only* (floor area 1445 m^2 or 15,550 ft^2) provided by a ground source heat pump system. The ground heat exchanger for this system utilizes 12 boreholes each 122m (400ft) in depth, oriented in a 2x6 rectangular field and spaced 7.6m (25ft) apart. An *in situ* thermal conductivity test was

performed on a test borehole, indicating a thermal conductivity of 3.25 W/m-K (1.88 Btu/hr-ft-°F) along with a grout thermal conductivity of 1.70 W/m-K (0.98 Btu/hr-ft-°F). The undisturbed ground temperature was determined at this time to be 19.4°C (67.0°F). The total system flow rate is approximately 9.5 L/s (150 GPM) of water.

The GHX system is monitored to provide experimental measurements of flow rate as well as entering and exiting fluid temperatures every 15 minutes. As with the other systems discussed in Chapter 5, Figures 6-1 and 6-2 below show the average daily heat pump entering and exiting fluid temperatures, as well as the daily heat extracted from the ground, for the first twelve months of *monitored* operation beginning in March 2010; data through the end of 2012 was used for this analysis. The gaps in September and November are periods when the system was not operational, or no data were reported.

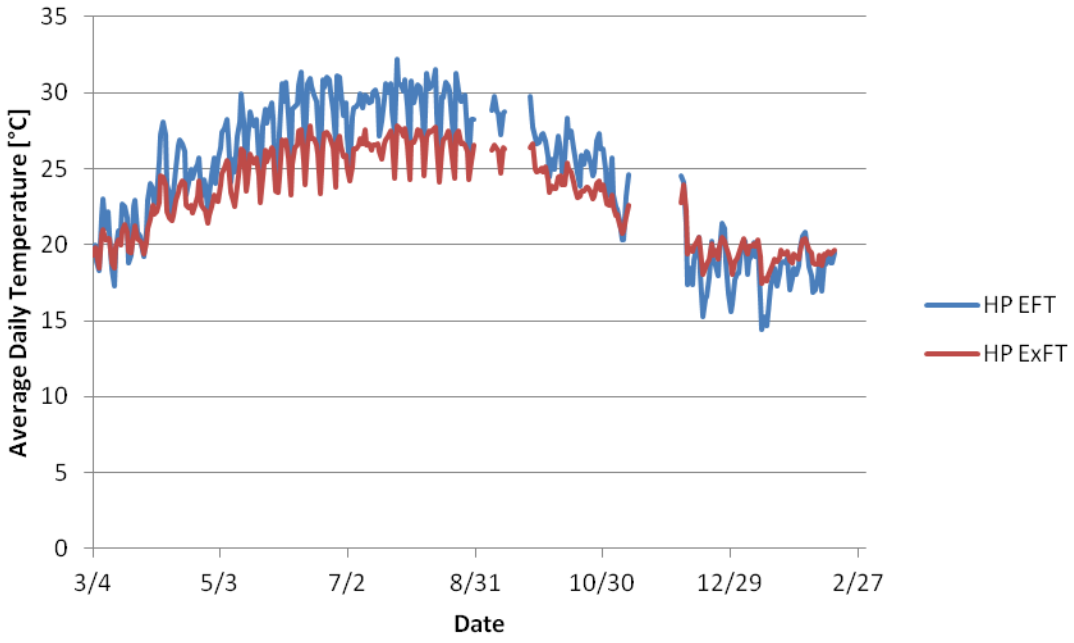

Figure 6-1: Atlanta experimental daily average temperatures

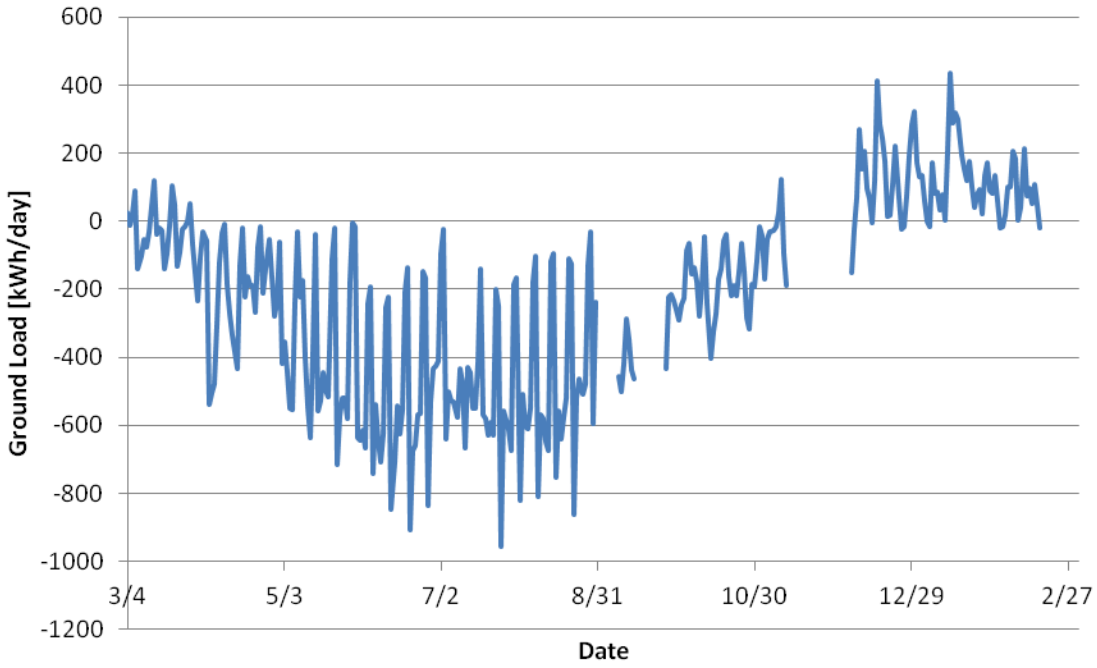

Figure 6-2: Atlanta experimental daily total ground heat extraction

This system was actually operational for 21 months prior to March 2010. However, changes in the data acquisition system resulted in data prior to March 2010 being lost. To investigate the best method to account for this lost data, a simple load prediction scheme was created to retrospectively "forecast" the loads on the system prior to commencement of monitoring. The past loads on the ground heat exchanger were predicted based on average daily air temperature, which is available from weather data for Atlanta. For the existing data, a cubic curve fit was created to fit the daily GHX load to the daily average air temperature. Thus, loads for the time before monitoring began were computed based on the air temperature for those days and the calculated curve fit. Figure 6-3 shows the monthly net heat rejection, both as estimated from the curve-fitting procedure and—once data measurement began—as measured. As Figure 6-7 shows, there is some year-to-year variation in the estimated loads, on the order of 10%. However, there is no evidence to suggest any long-term shift in the overall load pattern. Therefore, when validating the design procedures, the average of the three full years of actual measured data was used. The

peak loads used in the design procedures were the absolute highest loads from the latest year of data, as they corresponded to the maximum measured temperature. For the design period, however, since the system has been in operation for a total of five years, five years was chosen as the design period for both the simulation-based design tool and Handbook design equation to determine the required GHX length based on the experimental data.

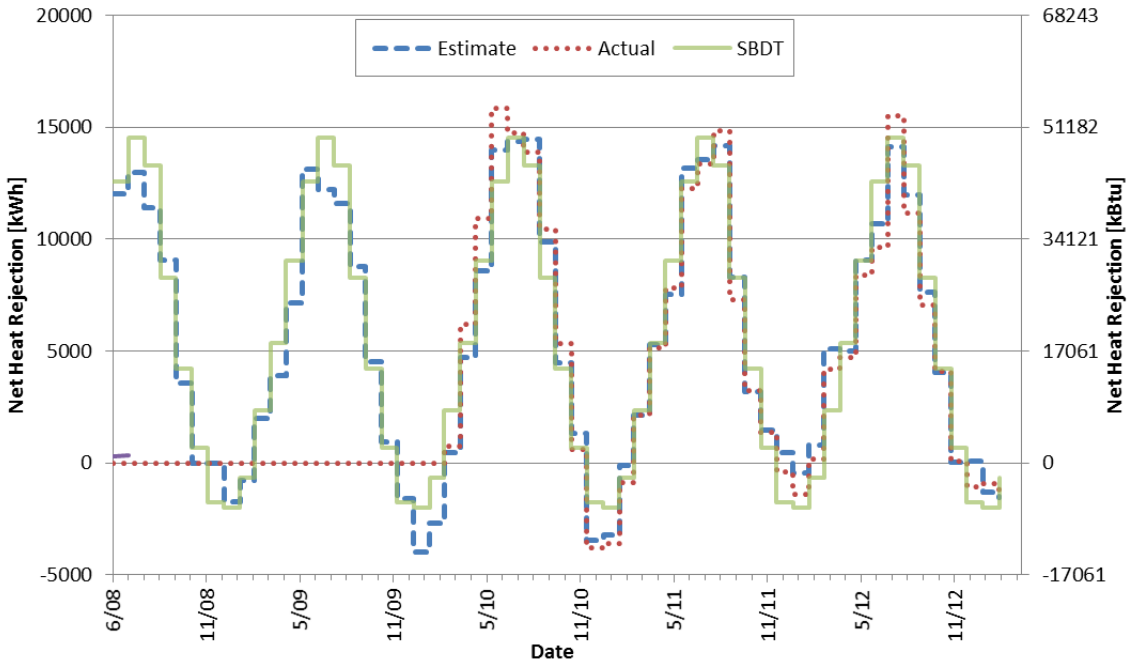

Figure 6-3: Atlanta predicted total daily heat rejection

6.1.4 Leicester, United Kingdom

Researchers at De Montfort University in Leicester, United Kingdom, designed and installed a large-scale domestic GSHP system consisting of 56 boreholes (Naicker and Rees, 2011). Operation and monitoring of the system began in December 2009. However, measurements of system flow rate were not available until March 2010. For those first months, then, flow data were filled in based off of similar patterns later in the experiment. All 24 months of available data, starting from December 2009, were used in the analysis, and a design period of two years was selected for both design methodologies. The peak temperatures utilized in the design are for

the times when there is flow; temperatures peak at 39°C (102°F) entering the ground loop, but during a time for which there is no flow, and thus no load on the system. This temperature has presumably drifted upward, influenced by the outside conditions while the fluid is stationary. Overall, this system provides much more cooling than heating, and thus is a good candidate for a long-term decrease in ground temperatures if this loading pattern persists for multiple years.

6.2 Methodology

This work compares the design lengths generated from the ASHRAE Handbook design equation—specifically, the detailed method published by Kavanaugh and Rafferty (1997)—are compared to design lengths from a validated simulation-based design tool. Specifically, the data and physical parameters from the experimental facilities outlined in the previous section are used as inputs for both methods, so that the resulting design lengths can also be assessed with respect to the actual installed GHX length from the real installations. Following is a detailed overview of both the simulation-based design tool and the ASHRAE Handbook method, including how the data and parameters from the experiment are used in each.

6.2.1 Simulation-Based Design Tool

The monthly design tool used for this analysis utilizes Eskilson's g-functions (1987) as its basis. For a single borehole, Eskilson computed the temperature response around the borehole due to a step change in heat input, using a two-dimensional finite difference method in radial-axial coordinates. By superimposing solutions for multiple boreholes, a non-dimensional response termed the "g-function" can be created that represents the thermal behavior of a specific ground heat exchanger as a function of time and heat input. The temperature at the borehole wall at the end of an arbitrary month *n* is then:

$$T_{borehole} = \sum_{i=1}^{n} \frac{(Q_i - Q_{i-1})}{2\pi k} g\left(\frac{t_i}{t_s}, \frac{r_B}{H}\right) + T_{UG} \quad (6\text{-}1)$$

Where:

$T_{borehole}$ is the borehole wall temperature [°C or °F];

Q_i is the heat injection rate per unit length of pipe [W/m or Btu/hr-ft];

n is the current time of interest [s];

k is the ground thermal conductivity [W/m-K or Btu/hr-ft-°F];

g is the value of the g-function at the specified point [-];

t_i is the time at the i^{th} time step [s];

t_s is the time scale [s];

r_B is the borehole radius [m or ft];

H is the depth of the borehole [m or ft]; and

T_{UG} is the undisturbed ground temperature [°C or °F].

The fluid temperature in the borehole, then, is based on the borehole wall temperature and thermal resistance:

$$T_f = T_{borehole} + R_B \cdot Q_i \quad (6\text{-}2)$$

Where:

T_f is the temperature of the working fluid [°C or °F];

R_B is the borehole thermal resistance [K/(W/m) or °F/(Btu/hr-ft)]; and

Q_i is the heat injection rate per unit length of pipe [W/m or Btu/hr-ft].

The borehole thermal resistance may be inferred from experimental values, or it can be computed analytically using an approach like the multipole method (Bennet et al., 1987; Claesson and Hellström, 2011). Finally, the heat pump entering and exiting fluid temperatures are calculated

by assuming that the temperature change between inlet and exit is linear. Thus, the heat pump entering fluid temperature is computed as

$$T_{in} = T_f - \frac{Q_i \cdot H \cdot NB}{2 \cdot \dot{m} \cdot c_p} \tag{6-3}$$

while the heat pump exiting fluid temperature is determined by

$$T_{out} = T_f + \frac{Q_i \cdot H \cdot NB}{2 \cdot \dot{m} \cdot c_p} \tag{6-4}$$

Where:

T_{in} is the heat pump entering fluid temperature [°C or °F];

T_{out} is the heat pump exiting fluid temperature [°C or °F];

NB is the number of boreholes in the system [-];

$\dot{m}$ is the mass flow rate of the working fluid [kg/s or lbm/s];

C_p is the specific heat of the working fluid [J/kg-K or Btu/lbm-°F]; and

other quantities are as described in Equations 4-4 and 4-5.

To determine a design length, the tool uses an initial guess and runs the monthly simulation. This produces a minimum and a maximum peak heat pump entering fluid temperature (EFT), which can be compared to the desired constraints. Here, the constraints are set as the minimum (if the system is heating-dominated) or maximum (if the system is cooling-dominated) measured value for the GHX exiting fluid temperature, as this will be nearly equal to the heat pump EFT.

Other parameters such as borehole diameter, ground thermal properties, and borefield configuration are taken from the specifications for each system. These parameters, and (as available) the sources from which they were obtained, are summarized in Table 1. With the exception of the shank spacing, all values were taken directly from the experimental descriptions and subsequent thermal response testing. For the Stillwater system, in which measurements were

taken for each borehole, the averages of the three measurements were used. The shank spacing in each case was assumed to follow the 'B' value given by Paul (1996)--the distance between the U-tube legs is equal to the distance between each leg and the borehole wall. When a U-tube is placed without spacers (which is assumed to be the case, as no indication to the contrary has been given), experiences show that the spacing tends toward the 'B' value, on average.

Table 6-1: Simulation-based design tool input parameters

Facility location	Valencia	Leicester	Atlanta	Stillwater
REFERENCE	Montagud et al., 2011	Naicker and Rees, 2011	---	Hern, 2004
Borehole depth, m (ft)	50 (164)	100 (328)	122 (400)	75 (246)
Borehole spacing, m (ft)	3 (10)	10 (33)	7.6 (25)	9 (30)
Borehole diameter, mm (in)	150 (5.9)	126 (5.0)	140 (5.5)	114 (4.5)
U-tube inner diameter, mm (in)	23.4 (0.92)	34.5 (1.36)	34.5 (1.36)	21.8 (0.89)
U-tube outer diameter, mm (in)	25.4 (1.00)	42.5 (1.66)	42.5 (1.66)	26.7 (1.05)
Shank spacing, mm (in)	44.6 (1.76)	13.9 (0.55)	18.5 (0.73)	20.2 (0.80)
Undisturbed ground temperature, °C (°F)	19.5 (67.1)	13.2 (55.8)	19.5 (67.1)	17.3 (63.1)
Ground thermal conductivity, W/m-K (Btu/hr-ft-°F)	1.6 (0.92)	3.2 (1.8)	3.3 (1.9)	2.3 (1.3)
Grout thermal conductivity, W/m-K (Btu/hr-ft-°F)	1.6 (0.92)	2.0 (1.2)	1.7 (0.98)	1.6 (0.92)

Loads are computed directly from the experimental data using the measured flow rate and temperature differential across the GHX; these loads are computed for each measured data point, and then processed into a monthly average/monthly peak format consistent with the hybrid time step procedure described by Cullin and Spitler (2011). Tables 6-2 through 6-5 show the simulation-based design tool load inputs—both total for the month and peak, for both heating and cooling—for each location; note that the month number '1' corresponds to the first month of

operation, which is not necessarily January in each case. Note that the Stillwater, Atlanta, and Valencia systems are cooling-dominated, while the Leicester system is heating-dominated. Further details on the simulation-based design tool, including development of the g-functions as well as experimental validation, may be found in the works of Spitler (2000) and Cullin (2008). Additional validation of the design tool itself was performed by Cullin, et al. (2014).

Table 6-2: SBDT GHX loads for Stillwater

Month	Total Heating, kWh (kBtu)	Total Cooling, kWh (kBtu)	Peak Heating, kW (kBtu/h)	Peak Cooling, kW (kBtu/h)
1	1959 (6683)	160 (545)	7.5 (25.5)	13.5 (46)
2	75 (255)	1320 (4503)	0.5 (1.7)	9 (30.6)
3	66 (225)	1701 (5802)	3.2 (10.8)	9.7 (32.9)
4	1 (4)	2704 (9227)	1 (3.3)	12.5 (42.8)
5	13 (44)	3271 (11161)	1.4 (4.8)	10.1 (34.6)
6	2 (8)	3775 (12881)	0.5 (1.8)	10.3 (35)
7	23 (77)	3366 (11486)	1.8 (6.1)	9.9 (33.7)
8	621 (2117)	1133 (3867)	4.8 (16.3)	9.4 (32.1)
9	452 (1542)	1009 (3441)	9 (30.6)	9.3 (31.8)
10	1504 (5132)	0 (0)	9.2 (31.4)	0 (0)
11	1698 (5795)	0 (0)	8.8 (30)	0 (0)
12	1609 (5489)	0 (0)	7.5 (25.7)	0 (0)

Table 6-3: SBDT GHX loads for Atlanta

Month	Total Heating, kWh (kBtu)	Total Cooling, kWh (kBtu)	Peak Heating, kW (kBtu/h)	Peak Cooling, kW (kBtu/h)
1	1314 (4485)	2476 (8448)	51.3 (175.1)	29.9 (102)
2	72 (244)	6104 (20828)	20.7 (70.7)	60.1 (205.1)
3	4 (13)	12063 (41158)	0.7 (2.4)	77.1 (262.9)
4	6 (20)	15414 (52591)	1.2 (4.2)	87 (296.9)
5	7 (24)	15023 (51259)	1.1 (3.8)	219.8 (750)
6	8 (27)	13624 (46486)	1.2 (4.1)	89.7 (306.1)
7	31 (107)	7568 (25820)	5.7 (19.6)	66.6 (227.3)
8	1358 (4633)	3307 (11284)	48.5 (165.3)	54.5 (186.1)
9	4719 (16100)	653 (2227)	49.6 (169.3)	14.7 (50.3)
10	4351 (14846)	750 (2559)	46.6 (159)	13.4 (45.9)
11	1698 (5795)	0 (0)	8.8 (30)	0 (0)
12	1609 (5489)	0 (0)	7.5 (25.7)	0 (0)

Table 6-4: SBDT GHX loads for Valencia

Month	Total Heating, kWh (kBtu)	Total Cooling, kWh (kBtu)	Peak Heating, kW (kBtu/h)	Peak Cooling, kW (kBtu/h)
1	1640 (5595)	0 (0)	12.3 (41.8)	0 (0)
2	1628 (5556)	0 (0)	12.4 (42.3)	0 (0)
3	1372 (4682)	0 (0)	12.1 (41.1)	0 (0)
4	745 (2543)	0 (0)	11.6 (39.4)	0 (0)
5	0 (0)	1542 (5260)	0 (0)	17.1 (58.3)
6	0 (0)	2405 (8207)	0 (0)	17.4 (59.2)
7	0 (0)	3081 (10513)	0 (0)	16.1 (54.9)
8	0 (0)	1759 (6001)	0 (0)	15.2 (52)
9	0 (0)	1578 (5383)	0 (0)	14.2 (48.5)
10	0 (0)	1123 (3833)	0 (0)	13.6 (46.5)
11	758 (2587)	0 (0)	9.8 (33.4)	0 (0)
12	1248 (4257)	0 (0)	11.3 (38.6)	0 (0)

Table 6-5: SBDT GHX loads for Leicester

Month	Total Heating, kWh (kBtu)	Total Cooling, kWh (kBtu)	Peak Heating, kW (kBtu/h)	Peak Cooling, kW (kBtu/h)
1	2618 (8932)	7989 (27259)	25.8 (88.1)	96.2 (328.3)
2	7391 (25218)	13665 (46623)	40.6 (138.4)	49.5 (168.7)
3	4536 (15478)	15106 (51543)	26.9 (91.6)	136.2 (464.7)
4	2226 (7596)	20903 (71319)	27.4 (93.6)	166 (566.4)
5	1497 (5107)	11052 (37709)	26.9 (91.6)	138.9 (474)
6	1870 (6379)	23886 (81500)	58.8 (200.5)	196.3 (669.7)
7	2431 (8295)	13764 (46961)	31.2 (106.4)	74.2 (253.2)
8	2821 (9626)	14830 (50599)	13.4 (45.6)	101.9 (347.8)
9	2771 (9454)	9935 (33899)	22.4 (76.5)	92.1 (314.2)
10	5631 (19214)	14356 (48981)	36.4 (124.2)	123.4 (421.1)
11	8146 (27795)	12789 (43637)	39.5 (134.7)	40.5 (138.1)
12	3125 (10663)	9249 (31558)	33.5 (114.2)	38.6 (131.8)

6.2.2 Handbook Method

The ASHRAE Handbook (2011) sets forth a ground heat exchanger design equation suitable for quick calculations, given as:

$$L_c = \frac{q_a R_{ga} + \left(q_{lc} - 3.41 W_c\right)\left(R_b + PLF_m R_{gm} + R_{gd} F_{sc}\right)}{t_g - \frac{t_{wi} + t_{wo}}{2} - t_p} \tag{6-5}$$

Where:

L_c is the required design length for cooling [m or ft]; and

all other variables are defined in Table 6-6.

Table 6-6 also lists the values provided for each experimental system, as taken from the experimental specifications, measurements, and estimations based on the recommended procedure of Kavanaugh and Rafferty (1997).

Table 6-6: Handbook method input parameters

Facility location	**Valencia**	**Leicester**	**Atlanta**	**Stillwater**
Average net hourly heat transfer rate to ground q_a, W (Btu/h)	-4.69E+02 (-1.60E+03)	-1.34E+04 (-4.57E+04)	-8.25E+03 (-2.81E+04)	-1.58E+03 (-5.39E+03)
Design block cooling/heating load q_{lc}, W (Btu/h)	-1.70E+04 (-5.80E+04)	-2.80E+05 (-9.55E+05)	-7.50E+04 (-2.56E+05)	-8.90E+03 (-3.03E+04)
Power at design load W_c, W (Btu/h)	---	---	---	---
Borehole thermal resistance R_b, m-K/W (h-ft-°F/Btu)	0.110 (0.190)	0.064 (0.110)	0.069 (0.120)	0.116 (0.200)
Ground thermal resistance for annual pulse R_{ga}, m-K/W (h-ft-°F/Btu)	0.193 (0.334)	0.059 (0.103)	0.086 (0.149)	0.078 (0.136)
Ground thermal resistance for monthly pulse R_{gm}, m-K/W (h-ft-°F/Btu)	0.244 (0.422)	0.119 (0.206)	0.117 (0.202)	0.153 (0.265)
Ground thermal resistance for sub-daily pulse R_{gd}, m-K/W (h-ft-°F/Btu)	0.169 (0.292)	0.094 (0.162)	0.095 (0.165)	0.129 (0.224)
Design month part load factor, PLF_m, unitless	0.27	0.42	0.33	0.55
Short-circuit heat loss factor	1.04	1.04	1.04	1.04
Undisturbed ground temperature t_g, °C (°F)	20 (67)	13 (56)	20 (67)	21 (70)
Borehole interference temperature penalty t_p, °C (°F)	-0.50 (-0.90)	-0.98 (-1.76)	-0.37 (-0.67)	-0.32 (-0.57)
Heat pump design inlet temperature t_{wi}, °C (°F)	27 (81)	18 (65)	30 (86)	27 (81)
Heat pump design outlet temperature t_{wo}, °C (°F)	33 (91)	24 (74)	38 (100)	31 (87)

Heat transfer rates were computed as the hourly average net heat extracted from the ground (q_a) using the experimental data; values are negative when heat is being rejected. (Note that, due to

this sign convention, compressor heat would add to the magnitude of the design block load term q_{lc}, although the equation may appear counterintuitive at first.) Since the loading directly on the ground was available instead of the experimental data, this was used instead of the combined design load/compressor work term. The part-load factor during the design month (PLF_m) was computed by dividing the peak load by the total load for the month in which it occurs, to determine the equivalent fraction of time that the system would run at peak conditions. The borehole thermal resistance value (R_b) was computed via the tabular data given in Kavanaugh and Rafferty (1997), even though these values were computed in greater detail as part of the monthly simulation tool analysis; this introduces some error, which will be discussed later. The undisturbed ground temperature (t_g) was measured directly prior to the experiments in concurrence with thermal conductivity testing, while the heat pump design temperatures (t_{wi} and t_{wo}) are the experimental values when the maximum or minimum temperature occurs in the system. All other values are either calculated directly or assumed based on the procedures given in Kavanaugh and Rafferty (1997), using experimental parameters not shown in the table (such as ground thermal conductivity) where required.

The temperature penalty may be determined either from tabulated values (ASHRAE, 2011), or via direct computation (Kavanaugh and Rafferty, 1997). For this work, the temperature penalty was computed directly, using Equation 6 below:

$$t_p = \frac{N_4 + 0.5N_3 + 0.25N_2 + 0.1N_1}{NB} \cdot t_{p1} \tag{6-6}$$

Where:

t_p is the temperature penalty for the borefield [°C or °F];

t_{p1} is the temperature penalty for a single borehole adjacent to four other boreholes [°C or °F]; and

N_i is the number of boreholes in the field adjacent to i other boreholes.

The temperature penalty of a single borehole t_{p1} is determined by finding the heat stored in successive cylinders surrounding the borehole, such that heat that would ordinarily be diffused beyond the borehole separation distance would instead be stored by the area around the borehole itself:

$$t_{p1} = \frac{Q_{stored}}{\rho c_p d_{sep}^2 L} \tag{6-7}$$

Where:

Q_{stored} is the total heat stored in a cylindrical region extending from the midpoint between boreholes to infinity [W orBtu/h];

ρ is the ground density [kg/m^3 or lb/ft^3];

c_p is the ground specific heat [J/kg-K or Btu/lb-°F];

d_{sep} is the borehole separation distance [m or ft]; and

L is the borehole length [m or ft].

The short-circuit heat loss factor (F_{sc}) was assumed as 1.04 in each case; this corresponds to a flow rate of approximately 3 GPM per ton (0.16 L/s per kW) of loading for a system with a single borehole per parallel loop, the closest available equivalent to each of the experimental configurations. A brief sensitivity analysis indicated that the specific value for this factor (which is only shown by the authors to range from 1.01-1.06) produces a variation of less than 1% in the design length, in any case. The annual, monthly, and daily resistance values (R_{ga}, R_{gm}, and R_{gd}, respectively) were also computed using the detailed method of Kavanaugh and Rafferty (1997). Fourier numbers for the total run time (one or more years, depending on system), monthly (30 days), and peak (six hours) pulses were computed, and the individual resistance terms were determined by using the "G-Factor" chart—not to be confused with the g-functions used in the simulation tool. It should be noted here that there is no real justification given by Kavanaugh and Rafferty (1997) for using six hours as the daily pulse, though it is used in examples. A more

thorough examination of the load representation, as will be explained in the next section, is very likely to produce better results.

6.3 Results

For each of the four buildings presented earlier, both the simulation-based design tool and the ASHRAE Handbook equation were used to size the VGHXs, and results were compared to the actual experimental depths. As shown in Table 6-7 below, the ASHRAE Handbook ("Handbook") method consistently produces incorrect sizes when actual experimental data is supplied as inputs. The simulation-based design tool ("Design tool"), on the other hand, is within 5% of the experimental depth ("Actual") each time.

Table 6-7: Actual and computed design lengths

Borehole Depth, m (ft)	Valencia	Leicester	Atlanta	Stillwater
Actual	50 (164)	100 (328)	122 (400)	75 (246)
Handbook	101 (333)	160 (524)	96 (314)	132 (432)
Design tool	52 (172)	106 (342)	125 (409)	76 (250)

This certainly shows a wide range of differences, particularly for the Handbook method. Table 6-8 shows the oversizing (positive values) or undersizing (negative value) error for each combination of method and location. As Table 6-8 shows, for both the Valencia and Leicester systems, the Handbook error is greater than 100%—in other words, the specified design length is more than double what is actually required. Additionally, the Valencia system is cooling-dominated, while that in Leicester is heating-dominated, so the error is large regardless of the dominant operational mode. For Atlanta, the Handbook method substantially undersizes the required system; this would lead to increasing loop temperatures over time, with an associated

decrease in efficiency or eventual equipment failure. In all cases, though, the length predicted by the design tool matches the experimental depth to within 5%.

Table 6-8: Over/undersizing errors for each design method

Over/Undersizing Error	Valencia	Leicester	Atlanta	Stillwater
Handbook	103%	60%	-21%	76%
Design tool	5%	6%	2%	2%

The differences between the simulation-based design tool and the Handbook equation can be demonstrated by incrementally changing the inputs to the design tool to more closely match what is assumed by the Handbook equation. Firstly, the Handbook uses a constant load throughout the course of operation, with a magnitude equal to the average value, plus a peak "block load" for which no guidance is given on how to determine magnitude or duration. The design tool, on the other hand, uses a monthly time step, with loads input as monthly totals plus a monthly peak for both heating and cooling; Cullin (2008) describes how the peaks are selected in terms of magnitude and duration, while Cullin and Spitler (2011) show that this method of load representation performs very well (within 7%) to an hourly time step. Using instead the Handbook-style load representation, with the same single average load applied every year plus a peak load applied for 6 hours, yielded a design length quite a bit closer to that obtained from the Handbook equation, accounting for at least half of the error. This can be seen in Figure 6-4 below ("Design tool w/ handbook loading").

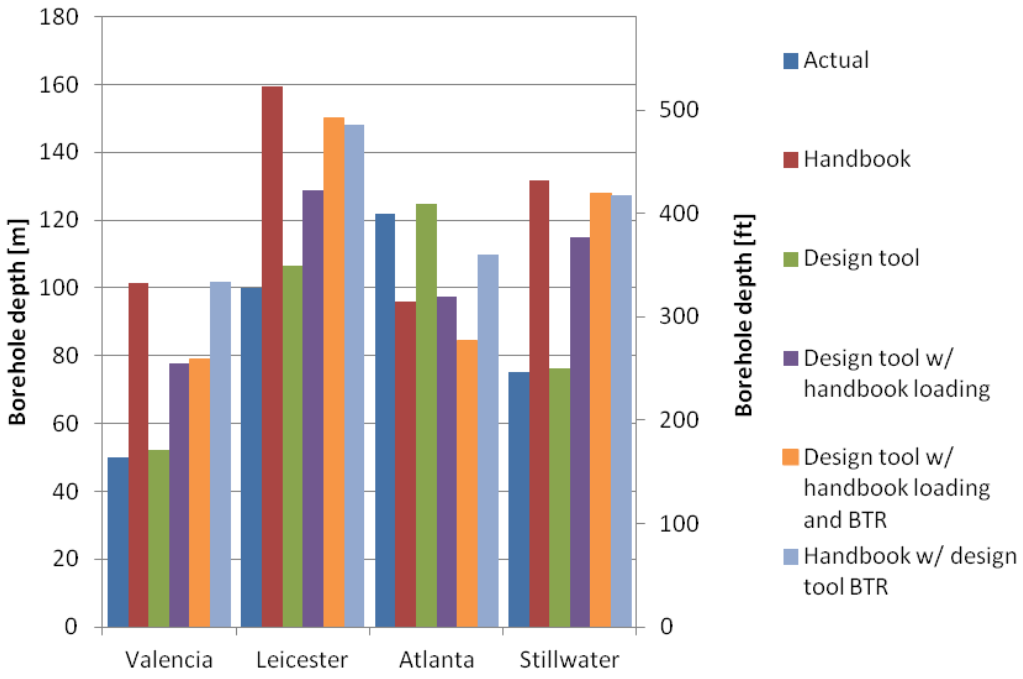

Figure 6-4: Extended comparison of design lengths

A secondary source of error in the Handbook method comes from the borehole thermal resistance. As detailed by Kavanaugh and Rafferty (1997), determination of the borehole thermal resistance involves two components: a base value determined from four U-tube diameters for either water or 20% propylene glycol at three discrete flows as the operating fluid, plus an "adjustment" for grouting dictated by the U-tube diameter, one of three discrete borehole diameters, and selection of three grout and three soil conductivities. Given that the differences between entries are nonlinear, interpolation (triple interpolation, at times) is of uncertain reliability. For this work, though, simple linear interpolation was used to determine the value used in the Handbook equation. As shown in Table 6-9, this is at times 30% or more different than the value used in the design tool. The design tool's borehole thermal resistance is computed with the multipole method (Bennet et al., 1987; Claesson and Hellström, 2011); for the Stillwater system at least, this value agrees with the value reported as a result of thermal response testing by Hern (2004).

Table 6-9: Borehole thermal resistance inputs

Borehole Thermal Resistance, m-K/W (h-ft-°F/Btu)	Valencia	Leicester	Atlanta	Stillwater
Handbook	0.110 (0.190)	0.0636 (0.110)	0.0693 (0.120)	0.115 (0.200)
Design Tool	0.111 (0.192)	0.0953 (0.165)	0.101 (0.175)	0.104 (0.180)

When the value for borehole thermal resistance determined from the Handbook tables is applied in the design tool, along with the simplified load representation, two of the four cases move substantially closer to the Handbook design length, as shown in Figure 6-4 and the error table in Table 6-10. One does not change much as the Handbook's resistance was actually very close (~2% difference) to the multipole value, and the final becomes even more undersized since this is the lone case for which the tabulated resistance is lower than that obtained with the multipole method. This is also visible in Figure 6-10 ("Design tool w/ handbook loading and BTR").

Table 6-10: Over/undersizing errors after exploration of differences

Over/Undersizing Error	Valencia	Leicester	Atlanta	Stillwater
Handbook	103%	60%	-21%	76%
Design tool	5%	6%	2%	2%
Design tool w/ handbook loading	55%	29%	-20%	53%
Design tool w/ handbook loading and BTR	58%	50%	-31%	70%
Handbook w/ design tool BTR	104%	48%	-10%	70%

Using the experimental parameters as inputs to the Handbook design equation, and following the detailed procedure of Kavanaugh and Rafferty (1997) for determining the remainder of the inputs, errors from +167% to -22% in the VGHX design length were encountered. Of this, the loading scheme seems uncorrectable, as any adaptation of the Handbook equation toward a more detailed loading scheme (even using monthly total and peak loads, as the simulation-based design tool does) would necessitate something akin to a complete system simulation—something that the

simulation-based design tool already achieves. Regardless, it can be inferred that the simple representation of loads in the Handbook equation can account for up to roughly half of the sizing error (in the Valencia and Leicester cases). Furthermore, inaccuracies in the borehole thermal resistance increase the error further, accounting for around a quarter of the error in the Leicester and Stillwater systems, and more in the Atlanta system (although the total error in this case is smaller, while the absolute error in borehole thermal resistance is largest). It is possible to apply a more accurate resistance value in the Handbook equation, whether it would be determined analytically by the multipole method or empirically from thermal response test results; the last entry in Table 6-10 ("Handbook w/ design tool BTR") shows the Handbook results with the multipole borehole thermal resistance used instead of the tabulated value. For Leicester and Atlanta, where the difference between the two resistances was more than 10%, using the multipole resistance in the Handbook equation brings the size closer to the actual value, while Stillwater improves a bit as well. However, this is only a secondary source of error, and it is still impossible to correct the load representation without drastically altering the Handbook equation.

6.4 Conclusions

This work has presented an assessment of two methods for sizing vertical ground heat exchangers for use in ground source heat pump systems: the ASHRAE Handbook design equation, as set forth in detail by Kavanaugh and Rafferty (1997); and a simulation-based design tool (Spitler, 2000; Cullin, 2008). This assessment was performed by using the two methods to "size" GHXs based on real systems, with specifications, loads, and temperature constraints dictated by physical parameters and experimental measurements.

The simulation-based design tool performs very well, predicting GHX lengths within 5% in all cases. Though experimental uncertainties are not readily available for all systems, Cullin et al. (2014) showed that, for Valencia, this error falls within the combined uncertainty of thermal conductivity and load measurements. In any case, Cullin and Spitler (2011) have shown that going from a pure hourly simulation to a hybrid monthly-plus-peak-hours time step introduces a difference of roughly 7% into the design length, over the course of a multi-year simulation. So, then, the simulation-based design tool is essentially as accurate as could be reasonably expected, given the limitations of a non-hourly simulation as well as experimental uncertainty.

The Handbook design equation, however produced results that are inconsistent, at best. The Stillwater system was sized at 75% more than the actual installed depth, while Valencia and Leicester were both greater than 100% in error—more than twice the size that was actually necessary. More seriously, perhaps, is that the Atlanta system was *under*sized by 20%; this could lead to serious equipment failure when heat pump temperatures become too high. Exploring the load representation and borehole thermal resistance explains some, if not most, of the differences between the Handbook equation and the simulation tool. While a more accurate borehole thermal resistance could easily be integrated by utilizing a more accurate method for determining it, it would be very difficult to modify the Handbook equation in such a way as to improve the load representation while still retaining computational simplicity. Even if a monthly (or even seasonal) profile were selected instead of one annual average value—plus peaks for each—it would require consideration of the effect of all previous loads on the current value; since this is, in essence, what the simulation-based design tool already does, it is likely not efficient to try to adapt the Handbook equation as it exists in its current form.

These four locations chosen for the comparison were those for which data were available and which came close to the ideal described there. As noted, such data sets are remarkably rare. The four data sets utilized here were collected at great expense and effort; presumably that is why there are so few publicly available data sets that even approach the ideal. Publication of other data sets would be most welcome. It would be particularly useful to collect and publish data for larger systems, systems that are cooling-dominated or heating-dominated, systems with deeper boreholes, and systems with groundwater-filled boreholes.

CHAPTER VII

CONCLUSIONS AND RECOMMENDATIONS

This work has, in several stages, detailed advancements in the simulation of ground source heat pump systems. Shortcomings in the present knowledge were identified, one preliminary study analyzed a common design assumption, a new and more detailed simulation model was developed, and both short time step simulations as well as design methodologies were validated against experimental data. In the process, several key insights into the behavior of ground heat exchangers have been gained.

7.1 Conclusions

Chapter 2 presented a detailed literature review of the current status of ground source heat pump system simulation. Numerous models were described, including both two- and three-dimensional models, as well as methods more suitable for utilization by practicing design engineers. Experimental validation and intermodal comparison of existing ground heat exchanger models was also discussed; in the process, general characteristics of an ideal experimental validation were presented. A list of common assumptions, typically made in the simulation of GSHP systems, was described in some depth—prior to this work, little consideration had been given to

these secondary factors, and whether they might need to be taken into account when designing these systems. Chapter 3 explored one such assumption, namely that the horizontal connective piping in a vertical borehole system plays no significant role in the performance of the system. To test the assumption, a horizontal ground heat exchanger was placed in series with the vertical ground heat exchanger, as a first approximation. Results showed that the HGHX does indeed affect the temperatures in the system, with the magnitude of the effect increased when the HGHX is closer to the ground surface, where it can interact more readily with the outside environment.

As the vertical ground heat exchanger size decreases (whether in general, or by intentional undersizing), the relative contribution of the horizontal piping grows. For an office building in heating-dominated Duluth, the horizontal piping contributed an effect equivalent to about 30% of the vertical design length. These results strongly suggest that the actual temperature constraints used in design are highly important in the expected behavior of a GSHP system, though the selection of the actual design temperatures should be done with care to avoid any unwanted long-term change in ground temperature.

Chapter 4 presented a new, multi-coordinate system model for the simulation of ground heat exchangers. This model can prove useful, as it does not necessarily require the application of the common assumptions presented in Chapter 2. This new model utilizes a coarse Cartesian grid afield of the boreholes, one radial grid representing the borehole region itself, and two smaller radial grids for each leg of the U-tube. After enhancing the *RC* network used in the model, a satisfactory match to the analytical line source solution was made; this required using five capacitance nodes in the grout region, plus three rings of radial cells in the soil outside the borehole, for sufficiently accurate results.

Chapter 5 provided a large-scale validation of both the existing g-function method, and the new multi-coordinate method, of simulating vertical ground heat exchangers. Experimental validation was performed with data from four separate facilities. For facilities in Stillwater and Valencia, both models produced reasonable matches to the experimental heat pump entering fluid temperatures, with RMSEs slightly higher for the multi-coordinate method than the g-function method. The g-function method also gave good results for the Leicester data, as well. The primary difference between these two models is that the multi-coordinate model uses a finite element simulation of a three-dimensional domain, while the g-function method works from a tabulated set of pre-computed response factors.

For the second Stillwater system, selected because it showcased very low flow rates, the multi-coordinate model matched very well, while the g-function method gave results that are obviously incorrect. This is due to the lack of consideration of thermal short-circuiting between the legs of the U-tube in the g-function model; in contrast, the multi-coordinate model explicitly models the thermal resistance between the two pipes, with the value determined by the analytical multipole method.

Chapter 6 performed a similar analysis to Chapter 5, this time with vertical ground heat exchanger design methodologies. Both a simulation-based design tool (which utilizes the g-function method) and the ASHRAE Handbook design equation were assessed against four different experimental facilities. In "sizing" VGHXs for each location using the available experimental data, the simulation-based design tool predicted design lengths within 5% of the actual installed depth, which is within the difference previously found between a pure hourly simulation and a hybrid monthly-plus-peak-hours time step. It is also likely within the bounds of

experimental uncertainty for all four systems analyzed, and is definitely within it for the Valencia data set.

In comparison, the ASHRAE Handbook design equation produced results that varied drastically. Errors ranged from 20% undersized (which could result in serious equipment failure) to more than 100% oversized (which would create tremendous excess cost). The difference in load representation between the two methods—the simulation tool uses the monthly-plus-hourly-peaks hybrid, while the equation utilizes only an annual average load and a peak block load—explains a lot of the difference between the two methods, with discrepancies in the borehole thermal resistance making up a substantial portion of the remainder.

7.2 Recommendations

The assessment of the impact of horizontal piping on a vertical ground heat exchanger showed that the horizontal piping may play an important role. The analysis, however, did not consider interaction between the horizontal and vertical pipes; adding this conductive interaction would likely mitigate the effect of the horizontal piping, although the extent of this should definitely be investigated. Furthermore, experimental testing to definitively quantify the impact would be most useful. However, the implementation and monitoring of an adequate facility would require multiple years to generate the necessary data; to date, this type of experiment has not yet been conducted.

The multi-coordinate method presented in Chapter 4 requires substantial computation time, enough to make it a model unsuitable for design calculations. It was unable to run the 56-

borehole Leicester system, and in fact was not seen to have made any noticeable progress given more than 24 hours to do so. This drawback could be lessened by hybridizing the multi-coordinate method with a more computationally efficient technique, so that the quicker (but presumably less accurate) model runs the vast majority of the simulation, while the MCM simulates critical times, such as around peak loads, when heat transfer rates are highest. Nevertheless, the MCM did prove useful in demonstrating the thermal short-circuiting in the low-flow Stillwater experimental system, something that the g-function model cannot handle at present.

The g-function model, as stated, currently does not include the effects of intra-borehole thermal short-circuiting. While it is certainly true that it may be accounted for by changing the effective borehole thermal resistance, any change in flow rate or other significant operational parameters will again cause inaccurate results. One possible approach, currently under investigation by other researchers, would be to modify the g-function method to incorporate an analytical representation of a resistance network that includes the short-circuiting effect. This would simultaneously necessitate a slight modification of thermal response testing procedures to report the additional resistance that would then be required, particularly for boreholes with long residence times when short-circuiting would be expected to become a significant factor.

The ASHRAE Handbook equation produced inaccurate design lengths for all four experimental systems used, primarily due to differences in the way loads are represented and the means of determining the borehole thermal resistance. It is certainly true that the process for applying the design equation could be tweaked slightly so as to utilize a more accurate method for determining the resistance, and that this adjustment would be fairly trivial in nature. However, the load

representation poses a much more complex problem. Any switch from the current method to one using even several intermediate "chunks" of loads (whether that be monthly, or even seasonal in nature) would by nature require the method to then consider past history for everything after the first "chunk". However, at a fundamental level, this is what the simulation-based design tool, as well as other similar simulation methods, do already. Given the effort required to redevelop the design equation into a more accurate form that considers the loading in greater detail, and subsequent necessary testing of the revised form, it is not currently seen as efficient to do so.

REFERENCES

ASHRAE, 2011. ASHRAE Handbook--HVAC Applications. Atlanta: ASHRAE.

Beier, R.A. 2011. Vertical temperature profile in ground heat exchanger during in-situ test. *Renewable Energy* 36(5): 1578-1587.

Beier, R.A., J. Acuna, P. Mogensen, and B. Palm. 2012. Vertical temperature profiles and borehole resistance in a U-tube borehole heat exchanger. *Geothermics* 44: 23-32.

Beier, R.A., M.D. Smith, and J.D. Spitler. 2011. Reference data sets for vertical borehole ground heat exchanger models and thermal response test analysis. *Geothermics* 40(1): 79-85.

Bennet, J., J. Claesson, and G. Hellström. 1987. Multipole Method to Compute the Conductive Heat Flows to and Between Pipes in a Composite Cylinder. Notes on Heat Transfer 3-1987, Department of Building Technology and Mathematical Physics, University of Lund, Sweden.

Bernier, M.A., P. Pinel, R. Labib, and R. Paillot. 2004. A multiple load aggregation algorithm for annual hourly simulations of GCHP systems. *HVAC&R Research* 10(4): 471-488.

Bertanoglio, S., M. Bernier, and M. Kummert. 2012. Comparing vertical ground heat exchanger models. *Journal of Building Performance Simulation* 5(6): 369-383.

Blomberg, T., J. Claesson, P. Eskilson, G. Hellström, and B. Sanner. Earth Energy Designer 3.0 Manual. Available online at http://www.buildingphysics.com/ manuals/EED3.pdf

Carslaw, H.S., and J.C. Jaeger. 1947. *Conduction of Heat in Solids*. Claremore Press: Oxford, United Kingdom.

Chiasson, A., S.J. Rees, and J.D. Spitler. 2000. A preliminary assessment of the effects of ground-water flow on closed-loop ground-source heat pump systems. *ASHRAE Transactions* 106(1): 380-393.

Claesson, J., and G. Hellström. 2011. Multipole method to calculate borehole thermal resistances in a borehole heat exchanger. *HVAC&R Research* 17(6): 895-911.

Claesson, J., and J. Bennet. 1987. Thermal Resistances to and Between Pipes in a Composite Cylinder. Department of Mathematical Physics and Building Technology, University of Lund, Sweden.

Claesson, J., and S. Javed. 2011. An analytical method to calculate borehole fluid temperatures for time scales from minutes to decades. *ASHRAE Transactions* 117(1): 3-12.

Crawley, D.B., L.K. Lawrie, F.C. Winkelmann, W.F. Buhl, Y.J. Huang, C.O. Pedersen, R.K. Strand, R.J. Liesen, D.E. Fisher, W.J. Witte, and J. Glazer. 2001. EnergyPlus: Creating a

new-generation building energy simulation program. *Energy and Buildings* 33(4): 319-331.

Cui, P., H. Yang, and Z. Fang. 2007. The simulation model and design optimization of ground source heat pump systems. *HKIE Transactions* 14(1):1-5.

Cullin, J.R. 2008. Improvements in design procedures for ground source and hybrid ground source heat pump systems. Master's Thesis, Oklahoma State University, Stillwater OK.

Cullin, J.R., and J.D. Spitler. 2011. A computationally efficient hybrid time step methodology for simulation of ground heat exchangers. *Geothermics* 40(2): 144-156.

Cullin, J.R., E. Lee, and J.D. Spitler. 2013. Preliminary investigation of the effect of horizontal piping on the performance of a vertical ground heat exchanger system. *ASHRAE Transactions*: 119(2):302-311.

Cullin, J.R., C. Montagud, F. Ruiz-Calvo, and J.D. Spitler. 2014. Experimental validation of ground heat exchanger design methodologies using real monitored data. *ASHRAE Transactions* 120(2): pages pending.

Eskilson, P. 1987. Thermal analysis of heat extraction boreholes. Doctoral Thesis, Lund University, Sweden.

Farouki, O.T. 1986. *Thermal properties of soils*. Clausthal-Zellerfeld, Germany: Trans Tech Publications.

Fisher, D.E., A. Murugappan, S.K. Padhmanabhan, and S.J. Rees. 2006. Implementation and validation of ground-source heat pump system models in an integrated building and system simulation environment. *HVAC&R Research* 12(3a): 693-710.

Fossa, M. 2011. The temperature penalty approach to the design of borehole heat exchangers for heat pump systems. *Energy and Buildings* 43: 1473-1479.

Gentry, J.E. 2007. Simulation and validation of hybrid ground source and water-loop heat pump systems. Master's thesis, Oklahoma State University, Stillwater OK.

Gnielinski, V. 1976. New equations for heat and mass transfer in turbulent pipe and channel flow. *International Chemical Engineering* 16: 359-368.

He, M. 2012. Numerical modelling [*sic*] of geothermal borehole heat exchanger systems. Ph.D. Dissertation, De Montfort University, Leicester, United Kingdom.

Hellström, G. 1989. Duct ground heat storage model. Manual for computer code. Department of Mathematical Physics, University of Lund, Sweden.

Hellström, G., and B. Sanner. 1994. Software for Dimensioning of Deep Boreholes for Heat Extraction. Proceedings of Calorstock Conference 1994, Espoo/Helsinki, Finland.

Hellström, G., B. Sanner, M. Klugescheid, T. Gonka, and S. Mårtensson. 1997. Experiences with the borehole heat exchanger software EED. Proceedings of Megastock Conference 1997, Sapporo, Japan.

Hern, S. 2004. Design of an experimental facility for hybrid ground source heat pump systems. M.S. Thesis, Oklahoma State University, Stillwater OK.

Hughes, P., and P. Im. 2012. Foundation heat exchanger final report: Demonstration, measured performance, and validated model and design tool. Oak Ridge National Laboratory report ORNL/TM-2012/27, available online at http://info.ornl.gov/sites/publications/files/Pub34532.pdf.

Ingersoll, L.R., O.J. Zobel, and A.C. Ingersoll. 1954. *Heat Conduction with Enginerering, Geological, and Other Applications*. The University of Wisconsin Press: Madison WI.

Judkoff, R.D. 1988. Validation of building energy analysis simulation programs at the Solar Energy Research Institute. *Energy and Buildings* 10: 221-239.

Kavanaugh, S.P. 1992. Simulation of ground-coupled heat pumps with an analytical solution. Proceedings of the ASME International Solar Energy Conference, Maui HI, 5-9 April.

Kavanaugh, S.P. 1995. A design method for commercial ground-coupled heat pumps. *ASHRAE Transactions* 101(2):1088-1094.

Kavanaugh, S.P., and K. Rafferty. 1997. Ground-source heat pumps: Design of geothermal systems for commercial and industrial buildings. Atlanta: ASHRAE.

Kelvin, W.T. 1884, *Mathematical and Physical Papers*. University Press: Cambridge, United Kingdom.

Kim, E.-J., J.-J. Roux, M.A. Bernier, and O. Cauret. 2011. Three-dimensional numerical modeling of vertical ground heat exchangers: Domain decomposition and state model reduction. *HVAC&R Research* 17(6): 912-927.

Kusuda, T., and P.R. Achenbach. 1965. Earth temperatures and thermal diffusivity at selected stations in the United States. *ASHRAE Transactions* 71(1): 61-74.

Lamarche, L., and M. Beauchamp. 2007. A new contribution to the finite line-source model for geothermal boreholes. *Energy and Buildings* 39(2): 188-198.

Lee, E.S. 2013. An improved hydronic loop system solution algorithm with a zone-coupled horizontal ground heat exchanger model for whole building energy simulation. Ph.D. dissertation, Oklahoma State University, Stillwater OK

Lee, E.S., D.E. Fisher, and J.D. Spitler. 2013. Efficient horizontal ground heat exchanger simulation with zone heat balance integration. *HVAC&R Research* 19(3): 307-323.

Liu, X. 2008. Enhanced design and energy analysis tool for geothermal water loop heat pump systems. Proceedings of the 9th International Energy Agency Heat Pump Conference, Zurich, Switzerland, 20-22 May.

Liu, X. 2013. Personal communications.

Liu, X., and G. Hellström. 2006. Enhancements of an integrated simulation tool for ground-source heat pump system design and energy analysis. Proceedings of Ecostock 2006, Pomona NJ.

Lund, J. 2011. Geothermal (Ground-source) heat pumps introduction. U.S. Department of Energy, Office of Energy Efficieny and Renewable Energy. Webinar, 23 June.

Malayappan, V., and J.D. Spitler. 2013. Limitations of using uniform heat flux assumptions in sizing vertical borehole heat exchanger fields. *Proceedings of Clima 2013*, Prague, Czech Republic, 16-19 June.

Marcotte, D., and P. Pasquier. 2008. On the estimation of thermal resistance in borehole thermal conductivity test. *Renewable Energy* 33: 2407-2415.

Mei, V.C. 1988. Heat pump ground coil analysis with thermal interference. *Journal of Solar Energy Engineering* 110(2): 67-73.

Mogensen, P. 1983. Fluid to duct wall heat transfer in duct system heat storages. Proceedings of the International Conference on Subsurface Heat Storage in Theory and Practice, Stockholm, Sweden, 6-8 June: 652-657.

Montagud, C., J.M. Corberán, Á. Montero, and J.F. Urcheguía. 2011. Analysis of the energy performance of a ground source heat pump system after five years of operation. *Energy and Buildings* 43(9): 3618-3626.

Naicker, S.S., and S.J. Rees. 2011. Monitoring and performance analysis of large non-domestic ground source heat pump installation. Proceedings of 2011 CIBSE Technical Symposium, Leicester UK, 6-7 September.

Nordell, B. 1985. The borehole heat store at Luleå, Sweden. Proceedings of Enerstock '85: 3rd International Conference on Energy Storage for Heating and Cooling, Toronto, Canada, 20-22 September.

Parsons, B. A living laboratory: ASHRAE's renovated headquarters. *Canadian Consuting Engineer* 49(7): 31-33.

Paul, N.D. 1996. The effect of grout thermal conductivity on vertical geothermal heat exchanger design and performance. M.S. Thesis, South Dakota State University.

Pertzborn, A., S. Hackel, G. Nellis, and S. Klein. 2011. Experimental validation of a ground heat exchanger model in a hybrid ground source heat pump. *HVAC&R Research* 17(6): 1101-1114.

Picard, D., and L. Helsen. 2014. Advanced hybrid model for borefield heat exchanger performance evaluation: An implementation in Modelica. Proceedings of the 10th International Modelica Conference, Lund, Sweden, 10-12 March.

Piechowski, M. 1996. A ground coupled heat pump system with energy storage. Ph.D. Dissertation, Melbourne University, Parkville, Australia.

Piechowski, M. 1999. Heat and mass transfer model of a ground heat exchanger: Theoretical development. *International Journal of Energy Research* 23(7): 571-588.

Rees, S.J., and M. He. 2013. A three-dimensional numerical model of borehole heat exchanger heat transfer and fluid flow. *Geothermics* 46(1): 1-13.

SEL. 2012. TRNSYS 17 – A Transient System Simulation Program. Version 17.1. Solar Energy Laboratory, University of Wisconsin-Madison.

Sheriff, F., and M.A. Bernier. 2008. (In French). Simulations de champs de puits géothermiques verticaux de charges thermiques différentes. Proceedings of IBPSA-Canada/eSim 2008, Ville de Québec, Canada: 17-24.

Shonder, J.A., V.D. Baxter, J.W. Thornton, and P.J. Hughes. 1996. A new comparison of vertical ground heat exchanger design methods for residential applications. *ASHRAE Transactions* 102(2): 1179-1188.

Shonder, J.A., V.D. Baxter, P.J. Hughes, and J.W. Thornton. 2000. A new comparison of vertical ground heat exchanger design methods for commercial applications. *ASHRAE Transactions* 106(1): 831-842.

Smith, M., and R. Perry. 1997. Vertical ground heat exchanger borehole grouting: Field application studies and in-situ thermal performance testing. EPRI Report RP3881-1, Electric Power Research Institute.

Spitler, J.D. 2000. GLHEPRO—A design tool for commercial building ground loop heat exchangers. Proceedings of the Fourth International Heat Pumps in Cold Climates Conference, Aylmer, Québec, 17-18 August.

Spitler, J.D., and J.R. Cullin. 2008. Misconceptions regarding design of ground-source heat pump systems. Proccedings of the World Renewable Energy Congress, Glasgow, Scotland, 20-25 July.

Spitler, J.D., and M. Bernier. 2011. Ground-source heat pump systems: The first century and beyond. *HVAC&R Research* 17(6): 891-894.

Spitler, J.D., D.E. Fisher, and D.C. Zietlow. 1989. A primer on the use of influence coefficients in building energy analysis. Proceedings of the Building Simulation '89 Conference, Vancouver, Canada, 23-24 June: 299-304.

Spitler, J.D., D.E. Fisher, J.R. Cullin, L. Xing, E. Lee, S.J. Rees, and D. Fan. 2011. Foundation heat exchanger model and design tool development and validation. Final report, Oak Ridge National Laboratory.

Spitler, J.D., J.R. Cullin, E. Lee, D.E. Fisher, M. Bernier, M. Cummert, P. Cui, and X. Liu. 2009. Preliminary intermodel comparison of ground heat exchanger simulation models. Proceedings of Effstock 2009: The 11th International Conference on Thermal Energy Storage, Stockholm, Sweden, 14-17 June.

Sutton, M.G., R.J. Couvillon, D.W. Nutter, and R.K. Davis. 2002. An algorithm for approximating the performance of vertical bore heat exchangers installed in a stratified geological regime. *ASHRAE Transactions* 118(2): 177-184.

U.S. Department of Energy. 2012. EnergyPlus Engineering Reference, Version 7.0.

Underwood, C.P., and J.D. Spitler. 2007. Analysis of vertical ground loop heat exchangers applied to buildings in the UK. *Building Service Engineering, Research and Technology* 28: 133-159.

Walter, I.A., R.G. Allen, R. Elliott, D. Itenfisu, M.E. Jensen, B. Mecham, T.A. Howell, R. Snyder, S. Eching, T. Spofford, M. Hattendorf, D. Martin, R.H. Cuenca, and J.L. Wright. 2005. The ASCE standardized reference evapotranspiration equation. Standardization of Reference Evapotranspiration Committee Final Report, American Society of Civil Engineers, and Environmental and Water Resources Institute.

Witte, H.J.L. 2012. Error analysis of thermal response tests (Extended version). Proceedings of Innostock 2012, Lleida, Spain, 16-18 May.

Xing, L. 2010. Analytical and numerical modeling of foundation heat exchangers. M.S. thesis, Oklahoma State University, Stillwater, Oklahoma.

Xu, H., and J.D. Spitler. 2011. Importance of moisture transport, snow cover and soil freezing to ground temperature predictions. Proceedings of the 9th Nordic Symposium on Building Physics, Tampere, Finland, 29 May-2 June.

Xu, X. 2007. Simulation and optimal control of hybrid ground source heat pump systems. Ph.D. dissertation, Oklahoma State University, Stillwater, Oklahoma.

Xu, X., and J.D. Spitler. 2006. Modeling of vertical ground loop heat exchangers with variable convective resistance and thermal mass of the fluid. Proceedings of Ecostock 2006, Pomona NJ, 31 May-2 June.

Yavuzturk, C., and J.D. Spitler. 1999. A short time step response factor model for vertical ground loop heat exchangers. *ASHRAE Transactions* 105(2): 475-485.

Yavuzturk, C., and J.D. Spitler. 2001. Field validation of a short time-step model for vertical ground loop heat exchangers. *ASHRAE Transactions* 107(1): 617-625.

Zeng, H.Y., N.R. Diao, and Z.H. Fang. 2002. A finite line-source model for boreholes in geothermal heat exchangers. *Heat Transfer Asian Research* 31(7): 558-567.

Zeng, H.Y., N.R. Diao, and Z.H. Fang. 2003. Efficiency of vertical geothermal heat exchangers in ground source heat pump systems. *Journal of Thermal Science* 12(1):77-81.

VITA

James Robert Cullin

Candidate for the Degree of

Doctor of Philosophy

Thesis: ADVANCEMENTS IN THE SIMULATION OF GROUND SOURCE HEAT PUMP SYSTEMS

Major Field: Mechanical Engineering

Biographical:

Personal: Born in Ponca City, Oklahoma, on 3 July 1984 to John F. and Celia R. Cullin. Married in Stillwater, Oklahoma, on 12 September 2010, to the former Cassandra O. Mickelson.

Education:

Completed the requirements for the Doctor of Philosophy in Mechanical Engineering at Oklahoma State University, Stillwater, Oklahoma, in May 2014.

Completed the requirements for the Master of Science in Mechanical Engineering at Oklahoma State University, Stillwater, Oklahoma, in 2009.

Completed the requirements for the Bachelor of Science in Mechanical Engineering and Aerospace Engineering (summa cum laude) at Oklahoma State University, Stillwater, Oklahoma, in 2006.

Experience: Employed as a graduate research assistant for the Oklahoma State University Building and Environmental Thermal Systems Research Group from 2006 to 2013. Lecturer (MAE 3233 - Heat Transfer) for the Department of Mechanical and Aerospace Engineering at Oklahoma State University, 2013-2014.

Professional Memberships: American Society of Heating, Refrigerating, and Air-Conditioning Engineers (ASHRAE), International Building Performance Simulation Association (IBPSA).